Sediment transport in the Slufter inlet channel, Texel, the Netherlands

Nynke Vellinga

MSc Thesis

Second version

December 13, 2010

Supervisors:

Prof. Dr. P. Hoekstra

Dr. M. van der Vegt

Utrecht University

Faculty of Geosciences

Department of Physical Geography

Sediment transport in the Slufter inlet channel, Texel, the Netherlands

Nynke Vellinga

MSc Thesis

Second version

December 13, 2010

Supervisors:

Prof. Dr. P. Hoekstra

Dr. M. van der Vegt

Utrecht University

Faculty of Geosciences

Department of Physical Geography

Preface

This master thesis about sediment transport in the Slufter inlet channel on the island of Texel is the result of the analysis of a fieldwork of seven weeks in the Slufter in the autumn of 2009. While a part of the fieldwork focussed on sediment transport in the Slufter inlet itself, another part of the research was focussed on wave processes on the nearby beach and the sediment transport accompanied by these processes. The results of this research can be found in the master theses of Marjolijn Witteveen, Hans Brockhus and Jurre de Vries (Witteveen, 2010, Brockhus, 2010 and de Vries, 2010).

As said, in this thesis the emphasis is on sediment transport in the Slufter inlet channel. With the analysis of measurements in and around the channel conclusions will be drawn on bedload as well suspended load transport. The sediment transport budgets under different weather conditions and on the long term will be analysed. With these computations, more can be said about the stability of the Slufter and other tidal inlet systems.

Although I put a lot of time and effort in this thesis, I could not have reached it without the help of some others, which I would like to thank:

- Piet Hoekstra, Maarten van der Vegt and Gerben Ruessink for the support and help with the analysis and the many useful remarks and ideas that helped me to keep focused on the important things and keep working in the direction of the end result, instead of swimming around in my own data.
- Marjolijn Witteveen, Jurre de Vries and Hans Brockhus for seven great weeks at the island of Texel and a good fieldwork cooperation, not only during the fieldwork itself, but also afterwards.
- All family and friends that supported me, listened to all boring stories about failed measurements and showed me the important things in life, which more often than not have nothing to do with seawater and suspended sediment.
- Staatsbosbeheer (National forestry service) and the municipality of Texel for giving us the opportunity to work in the Slufter.

- Chris Roosendaal, Henk Markies and Marcel van Maarsseveen. One can do a lot of fieldwork without fieldwork partners, a lot of analysis without a professor, very well finish a thesis without the distraction of family and friends, but I certainly could not have done any fieldwork at all without the 24/7, on-demand assistance of technicians.

List of contents

List of figures

List of tables

List of Photographs

Summary

Tidal inlets are a very dynamic coastal form. Sediment transport patterns and net sediment transport directions are of great importance with respect to tidal inlet stability. In this research, bedload and suspended load sediment transport and the factors governing this transport are investigated in the inlet channel of the small Slufter tidal inlet on the island of Texel, in the northwestern Netherlands.
A triangular frame was place in the inlet channel, to which three Acoustic Doppler Velocimeters (ADV) for measuring flow velocity, three Optical Backscatter Sensors (OBS) for measuring suspended sediment concentrations and a wave gauge for measuring water levels and water depths were mounted. Channel migration was monitored using a DGPS.

Migration of the channel only takes place where the channel crosses the sand flat and is very dependent on flow velocities. Bedforms showed a highly three dimensional pattern with lengths in the order of meters and heights in the order of decimetres. No migration of bedforms took place for flow velocities below 0.6 m/s. Inflow takes place in two pulses, while outflow occurs in one single pulse. The higher the tidal amplitude and the setup, the higher the flow velocities in the channel. The system as a whole is ebb dominated. Only during storm, water flows in over the large sand flats on each side of the channel, but flows out via the channel. No waves enter the inlet, except for infragravity waves under storm conditions.

Quantifying bedload sediment transport with dune tracking techniques was not possible. The OBS and ADV measurements of suspended sediment concentration could only be used to deduce a general pattern in transport rates, but could not be quantified. The suspended sediment concentration is a result of local flow velocities. The concentration profiles from the ADV and OBS showed very good mixing of suspended sediment and show that in the Slufter a sand/mud mixture is in suspension.
For bedload as well as suspended load, calculations showed almost no transport under calm weather conditions, an export of several cubic meters per fifty hours for more

energetic weather conditions and an export of several tens of cubic meters under storm conditions. For the total transport, bedload as well as suspended load are important contributors. The amount and magnitude of storms is very important to the total net export through the Slufter inlet channel on the long term.

For the Slufter system as a whole, import of sediment takes place during storm over the beach flat and mud is captured in the backbasin. These processes reduce the export of sediment for the system as a whole and thereby bring the system closer to equilibrium.

1 Introduction

1.1 problem definition/general problem

Barrier coasts make up 15% of the world's coastlines (de Swart & Zimmerman, 2009) and are a very dynamic coastal form. Depending on tidal and wave conditions barrier islands are more or less elongated and are often interrupted by tidal channels. These tidal channels are very important with respect to sediment transport since they are the only pathway of import or export for the back-barrier basin (Figure 1.1). Due to confined flow in the inlet itself and decreasing velocities in the open sea and backbarrier basin, deltas are formed at both sides of the inlet. In areas with a relatively large tidal amplitude and relatively small wave influence, the ebb tidal delta on the open sea side is generally the largest and best developed one.

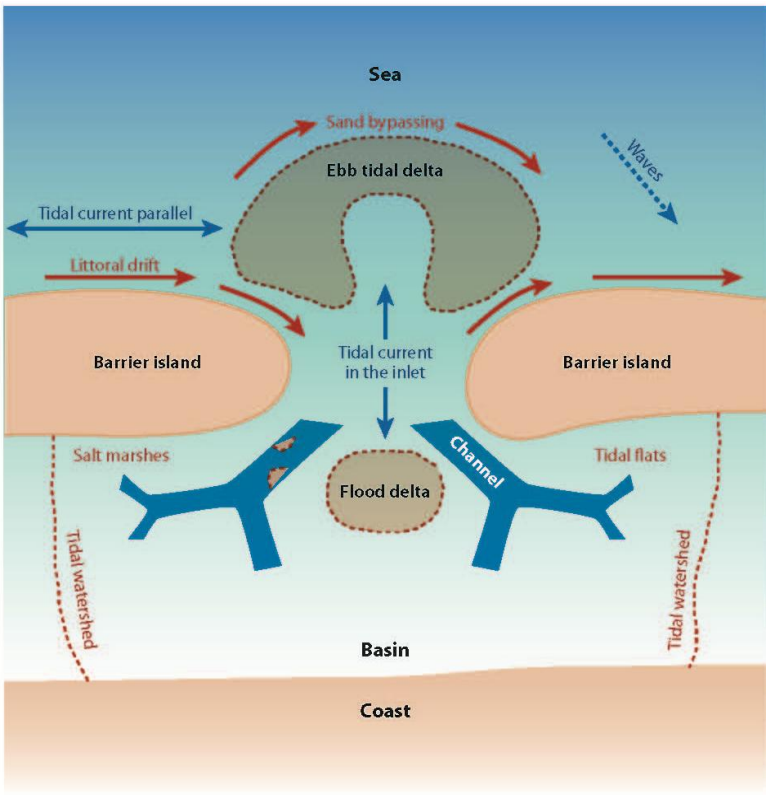

Figure 1.1 Schematic overview of a tidal inlet system between two barrier islands. (de Swart and Zimmerman, 2009).

Sediment transport patterns and net sediment transport directions are of great importance with respect to tidal inlet stability and the stability of the adjacent basin. Stable inlets have been studied by many authors (e.g. Gao & Collins, 1994; Nield, Walker, & Lambert, 2005; Pacheco et al., 2008; Van Goor et al., 2003) and often have relationships between different inlet parameters such as, for instance, inlet cross-sectional area and tidal prism. Tidal inlets can be considered stable when there is no or very little net transport or when certain inlet parameters, such as for example the cross-sectional area of the inlet channel, do not change. However, as Pacheco et al (2008) state, the establishing of inlet parameter stability not necessarily means that there is no net sediment transport in the system as a whole. When external factors such as jetties and resistant bed layers prevent an inlet to migrate or adapt its width or depth, the inlet might still show a net import or export of sediment. Although the inlet itself does not change (i.e. its parameters are stable), the system as a whole has not reached an equilibrium stage yet.
Dominating processes and relations between inlet parameters probably are very different for tidal inlet systems of different size. This means that the influence of certain weather conditions or processes (e.g. storms or longshore drift) on large tidal inlets, might be different than expected in a relatively small system such as the Slufter.

Since a lot of different factors influence sediment transport, it is very difficult to make a general statement about sediment transport fluxes in tidal inlets. For suspended as well as bedload transport, net transport might be offshore as well as onshore, dependent on the dominant sediment transport mechanisms and prevailing hydro-meteorological conditions. Investigating sediment transport patterns in small tidal inlets can give more insight in the different mechanisms at work and their contributions to the total sediment transport and inlet stability.

1.2 objectives of research

Bed load and suspended load transport cause the import as well as the export of sediment in the Slufter area at Texel. The fact that the Slufter is already in existence for over 150 years, shows that the balance between incoming and outgoing sediment is quite delicate.

It is however not clear whether there is net import or export, or that there is no gain or loss of sediment at all.
Understanding sediment budgets for a relatively small system like the Slufter inlet can help improving the general understanding of sediment budgets in tidal inlets. For large tidal inlets between barrier islands, a lot of research has been done and a basic understanding of stability has been gained. Investigating sediment budgets in small tidal inlets such as the Slufter can be of help for the understanding of small systems as well, thereby broadening our insight in a wider range of inlet systems.
Since a large part of the sediment transport takes place in the Slufter inlet, the focus of this study will be on that inlet. Bedload as well as suspended sediment transport will be studied, since both play an important, but not by definition comparable role, to the sediment budgets of the Slufter.
The aim of this research can be described as:

"With this study we want to investigate bedload and suspended load sediment transport in the Slufter inlet and the main factors governing this transport, under spring as well as neap tide conditions and during storm and calm weather."

1.2.1 Formulation of hypothesis

Tidal asymmetry plays an important role in the transport of sediment, but also waves and wind can have a large influence. During calm weather, the sediment transport in the inlet will depend mostly on tidal asymmetry. During storms the whole Slufter basin and inlet is flooded. Water is in that case also imported over the beach plain during the flood tide, while the system empties through the main inlet channel. Waves also cause sediment transport in this case and swell waves and infragravity waves may induce sediment transport in different directions. Therefore, our hypothesis is as follows:

"During calm weather conditions, the Slufter inlet throat will show an import of sediment, for bedload as well as suspended load sediment transport. During storms,

export of sediment will take place through the inlet due to increased seaward flow, which compensates landward flow over the shoals".

1.2.2 Formulation of research questions

In order to answer the main research question and to test our research hypothesis, subquestions need to be answered which together will give a full answer to the question whether the Slufter has a positive, a negative or a neutral sediment budget.

The research questions of this study are defined as follows:

- Is the tidal flow in the inlet ebb or flood dominated and what is the dominant flow direction due to wave action, during storm as well as during calm conditions?
- How large and in which direction is bedload transport under different energetic conditions and on the long term?
    - Which bedforms are occurring in the channel and what are their dimensions and migration rates, during spring as well as neap tide and during storm as well as calm weather conditions?
    - What is the net bedload transport direction, during spring as well as neap tide and during storm as well as calm weather conditions?
- How large and in which direction is suspended load transport under different energetic conditions and on the long term?
    - How do suspended sediment concentrations change with different energetic conditions and what do the concentration profiles look like?
    - What are the magnitudes of suspended sediment fluxes, during spring as well as neap tide and during storm as well as calm weather conditions?
    - What is the relative contribution of sand and mud to the suspended load sediment fluxes?
- What is the relative importance of bedload and suspended load transport through the Slufter inlet channel?

The answer to the above questions will be obtained by performing measurements in the inlet channel on flow velocity, morphology and water levels (see paragraph 3.1). Furthermore, sediment transport models will be used to predict sediment transport rates an net transports on the longer term (see paragraph 2.4 and 2.5).

1.3 thesis outline

- Chapter 2 gives the theoretical background of the subjects important to this research: a description of the Slufter inlet, the morphology and stability of tidal inlet systems, hydrodynamics and deformation of tides, theoretical background and used equations for bedload and suspended load sediment transport.
- Chapter 3 describes the details about the fieldwork campaign and the elaboration of the results. The measurement setup is described, followed by an outline of the data analysis and laboratory work performed.
- Chapter 4 gives a short overview of the meteorological and hydrodynamic conditions during the fieldwork campaign.
- Chapters 5,6 and 7 give the results of measurements and analysis with respect to, respectively, morphology, hydrodynamics and sediment transport.
- Chapter 8 discusses the results and gives suggestions for further research
- In chapter 9, the main conclusions are outlined and the research questions answered.

2 Fieldwork location and theoretical background

In this chapter, some background information is provided on the fieldwork location and on the theory which is used for the elaboration of the measurements. The emphasis lies on sediment transport, split in the factors influencing the transport, bedload transport and suspended load transport.

2.1 Fieldwork location

The Slufter is a small tidal inlet that connects the North Sea with a backbarrier basin on the island of Texel, located in the northern Netherlands (Figure 2.1). It is approximately 4 km² in size and has one outlet to the North Sea. Parts of the Slufter are inundated every flood, whilst other parts are only inundated during storms when the flood water levels are increased due to storm surges.

The island of Texel is the product of two smaller islands that existed in the 13th and 14th century: Texel and Eijerland. Due to the construction of dikes (the so called *stuifdijken*, or sand drift dikes), the two islands merged into one large island Texel. However, in 1858 a storm caused three breaches in the dikes, generating three Slufter-systems as a consequence: the *Muy,* the *Grote Slufter* and the *Kleine Slufter*. The former two were successfully closed by dikes, but despite several attempts, the *Kleine Slufter* remained an open connection to the sea and even grew larger (Hisgen & Laane, 2008; van Puijvelde, 2009). The Slufter is now recognized as a valuable nature reserve due to its fresh/saltwater gradient and its semidiurnal flooding.

The inlet of the Slufter is approximately 30 m wide and has a very variable depth. The deepest part is located some 300 m from the sea and has a depth of about 1.5 m at low tide. More seaward and more landward, the depth of the channel is only a few decimetres, with a minimum of 10 cm at low tide. The channel widens at the mouth, up to a width of 60m. At high tide, the width of the channel increases, specially where the banks have a low slope. Landward of the beach, just inside the tidal basin, the shoals near the main channel flood, causing a large increase in width of the channel. During storm surges, water does not only enter the Slufter via the channel, but also by flowing over the

adjacent beach plains. The width of the inlet of the Slufter then equals the gap in the dune row, being 400 m. Outflow occurs mainly via the channel, due to decreased water levels at the falling tide.

The flow of water through unconsolidated sand causes erosion at the northern bank and deposition on the southern bank of the inlet between the dunes. This results in a northward migration of the channel. At a certain moment, the channel reaches and starts eroding the northern dunes, thereby attacking the primary sea defence. To prevent this erosion, the channel is artificially relocated every time it reaches the dunes, being every three to five years.

Figure 2.1 Location of the Slufter on Texel

The mean tidal range is 1.5 m, varying from 1m at neap tide to 2 m at spring tide (source: www.actuelewaterdata.nl). The spring tidal prism of the Slufter equals 4.36 10^5 m³ (van Puijvelde, 2009). When due to a setup on the normal water levels the supratidal marshes of the Slufter flood with an average water depth of half a meter, the tidal prism increases with another 2 10^6 m³.

Wind direction is dominantly from the southwest, as KNMI-observations from the Texelhors show (KNMI, Verkaik, pers. comm. in van der Molen, 2002). Moderate storms from the southwest dominate in the wind climate (Figure 2.2)(van der Molen, 2002).

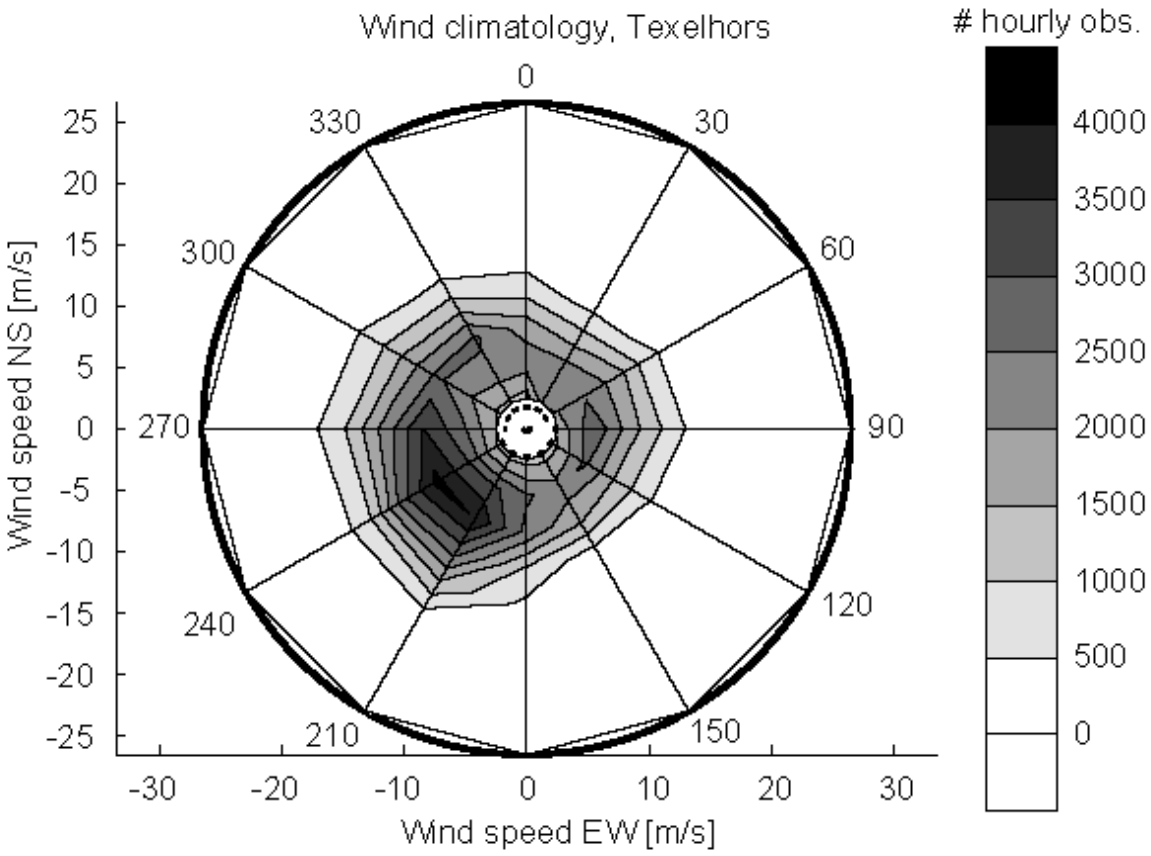

Figure 2.2 10-year period wind climate for Texel, obtained from the Texelhors meteorological station. Wind directions are set from the North (0 degrees) and wind speed increases from the centre to the outside. The areas denote the number of hourly observations. Moderate southwesterly storms dominate (van der Molen, 2002).

2.2 Hydrodynamics

As with gravity wind waves, tidal waves deform when they enter shallow water. Second and higher order waves are superimposed on the original tidal wave. Because in shallow water wave celerity depends on water depth, the wave crest has a larger celerity than the wave trough, causing asymmetrical tides. These deformations have a profound effect on

maximum flow velocities and the duration of tidal stages. The tidal stage with the highest flow velocities has the shortest duration.

Likewise, the asymmetry of the tide caused by wave deformation is of great importance for sediment transport. Since sediment transport is not linearly related to flow velocity, but related with a power of three to five, increased flow velocities during the flood stage cause sediment transport during the flood stage to be much larger than during the ebb stage. This implies a net sediment transport in the direction of the flood flow. However, this dominant direction of sediment transport is partially cancelled out by the longer duration of the ebb flow, giving more time for sediment transport in the ebb flow direction. However, this only holds if flow velocities exceed critical flow velocities for sediment transport. For bedload sediment transport the net transport direction mostly depends on the absolute flow velocities, since bedload transport reacts immediately to changing flow velocity. For suspended load sediment transport, however, the duration of the change of the tide also plays a role; when flow velocities drop below values critical for sediment transport, sediment in suspension is still taken with the flow. The stage between two tides therefore has influence on the suspended sediment transport, although flow velocities are very low.

Besides the formation of Stokes and sawtooth wave patterns, the local morphology of a tidal inlet can be important for the propagation and deformation of the incoming tidal wave. Flow velocity patterns and differences in the duration of the ebb and flood which are caused by local morphology, can therefore be of major importance with respect to net sediment fluxes. Specially the relative amounts of intertidal area in a tidal basin influences the tidal wave and thus local flow velocities.

2.3 Factors influencing sediment transport

The most important factor determining net suspended as well as net bedload sediment transport in tidal channels is tidal asymmetry (Fiechter et al., 2006; Ranasinghe & Pattiaratchi, 2000; van de Kreeke & Hibma, 2005). Tidal asymmetry is not only important in determining the net in- or export of sediment, but also relevant for the spatial

(re)distribution of sediment within a tidal inlet system (Fiechter et al., 2006; Stanev, Brink-Spalingk, & Wolff, 2007).

For the sand-sized fraction of the sediment, wave action is an important factor of influence on transport. Wave action influences sediment transport in different ways:

A) wave deformation: in shallow water, flow velocities under wave crests increase with respect to those under troughs (L. C. van Rijn, 1990). This process enhances sediment transport under the crest of a wave.
B) Stirring up sediment: when waves enter shallow water, they generate extra bed shear stress to stir up sediment from the bottom. This sediment can then be further transported by the wave itself or by tidal currents. Without the presence of waves, sediment transport might not have been possible despite the presence of tidal currents (Green & MacDonald, 2001).
C) Longshore currents: Oblique incoming breaking waves induce longshore currents which in turn can enhance longshore sediment transport. The ebb tidal deltas and inlets along a coast can function as a trap of this longshore sediment transport (Elias & van der Spek, 2006). The magnitude of the longshore current and thus the amount of sediment that enters the system via this current depends on the angle of wave approach and the wave breaker height. Sediment can either be trapped in the inlet itself, be trapped in the ebb-tidal delta or pass by the delta to the adjecent shore (sediment bypassing) (Hoque, Ahad, & Saleh, 2009; Liu & Hou, 1997; Vila-Concejo et al., 2003; Vinther, Nielsen, & Aagaard, 2004)
D) Wave-wave interaction: infragravity waves, which form in gravity wave groups, can, in combination with sediment stirring of gravity waves, have a distinct effect on sediment transport. Under the highest waves of a wave group, sediment is stirred up. Under the highest waves of a group, however, the bound infragravity wave produces an offshore directed low-frequency orbital velocity, so that the stirred up sediment will be transported offshore as well. With this mechanism, infragravity waves can cause offshore suspended sediment transport (Green & MacDonald, 2001)

As with waves, wind-induced currents can have a significant effect on sediment transport in tidal inlets (Elias & van der Spek, 2006; Elias et al., 2006; Green & MacDonald, 2001). The same holds for river outflow in estuaries (Siegle, Huntley, & Davidson, 2004).

Factors which are mostly caused by tidal currents often play a role in the concentration and distribution of suspended sediment, of which the settling and scour lag mechanisms are the most important. When flow velocities fall below the threshold for keeping sediment in suspension, the sediment is not deposited at that precise location, but travels further with the still flowing water. This is called the settling lag. Because the picking up of sediment takes a higher flow velocity than is needed to keep it in suspension, the parcel of water that carried the sediment grain initially will not pick it up after the turn of the tide, but a parcel of water from a more landward location will do this. This delay due to the difference in the location of water parcels that pick up the sediment is called scour lag. Settling and scour lag together always cause net landward transport of fine suspended sediment.

2.4 Bedload sediment transport

When bed shear stresses are high enough, sediment on the bed are transported with the flow. When transport is only just possible, it takes place along a flat bed. However, increased flow velocities and shear stresses cause the formation of bedforms. Sediment is then transported over the stoss side of the bedform and deposited in the trough, at the leeside. As a consequence, the bedform as a whole migrates in the dominant transport direction. This offers a way of calculating bedload transport: the migration of the bedforms equals the net bedload transport.

2.4.1 Bedforms in intertidal and subtidal areas

Bedforms in intertidal and subtidal areas have been less intensively investigated than bedforms in rivers. In contrast with rivers, flow in tidal areas is bidirectional, or even

multi-directional, which highly complicates the formation and behaviour of bedforms. Due to a large variability in flow velocity and water depth in tidal areas, a large variety of bedforms is reported. A distinction can be made between bedforms in intertidal areas and bedforms in subtidal environments, since bedforms in subtidal environments generally have much larger lengths and heights than those in intertidal environments.

In subtidal areas bedforms develop when tidal flow velocities are high enough to induce bedload sediment transport. Because in subtidal areas water depth is only very seldom a limiting factor, bedforms can reach considerable lengths and heights of tens of meters and meters, respectively (e.g. (Anthony & Leth, 2002; Buijsman & Ridderinkhof, 2008a; Buijsman & Ridderinkhof, 2008b; Kotaschuk & Best, 2005).

Intertidal areas where bedforms occur are mostly sand flats on ebb tidal deltas or shoals in inlets of tidal basins or estuaries. When these intertidal areas are submerged, water depths are much less than in subtidal areas and are mainly determined by the tidal range. Bedforms have typical lengths in the order of meters, while heights are in the order of decimetres (e.g. (Allen et al., 1994; Hawkins & Sebbage, 1972).

Bedforms in subtidal areas are in general much larger than bedforms in intertidal areas, due to larger water depths. This general rule is, however, not applicable for the prediction of bedform dimensions, because on a more detailed level water depth and bedform dimension show no correlation (Bartholdy, Bartholomae, & Flemming, 2002). For specific cases, other factors such as grain size, flow velocities and bed shear stress have a more important influence on dune dimensions than water depth (e.g. (Ernstsen et al., 2005; Kotaschuk & Best, 2005; Masselink et al., 2009). In the case of the Slufter, with a subtidal environment and limited water levels, dunes with heights of decimetres and lengths of meters are the dominant bedforms which are expected to be found.

2.4.2 Bedload transport calculation

Bedload transport is calculated from measured dune parameters (celerity, height and length). The transports obtained with this dune tracking technique can be compared with models for the calculation of bedload transport. Below the dune tracking technique is outlined, which is based on field measurements on dunes, followed by several transport

formulae, which are based on measurements of hydrodynamic processes (flow velocity, water depth) and sediment characteristics.

Dune tracking technique

The technique of dune tracking is quite often applied in rivers, where unidirectional flow leaves no doubt about sediment transport direction. In coastal environments, however, flow is bidirectional or even multidirectional and there is more than one direction of sediment transport. When tidal flow is stronger during a particular phase of the tide, the bedforms will propagate in the direction with the largest flow velocity. Calculating bedload transport with the help of the migration rates of these dominant bedforms then is a good way of estimating net bedload sediment transport.

Hoekstra et al. (2004) used the conservation of sediment mass and the kinetic equation to calculate mean sediment transport rates. The methods were derived from different authors who applied these formulas mainly in rivers (Engel & Lau, 1980; Jinchi, 1992; Ten Brinke, Wilbers, & Wesseling, 1999). Only Van den Berg (1987) used these formulas in tidal environments. The time-averaged bedload transport ($\overline{q_b}$) per unit meter width (m²/s) can be calculated with:

$$\overline{q_b} = cfH \qquad (2.1)$$

in which c is the celerity of the bedforms (m/s), H is the bedform height (m), $f = V / H\lambda$ is the dimensionless form or shape factor, λ is the bedform length and V is the bedform volume per unit width (m²). A number of other processes influence bedload transport and thus alter the equation (3.1), but these factors appear to cancel each other out. Equation (3.1) therefore gives a good estimation of time-averaged bedload transport (Hoekstra et al., 2004).

Bagnold

Bagnold (1966, from van Rijn (1993)) assumed that the bedload transport is a result of the total available kinetic energy in the fluid times an efficiency factor e_b. Bedload transport can then be calculated with:

$$q_{b,c} = \frac{e_b \tau_b \bar{u}}{(\rho_s - \rho) g \cos\beta (\tan\phi - \tan\beta)} \quad (2.2)$$

In which:

$q_{b,c}$	Volumetric bedload transport (m^2/s)
τ_b	Overall bed-shear stress (N/m^2)
$\bar{u}$	Depth-averaged velocity (m/s)
e_b	Efficiency factor (0.1-0.2)
$\tan\phi$	Dynamic friction coefficient (-)
$\tan\beta = I_b$	Bed slope (-)
h	Water depth (m)
g	Acceleration of gravity (m/s^2)

Since the bed slope β is very small, tan β nears zero and cos β nears one, so eq (2.2) is simplified to

$$q_{b,c} = \frac{e_b \tau_b \bar{u}}{(\rho_s - \rho) g \tan\phi} \quad (2.3)$$

Bailard

Using the efficiency factor Bagnold (1966) introduced, Bailard (1981) derived another transport model, in which both wave orbital velocities and depth averaged current velocities are taken into account. For a flat bed, it reads as (Bailard (1981), from Camenen and Larroudé (2003)):

$$q_b = \left(\frac{0.5 f_{cw}}{g(s-1)}\right)\left(\frac{e_b}{\tan\phi}\left\langle |\vec{u}|^2 u \right\rangle\right) \quad (2.4)$$

u represents the instantaneous velocity vector, $\vec{u} = \bar{u} + \vec{u}_w$, $\bar{u}$: depth-averaged velocity and u_w instantaneous wave orbital velocity. $\langle\ \rangle$ stands for the average value over several periods of the wave. Since no waves enter the inlet (see paragraph 6.3), wave orbital velocities do not have to be taken into account and Bailard's formula can be simplified to:

$$q_b = \left(\frac{0.5 f_{cw}}{g(s-1)} \right) \left(\frac{e_b}{\tan\phi} \bar{u}^3 \right) \tag{2.5}$$

In which:

q_b	Volumetric bedload transport (m^2/s)
$f_{c,w}$	Friction coefficient due to waves and currents
g	Acceleration of gravity (m/s^2)
$s = \rho_s / \rho$	Relative density (-)
ρ_s	Sediment density (kg/m^3)
ρ	Fluid density (kg/m^3)
$\bar{u}$	Depth-averaged velocity (m/s)
e_b	Efficiency factor (0.1)

For the friction coefficient, Soulsby's (1997) method is used (from Camenen and Larroudé (2003)):

$$f_{c,w} = \frac{\tau_{cw,\max}}{0.5\rho \left\langle |\vec{u}|^2 \right\rangle} \tag{2.6}$$

Where the subscripts c and w represent currents and waves, respectively. However, since no waves enter the Slufter inlet channel, bed shear stress due to waves has not been taken into account. Using the above reasoning for wave orbital velocities, the equation for friction coefficient can be simplified to:

$$f_c = \frac{\tau_b}{0.5\rho\bar{u}^2} \quad (2.7)$$

In which τ_b represents overall bed shear stress (N/m²).

Van Rijn

Van Rijn (1984, from van Rijn (1993)) assumed that het motion of the bedload particles is dominated by saltation under the influence of hydrodynamic fluid forces and gravity forces. The bedload transport rate is believed to be the product of particle velocity ($\bar{u}_b$ in m/s), the saltation height (δ_b in m) and bedload concentration (c_b, dimensionless). From 130 flume experiments, van Rijn (1984, from van Rijn (1993)) concluded that the bedload transport rate for particles in the range of 200 to 2000 μm can be computed with:

$$q_{b,c} = 0.053\sqrt{s-1}\sqrt{g}\,d_{50}^{1.5} D_*^{-0.3} T^{2.1} \quad (2.8)$$

In which:

$q_{b,c}$	Volumetric bedload transport rate (m^2/s)
$T = (\tau'_{b,c} - \tau_{b,cr}) / \tau_{b,cr}$	Dimensionless bed-shear parameter
$\tau'_{b,c} = \rho g(\bar{u} / C')^2$	Effective bed-shear stress (N/m^2)
$C' = 18\log(12h / 3d_{90})$	Grain-related Chézy coefficient ($m^{1/2}/s$)
h	Water depth (m)
d_{50}, d_{90}	Particle diameters (m)
$\bar{u}$	Depth-averaged velocity (m/s)
$\tau_{b,cr}$	Critical bed-shear stress (N/m^2)
$D_* = d_{50}[(s-1)g / \nu^2]^{1/3}$	Dimensionless particle diameter
$s = \rho_s / \rho$	Relative density (-)
ρ_s	Sediment density (kg/m^3)

ρ	Fluid density (kg/m^3)
ν	Kinematic viscosity coefficient (m^2/s)
g	Acceleration of gravity (m/s^2)

Eq (3.8) was found to overpredict the transport rates for T≥3. Therefore, a modified expression is proposed for this range:

$$q_{b,c} = 0.1\sqrt{s-1}\sqrt{g}\,d_{50}{}^{1.5} D_*^{-0.3} T^{1.5} \quad \text{for T}\geq 3 \qquad (2.9)$$

2.4.3 Bed shear stress

The Bagnold (1966) as well as the Bailard (1981) sediment transport calculations use bed shear stress τ_b as a measure of roughness of the bed. For rivers with steady uniform flow, this bed shear stress is computed with the help of the water level gradient, but this is not applicable to the acceleration and multidirectional flow of the Slufter. Kim et al (2000) proposed four different methods to determine bed shear stress in marine environments using ADV measurements. Although each method had its own drawbacks, the TKE method is considered to be a very robust and reliable one (Kim et al., 2000; Thompson et al., 2003; Dyer et al., 2004, last two from Pope et al., 2006). Also, the other three methods proposed by Kim et al. (2000) used assumptions and extra information about instrument build-up which could not be met or obtained in the case of the Slufter.

The TKE factor is computed as follows:

$$TKE = \frac{1}{2}\rho\left(\overline{u'^2} + \overline{v'^2} + \overline{w'^2}\right) \qquad (2.10)$$

The flow velocity is composed of an average value and a fluctuation part. The variance of the fluctuating part is used as a measure for turbulence and thus bed shear stress. u', v' and w' represent the fluctuating part of total flow in the alongchannel, crosschannel and vertical direction, respectively.

Bed shear stress is assumed to be linearly related to the TKE factor:

$$\tau_b = C_1 TKE \qquad (2.11)$$

In which C_1 is a proportionality constant. Values for C_1 of 0.19 and 0.20 have been proposed (Kim et al., 2000 and Pope et al., 2006), in this study a value of 0.20 is adopted.

2.5 Suspended load sediment transport

Suspended sediment transport can make up an important fraction of total sediment transport in flows and is sometimes even considered to be the only significant way of sediment transport in tidal inlets (van de Kreeke & Hibma, 2005). When the flow becomes sufficiently strong, sediment is taken up in the flow and remains there in suspension. When flow velocities decrease again, suspended sediment can fall out of the fluid to the bed. The amount of suspended sediment in the flow is not linearly related to flow velocities, but related to a third or fifth power (van Rijn, 1993).

In tidal environments, the concentration of suspended sediment in the water is very much dependent on the stage of the tide. During slack, suspended sediment falls out of the water, whilst during maximum ebb- or flood flow the sediment concentration is higher. When coastal environments are ebb- or flood dominated, this domination becomes even more pronounced in the suspended sediment load due to the non-linearity between flow and sediment concentrations.

2.5.1 Mixtures of sand and mud in suspension

In coastal and tidal environments, two types of suspended sediment are observed: fine sand and mud. The concentration of fine sand is mostly dependent on flow velocity; a decrease in flow velocity causes sand to deposit quickly. Mud, on the contrary, has a very low fall velocity and concentrations can lag behind changes in flow velocities.

Mud transport is very difficult to capture in formula's. All kinds of complications occur which are extremely difficult to model. Examples of these complications are lags in

deposition and erosion (settling lag and scour lag), flocculation and aggregation of sediment particles, biological activity influencing flocculation and settling and different transport characteristics for different salinity. Sand in suspension can be calculated with the help of suspended sediment transport formulas (e.g. (Bagnold, 1966; van Rijn, 1984).
To even further complicate things, the measurement of a mixture of suspended sand and mud is also very difficult due to calibration problems with the two different kinds of sediment in suspension. Most measurement instruments are very sensitive to the grainsize of the suspended sediment. Some sensors are only suitable for measuring sand in suspension, or they are only suitable for measuring mud in suspension. When one grainsize is dominant, or a mixture is present that does not change in composition, instruments can be calibrated. However, when the composition of sand/mud mixtures changes through time, calibration of instruments becomes practically impossible.

2.5.2 Suspended load calculations

Suspended sediment transport is calculated using different methods for comparison with fluxes based on measured velocities and observed OBS values. The calibration method for the OBS is outlined in paragraph 3.3.3. Below the different calculation methods for the suspended sediment transport are given.

Bagnold

As is outlined in paragraph 2.4.2, Bagnold (1966) assumed that the bedload transport is a result of the total available fluid energy times an efficiency factor e_b. For suspended load transport, the same holds: the transport rate is a result of the total available fluid energy minus the energy used for bedload transport, times an efficiency factor for suspended load e_s. The equation for suspended load transport thus yields:

$$q_{s,c} = \frac{e_s\left(1-e_b\right)\tau_b\bar{u}}{\left(\rho_s-\rho\right)g\cos\beta\left(\left(w_s/\bar{u}\right)-\tan\beta\right)} \qquad (2.12)$$

In which:

$q_{s,c}$	Volumetric bedload transport (m^2/s)
τ_b	Overall bed-shear stress (N/m^2)
$\bar{u}$	Depth-averaged velocity (m/s)
e_b	Efficiency factor for bedload (0.1to 0.2)
e_s	Efficiency factor for suspended load (0.1 to 0.2)
w_s	Fall velocity of sediment (m/s)
β	Bed slope (-)
h	Water depth (m)
g	Acceleration of gravity (m/s^2)

Since the bed slope β is very small, tan β nears zero and cos β nears one, eq (3.12) is simplified to

$$q_{s,c} = \frac{e_s\left(1-e_b\right)\tau_b\bar{u}}{\left(\rho_s-\rho\right)g\left(w_s/\bar{u}\right)} \qquad (2.13)$$

Bailard

The suspended load transport formula by Bailard (1981) is similar to the bedload transport formula and again based on the efficiency factor principle introduced by Bagnold (1966). The suspended load transport on a flat bed is written as (Bailard, 1981, from Camenen and Larroudé, 2003):

$$q_s = \left(\frac{0.5 f_{cw}}{g(s-1)}\right)\left(\frac{e_s}{w_s}\left\langle|\vec{u}|^3 u\right\rangle\right) \qquad (2.14)$$

Which, similar to the bedload transport calculations, can be simplified to:

$$q_s = \left(\frac{0.5 f_c}{g(s-1)} \right) \left(\frac{e_s}{w_s} \bar{u}^4 \right) \quad (2.15)$$

In which:

q_s	Volumetric bedload transport (m^2/s)
f_c	Friction coefficient
g	Acceleration of gravity (m/s^2)
$s = \rho_s / \rho$	Relative density (-)
ρ_s	Sediment density (kg/m^3)
ρ	Fluid density (kg/m^3)
$\bar{u}$	Depth-averaged velocity (m/s)
e_s	Efficiency factor (0.02)

For the calculation of the friction coefficient, see paragraph 2.4.2.

Van Rijn

According to van Rijn (1984b), the suspended load transport in m^2/s can be computed with:

$$q_{s,c} = F \bar{u} h c_a \quad (2.16)$$

In which:

$c_a = 0.015 \frac{d_{50}}{a} \frac{T^{1.5}}{D_*^{0.3}}$	Reference concentration at height a above the bed (-)
$F = \frac{(a/h)^{Z'} - (a/h)^{1.2}}{(1-a/h)^{Z'}(1.2-Z')}$	Shape factor of suspended sediment distribution in the vertical(-)

$$D_* = \left[\frac{(s-1)g}{\nu^2}\right]^{1/3} d_{50}$$ Particle parameter (-)

$$T = \frac{\tau'_b - \tau_{b,cr}}{\tau_{b,cr}}$$ Bed-shear stress parameter (-)

$$\tau'_b = \rho g\left(\frac{\bar{u}}{C'}\right)^2$$ Current-related effective bed-shear stress (N/m^2)

$$u_* = \frac{\sqrt{g}}{C}\bar{u}$$ Current-related overall bed-shear velocity (m/s)

$$C' = 18\log\left(\frac{12h}{3d_{90}}\right)$$ Grain-related Chézy coefficient (m$^{0.5}$/s)

$$C = 18\log\left(\frac{12h}{k_s}\right)$$ Overall Chézy coefficient (m$^{0.5}$/s)

$$\tau_{b,cr} = (\rho_s - \rho) g d_{50} \theta_{cr}$$ Critical bed-shear stress (N/m^2) according to Shields

$$Z' = Z + \psi$$ Suspension number (-)

$$Z = \frac{w_s}{\beta\kappa u_*}$$ Suspension number (-)

$$\psi = 2.5\left(\frac{w_s}{u_*}\right)^{0.8}\left(\frac{c_a}{c_0}\right)^{0.4}$$ Stratification correction

$$\beta = 1 + 2\left(\frac{w_s}{u_*}\right)^2$$ Ratio of sediment and fluid mixing coefficient ($\beta_{max} = 2$)

$q_{s,c}$	Volumetric current-related suspended load transport (m^2/s)
$\bar{u}$	Depth-averaged velocity (m/s)
h	Water depth (m)
a	Reference level (m), $a = \frac{1}{2}\Delta$ or a=k$_s$
k_s	Overall roughness height (m)
Δ	Bed form height (m)
d_{50}	Median particle diameter of bed material (m)
d_{16}, d_{84}, d_{90}	Characteristic diameter of bed material (m)

w_s	Fall velocity of suspended sediment (m/s)
c_0	Maximum relative concentration (=0.65)
s	Specific density (= ρ_s / ρ)
ρ_s	Sediment density (=2650 kg/m^3)
ρ	Fluid density (=1025 kg/m^3)
ν	Kinematic viscosity coefficient (m^2/s)
κ	Constant of Von Karman (= 0.4)
g	Acceleration of gravity (m/s^2)

2.5.3 Concentration profiles

Suspended sediment concentrations decrease with increasing height from the bed and concentration profiles can be calculated. Since low concentrations (c<10 kg/m^3) are assumed, hindered settling and turbulence damping effects are neglected.

Concentration is assumed to have a parabolic profile in the lower half of the water column and a linear profile in the upper half of the water colum. Concentration is expressed as (van Rijn, 1993):

$$c = c_a \left(\frac{h-z}{z} \frac{a}{h-a} \right)^Z \qquad \text{for } \frac{z}{h} < 0.5 \qquad (2.17)$$

$$c = c_a \left(\frac{a}{h-a} \right)^Z e^{-4Z(z/h-0.5)} \qquad \text{for } \frac{z}{h} \geq 0.5$$

In which:

c	Concentration at height z above the mean bed level (kg/m^3)
c_a	Reference concentration at height z=a above bed (-)
h	Water depth (m)
w_s	Fall velocity in clear water (m/s)
u_*	Bed-shear velocity (m/s)
β	Ratio of sediment and fluid mixing coefficient ($\beta_{\max} = 2$)

z Height above bed (m)

The parameter Z is termed the suspension number:

$$Z = \frac{w_s}{\beta \kappa u_*} \tag{2.18}$$

3 Measurement campaign and data analysis

From September 15 to November 1 2009, a field campaign has been carried out in the Slufter inlet area. Measurements have been carried out in the inlet with a large triangular frame and on the beach with one large an three small frames. For a detailed description of the instrument setup and measurement results of the beach measurements, see Witteveen (2010), de Vries (2010) and Brockhus (2010). Below a description of the fieldwork location and instrument setup in the Slufter inlet is given.

3.1 Required measurements and instrument set-up

In order to answer the research questions stated in paragraph 1.2, the following parameters have been measured:

- Flow velocity in the inlet
- Water level, wave height and period
- Bed level elevation, including shape and dimensions of bedforms
- Suspended sediment concentration
- Channel morphology

The instrument setup in the Slufter inlet consisted of a triangular frame with sides of three meters, with three Acoustic Doppler Velocimeters (ADV) for measuring flow velocity, three Optical Backscatter Sensors (OBS) for measuring suspended sediment concentrations and a wave gauge for measuring water levels and water depths (Photograph 3.1). Attached to the OBS's were plastic tubes which were used for pumping of water samples.

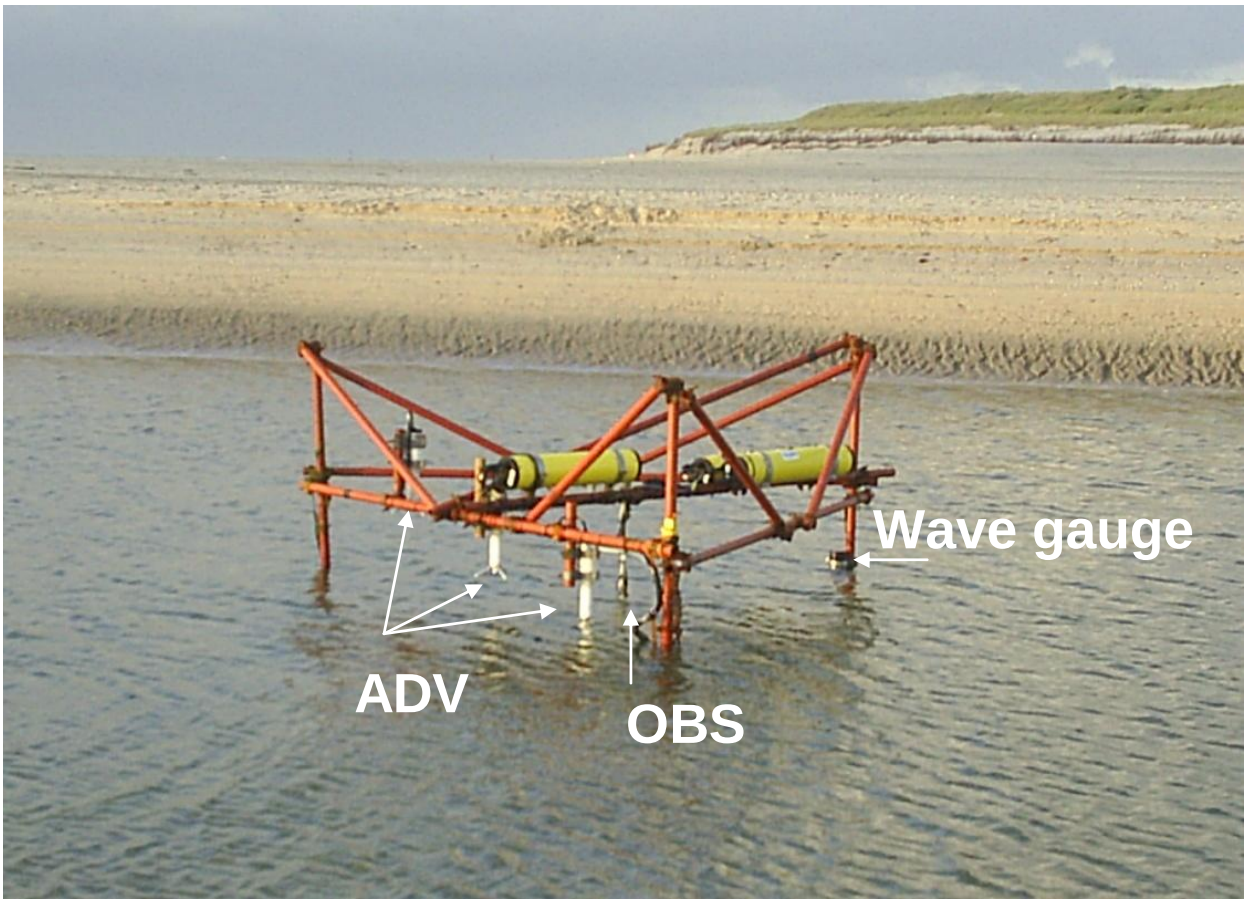

Photograph 3.1 The frame in the Slufter inlet. The different instruments mounted on the frame are pointed out.

The instrument frame was located at the deepest part of the channel, where water depths around low water level were still 1 to 1.5 m. The frame was placed as far north in the channel as possible, to prevent burial by sediment due to northward channel migration.
The three ADV's had a spatial interval of 0.5 m, which gives a total measurement section of 1 m, which was considered sufficient to measure the migration of the bedforms which had lengths in the order of meters. The ADVs were placed in the alongchannel direction because no variation in bedforms in crosschannel direction was expected. The lowest and the middle ADV had a vertical distance of 0.18 m, the middle and the highest ADV of 0.23 m. During low tide, only the lowest ADV was submerged. The OBS's were mounted on the frame at the same heights and with the same vertical distance as the ADV's, but it should be noted that the measurement volume of the ADVs lies twenty centimetre below

the instrument itself. The wave gauge was mounted so that it was permanently submerged.
The channel showed a continuous migration towards the north, which caused a relative shift of the frame to the south of the channel. During a storm, migration rates were so high that the frame was located at the southern bank of the channel after the storm. Relocation was necessary and the frame was again placed as far north as possible, at the deepest part of the channel. After relocation, absolute heights of the ADV's relative to NAP (Dutch ordnance level) did not change. Also the distance between the ADV's remained the same. The OBS's were now placed 20 cm deeper than the ADVs, to be at the same height as the measurement volume of the ADV.

Data cables from the instrument package were connected to a pole at the southern channel bank to facilitate daily data-retrieval. The wave gauge data was obtained every two weeks, during the service checks and replacement of batteries.

Channel morphology has been measured with the help of a Differential Global Positioning System (DGPS) and a leveling instrument. Three times during the field campaign, on September 19, October 15 and October 31, cross sections through the channel have been determined.

3.2 Instruments

3.2.1 ADV

An Acoustic Doppler Velocimeter (ADV) obtains flow velocities by measuring the Doppler shift of acoustic signals. The ADV sends a high-frequency sound signal (transmit beam) which is reflected by suspended particles in the water column and caught by the receive beam. The movement of these suspended particles causes a Doppler shift in the return signal, from which the absolute flow velocity is calculated. Fifty measurements per second are made, but flow velocities are averaged over a few measurements to a lower output frequency, for example 4 Hz. Three receivers of the ADV measure flow velocities, resulting in an output in x-, y- and z-direction (Figure 3.1).

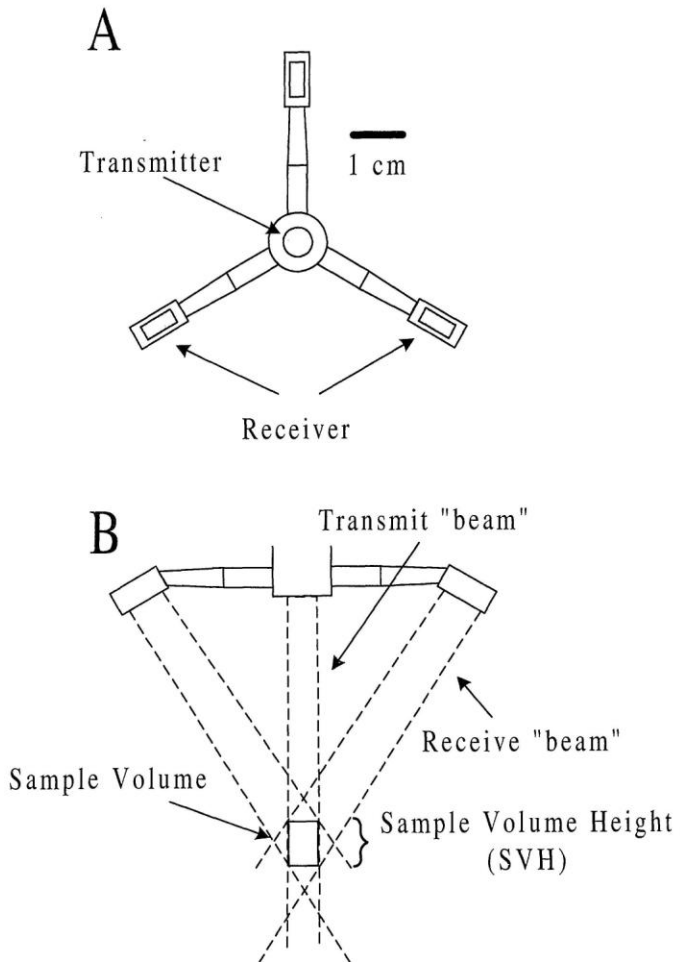

Figure 3.1(A) Bottom view of the ADV probe showing the locations of the central transmitter and three acoustic receivers. (B) Side view showing acoustic transmit and receive 'beams' and the approximate position and height of the sample volume. From (Finelli, Hart, & Fonseca, 1999)

In general, the flow velocity measurements of an ADV are quite accurate, but performance near the bottom can be very poor, because the water volume over which the actual measurement takes place is larger than described by the producer, while velocity gradients near the bed are also larger than higher up in the water column (Elgar, Raubenheimer, & Guza, 2005; Finelli et al., 1999; Huettel, Precht, & Janssen, 2006). Other factors that can influence velocity measurements are air bubbles (Mori, Suzuki, & Kakuno, 2007), lack of submergence, biofouling or blockage (Elgar et al., 2005). Bubbles and a lack of submergence will mostly be present under breaking waves and are thus of minor importance for research in the Slufter inlet. Biofouling and blockage by seaweed however occurred often, especially in high energetic conditions. The ADV's have to be

deployed with care; if they are located too close to the bed, there will be a large negative effect on measured flow velocities.
The ADV measures the distance to the bed at the beginning of each measurement burst. These measurements will be used for dune tracking analysis and thus the height of the ADV with respect to NAP and the relative vertical and horizontal distance between the ADV's must be exactly known. ADV's give quality information about the data they produce, with which spikes or bad bursts can be recognized and removed.
The measurement frequency of the ADV should be chosen such that a reliable flow velocity (i.e. low measurement frequency) and reliable wave characteristics (i.e. high measurement frequency) could be obtained. Measurement bursts should be sufficiently long to be able to measure a tidal signal, but a frequent measurement of bed level was required to be able to track migrating dunes. Taking these arguments into account, the measurement frequency of the ADV's was set at 4 Hz, the burst length was set at 10 minutes.

The ADV data is processed with the help of a Matlab routine. When flow velocities exceed the measurement range of the ADV, data also has to be processed by hand to avoid erroneous results.

3.2.2 OBS

An Optical Backscatter Sensor (OBS) is used for measuring suspended sediment concentrations in flowing water. The OBS sends an infrared light-signal and measures the amount of backscatter from the sediment in suspension. Each type of sediment and each specific grain size has its own backscatter properties, which means that the OBS needs to be calibrated for every location at which it measures. Since the OBS is designed for measuring either sand or mud in suspension, extra calibrations have to be performed for the slufter inlet, where sand/mud mixtures are common.
Factors that can influence the quality of OBS measurements are air bubbles and the growth of particularly Sessilia (*Semibalanus balanoides)* on the smooth surface.

When only sand is in suspension and thus measured, a laboratory calibration with local sand from the field site is sufficient. However, for calibration of sand/mud mixtures, OBS ouput (in counts) has to be compared with real sediment concentrations, measured from water samples. Therefore, water samples of Slufter water have been taken with a pump. Each sample contained approximately 0.5 L water. In the ideal case, the water is pumped out of the channel with the same velocity as the flow velocity of that moment. However, only one pump speed could be used. The pumping rate was approximately 0.01 L/s, corresponding to a velocity of 0.8 m/s.

Since ADV and OBS data were processed by the field measurement software at the same time, the OBS output was the same as the ADV output: 4 Hz in bursts of 10 minutes.

3.2.3 Wave gauge

Water level, wave height and wave period was measured using a 5 Hz wave gauge. The gauge itself measures pressure, which is recalculated to water level relative to NAP using

$$H_w = \frac{p_{meas} - p_{air}}{\rho g} + H_s \qquad (3.1)$$

In which:

H_w = water level relative to NAP (m)

p_{meas} = measured pressure (Pa)

p_{air} = air pressure (Pa)

ρ = density of (sea)water (kg/m^3)

g = acceleration of gravity (m/s^2)

H_s = height of gauge relative to NAP (m)

Air pressure was measured with a small air pressure station at a ten minute interval.

3.2.4 DGPS and levelling instrument

A Differential Global Positioning System (DGPS) system works similar with ordinary GPS systems, i.e. they measure location and height with the help of satellites. The main

difference is that a DGPS uses a ground station of which the spatial coordinates, including height, are very precisely known. The difference between the ground station coordinates and the coordinates obtained by the satellites is calculated. This difference is assumed to be the same for the mobile GPS receiver which is used in the field. With this difference, the real coordinates of the mobile GPS receiver are calculated with a horizontal precision of 1 cm and a vertical precision of 5 cm.
At locations where the use of the DGPS system was impossible due to large water depths, a levelling instrument was used. Coordinates were measured from a known point, measured with the DGPS. With a beacon, heights and distances with respect to this known point were measured.

3.3 Data analysis methodology

3.3.1 Fourier analysis

In order to determine the presence of waves in the channel and on the beach, a Fourier analysis was performed on measurements of water depth.
With Fourier analysis, a dataset is split in a large number of individual sines. The more dominant a frequency is in the original dataset, the higher the spectral density in the analysis. In a formula this can be represented as follows:

$$X = a_0 + \sum_{p=1}^{(N/2)-1} \left[a_p \cos\left(2\pi pt / N\right) + b_p \sin\left(2\pi pt / N\right) \right] + a_{N/2} \cos\left(\pi t\right) \qquad (3.2)$$

In which:

$t = 1...N$	Datapoint
$p = 1...\left(N/2\right)-1$	Amount of frequencies to fit
$a = 0...(N/2)$	Coefficient
$b = 0...\left(N/2\right); b_0 = 0$	Coefficient

The amplitudes of the individual waves is given by:

$$R_p = \sqrt{a_p^2 + b_p^2} \tag{3.3}$$

The phase of each wave is given by:

$$\theta_p = \tan^{-1}\left(-b_p / a_p\right) \tag{3.4}$$

In order to improve the confidence of the spectrum, the used dataset can be divided in blocks with 50% overlap. A spectrum is then computed for each block, after which the average for all spectra is regarded as the best spectrum for the whole dataset:

$$\overline{G}(f) = \frac{1}{N_{blocks}} \sum_{i=1}^{N_{blocks}} G_i(f) \tag{3.5}$$

The drawback of this increased confidence is a lower frequency resolution; i.e. the spectrum is calculated for less individual frequencies.

Before analysis, a Hamming filter is applied on the data to make it fit for Fourier analysis. This so called windowing transforms the data so that the beginning and the end of the dataset near zero.

3.3.2 Analysis of bed level measurements

Bed level is measured by the ADV's as a distance below the instrument. When the heights of the instrument relative to NAP (Dutch Ordnance Level) was known, bed level measurements were re-calculated to height relative to NAP. When the height of the instruments was not exactly known, it was assumed that the relative distance of the ADV's with respect to each other did not change through time. This still made it possible to observe relative bed level changes under the three ADV's and to determine bed slope and bedform dimensions.

When bedform dimensions were determined from the bed level measurements, bedload transport was calculated using Hoekstra's method (Hoekstra, 2004. See paragraph 2.4.2).

3.3.3 Calibration of OBS measurements

Output of the Optical Backscatter Sensors (OBS) is given in counts. For conversion to grams per litre, two calibrations have to be performed:

1) an internal calibration to convert the output in counts to an output in millivolts. This calibration gives a good and reliable outcome.
2) A calibration in the laboratory from millivolts to grams per litre. For this calibration, samples are prepared with well-defined concentrations and measured with the OBS. Performing these measurements for different sediment concentrations, a second order regression line is found. This calibration has been carried out with local sediment from the bed.

For sand in suspension, the above regression method works well and can be directly applied. However, since OBS measurements are very sensitive to grain size distributions, the second calibration step cannot be directly applied with just sand samples, since there is also mud in suspension. This mixed composition makes calibration with a sample containing just sand useless.
For comparison of the OBS measurements, the measurements were first recalculated to concentrations using the sand-calibration curve (step two in the above calibration procedure). These calculated concentrations were then compared with real concentration measurements from water samples. First, water samples were filtered and the residue was dried to remove all water. Then the samples were weighed and the sediment concentration in grams per litre was calculated. These concentrations were compared with OBS measurements (recalculated to mg/L) from exactly the same time interval as the samples were taken. The comparison was used to obtain a new calibration curve for the sand/mud mixtures found in the Slufter inlet.

4 General overview of conditions during fieldwork period.

During the fieldwork period different weather conditions occurred, which caused different boundary conditions for the Slufter inlet channel.

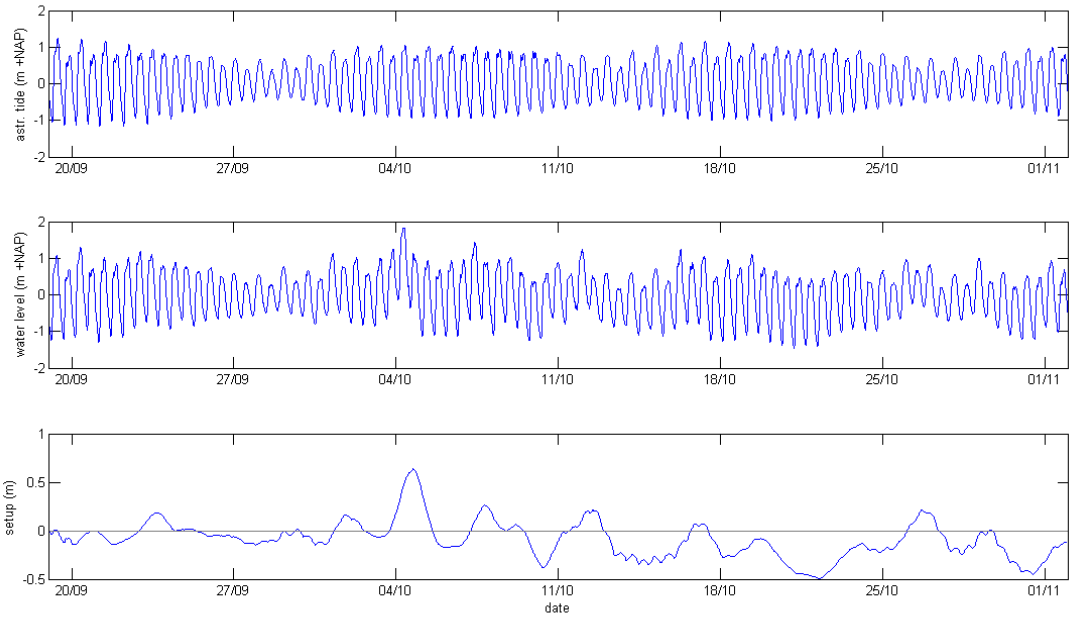

Figure 4.1 Water level offshore the Texel coastline. Top: astronomical tide, center: real tidal signal, bottom: setup. Source: Rijkswaterstaat

The tidal range offshore the coast of Texel varies from 1 m at neap tide to 2 m at spring tide. However, winds can significantly alter the real water level with respect to the astronomical tide (Figure 4.1). During the course of the fieldwork, a storm hit the coast at October 4. This can be recognized in the water levels and the large setup that day. The coincidence of a large setup due to storm and spring tidal conditions caused the flooding of the entire beach plane between the two dune rows at the Texel inlet.

From offshore wave records can be seen that the maximum offshore significant wave height during the storm was 4 m, but this was not the maximum recorded wave height during the fieldwork, which was 6 m at October 17 (Figure 4.2). Although wave heights

were large from October 16 to 18, the beach flat was not inundated because of the northern wind, which generates not a high setup. The western winds of October 3 and 4 however, did generate a high setup. Due to the lack of setup, the high wave event of October 16 and 17 will not be classified as a storm.

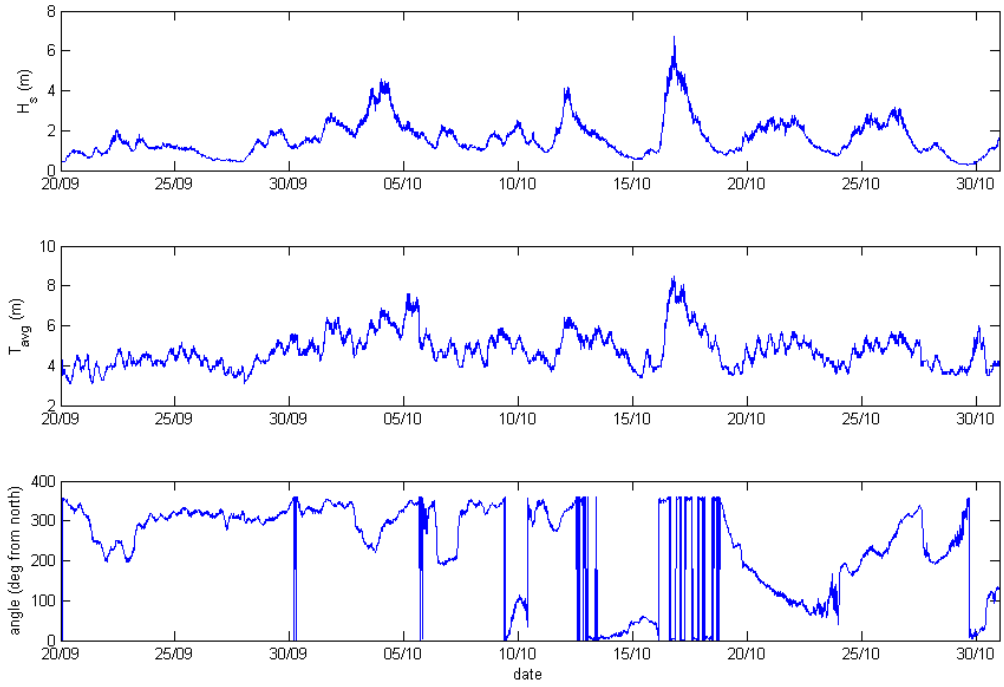

Figure 4.2 Wave characteristics offshore the Texel coastline. A) Significant wave height, B) average wave period, C) incoming wave angle. Source: Rijkswaterstaat

The different conditions which occurred at sea during the fieldwork are very well reflected in the water depth and flow velocity recordings in the Slufter inlet itself. During the storm on October 4, water levels in the channel increased to a value of more than 2.5 m above NAP (Figure 4.3). This water level is higher than the one measured offshore, due to additional wind setup and wave setup near the coast. High water levels coincide with large flow velocities, of which the storm event is the best example. However, also for example from October 16 to 18, increased water levels in the inlet coincided with higher flow velocities. The dominant mechanism behind this correlation is simple: the higher the water level, the more water flows in and out of the Slufter system in a given amount of time and thus the higher the flow velocities.

From the flow velocity record it can be seen that from October 20 on, calm weather prevailed (Figure 4.3) with low flow velocities.

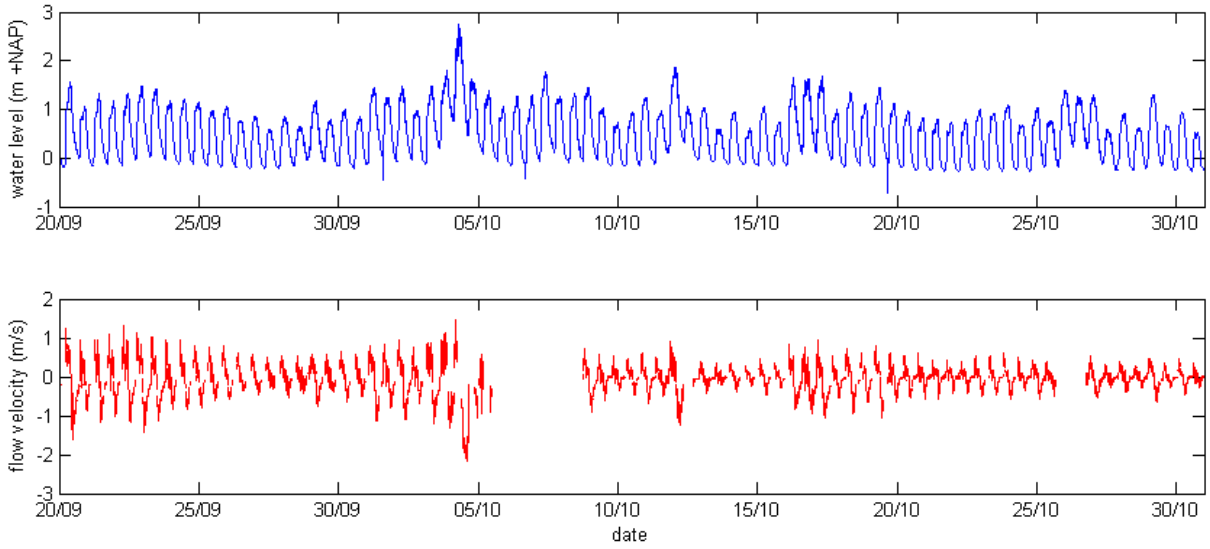

Figure 4.3 Overview of conditions in the inlet during the fieldwork period. A) water level in the channel, B) flow velocity in the channel, as measured by ADV2. The gap in the data after October 5 reflects the submergence of the ADV in the channel bank, so no flow could be measured. The gap just after October 25 reflects empty batteries.

5 Channel morphology and bedforms

5.1 location and migration of inlet channel

Due to a relocation of the inlet in the summer of 2009, the location of the channel during the fieldwork was approximately in the centre of the gap between the two dunes (Figure 5.1). A photo mosaic made on September 18 gives a good overview of the situation at the beginning of the fieldwork. Ten cross sections have been defined through the channel to monitor channel migration during the fieldwork (Figure 5.2). Section 6 is defined along the measurement frame, sections 7 up to 10 are located more seaward, sections 1 up to 5 more landward to get a good idea of channel migration at different locations.

Figure 5.1 The location of the Slufter inlet channel with respect to the dunes. Light blue line: location summer 2009; dark blue line: location during fieldwork period.

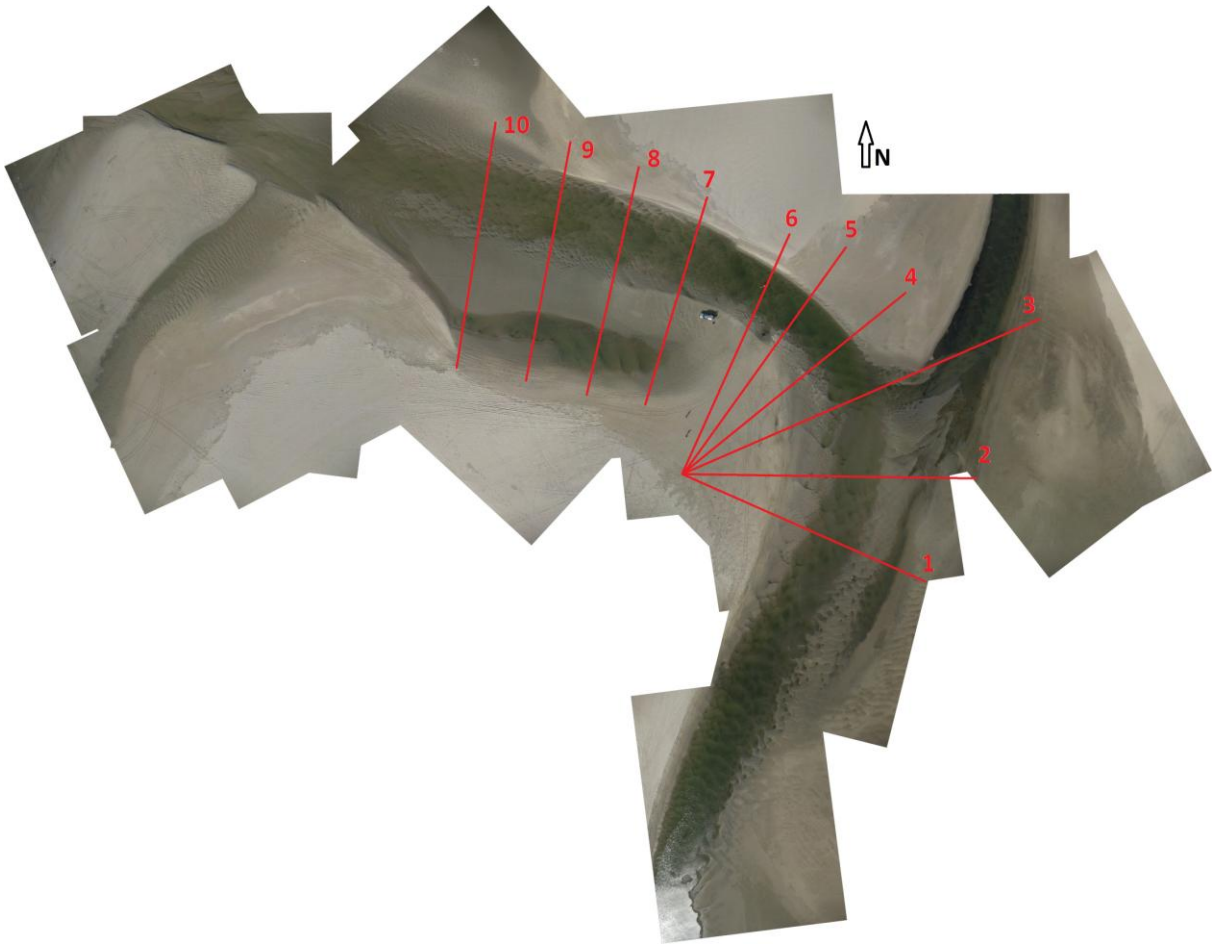

Figure 5.2 A compilation of different aerial photographs of the Slufter inlet channel. The red lines represent the ten cross sections which have been defined in the channel.

The migration of the Slufter inlet channel has been monitored with DGPS measurements. Several cross sections have been defined (Figure 5.2) and cross sectional profiles have been measured on three moments: before the storm, at the beginning of the fieldwork campaign (September 19); after the storm (October 15) and at the end of the fieldwork campaign (October 31). Between the second and the third survey was a two week period of calm weather.

From the DGPS measurements it appeared that migration only took place where the channel crossed the sand flat. The cross sections 1, 2 and 3 show no migration (Figure 5.3) and also more landward no migration of the channel was observed. Cross sections 4 up to 7 show a migration of the channel to the north of ten to twenty meters. Practically all of this migration took place between September 19 and October 15. Within this

period, most of the migration was observed during the storm on October 4. Between October 15 and October 31, hardly any migration took place.

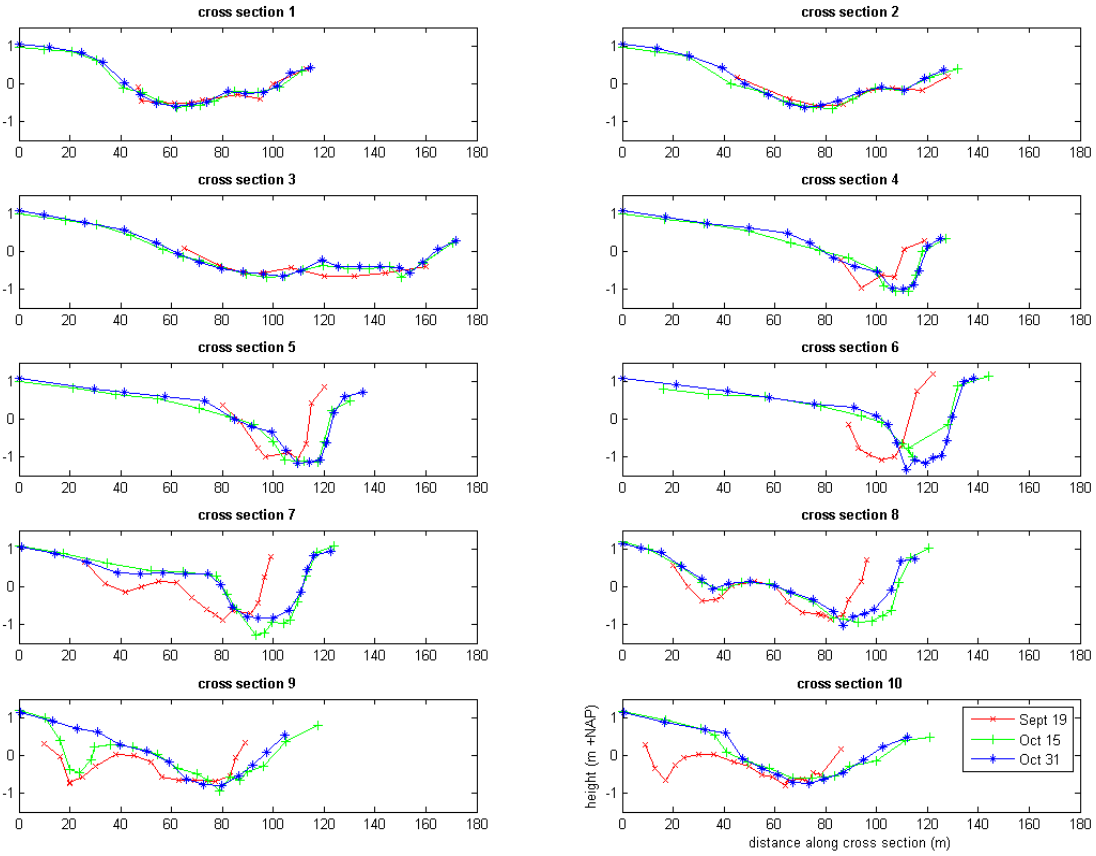

Figure 5.3 Cross section profiles of the Slufter inlet as measured on September 19, October 15 and October 31.

The migration of the channel is very dependent on flow velocities in the channel, which in turn are mostly determined by weather conditions. The outer bank –the northern one- is the one to suffer from erosion due to the flow in the channel. However, during calm weather, flow velocities are too low to cause significant erosion. The northern bank becomes less steep as calm weather prevails and erosion hardly takes place. When tidal flow velocities and associated discharges increase due to increased setup and larger tidal amplitudes, the channel starts eroding its northern bank. Within a day, the northern bank shows a fresh cut. The bank is undercut by the flow and blocks of sand can be seen falling into the channel. With the datacable pole as a fixed reference point, it was

observed that the channel hardly migrated during calm weather, but up to three meters a week when winds were stronger and the astronomical tide was modified by a small setup.
During storm, currents are much stronger than usual, which causes the outer bank of the channel to erode strongly. However, during high water the entire gap between the two dunes is flooded and the inflow of water is not only restricted to the channel. Whether this enhances or decreases the erosion and migration of the channel is difficult to say. On one hand, erosion can be enhanced because the beach plane is entirely saturated with water, which greatly decreases its strength and thereby enhances erosion. On the other hand, flow velocities in the channel decrease because a relative small amount of the total amount of water flows through the channel. This would decrease erosion of the banks. Because observations at the channel banks are impossible during storm, it is difficult to say which process is most important. It is however very likely that with channel inflow during a storm, significant erosion of the northern bank takes place.
When during a storm the water level lowers, all the water that flowed in the Slufter system over the sand flats has to be exported again via the inlet channel. Flow velocities are therefore extremely high, up to 2 m/s. These high outflow velocities cause continuous erosion and undercutting of the northern bank and therefore large migration of the channel. The saturation of the sand of the banks decreases bank strength and thus increases erosion rates. Large amounts of water enter the Slufter basin during storm via the beachflats and not via the channel. However, all water has to flow out via the channel. Despite high flow velocities, one ebb tidal stage does not last long enough to empty the basin to its normal low-water levels, also because water that is trapped on the mudflats requires more time to flow back to the channel. Low water levels in the basin will be higher than normal and during the next outflow stage, this remaining water also has to flow out of the basin, again causing higher than normal outflow velocities. These higher flow velocities cause an additional erosion of the outer banks and thus an additional migration of the channel.

5.2 bedform dimensions and migration

The distribution and length of the bedforms in the Slufter channel are very well visible on the aerial photograph of September 18 (Figure 5.4). Striking is the strong three-dimensional character of the bedforms and their dominant ebb-flow direction. Nowhere along the channel is a two-dimensional pattern of the bedforms visible, although such a two-dimensional pattern has been observed in the channel in 2008 (van der Vegt, personal communication). The aerial photo also shows that bedforms in the centre of the channel are longer than those at the banks, which fall dry every low tide. This would suggest that bedform size is related to water depth, since water depths in the centre of the channel are larger than at the banks. However, bedform dimensions at different locations in the channel do not support this suggestion. At the southern part of the photograph, bedforms are not smaller than those near the frame, although water depth at the southern part was much less than at the frame location. The same holds for the seaward part of the channel: water depths there were smaller than at the measurement frame, but bedform dimensions were not.

Looking in more detail at the bedforms near the frame (Figure 5.4), a typical length scale of two to four meters can be seen, although the strong three-dimensional character of the forms makes it difficult to determine typical lengths. Shorter as well as longer lengths are abundant. Typical bedform heights vary from 0.3 meters at the banks and at the shallow areas to 0.5 meter at the deepest parts of the channel. The bedforms themselves are not very high, but in between scour holes occur.

Figure 5.4 Close ups of the photo compilation, on which the 3D morphology of the bedforms is visible.

The ADV's which were mounted on the measurement frame in the channel measured distance to the bed every ten minutes. The horizontal distance between the ADV's was 0.5 m, ADV1 being the most landward one, ADV3 the most seaward. When bed level (relative to NAP) is compared with flow velocity in the channel (Figure 5.5 and Figure 5.6), it can be seen that bed level does not change when flow velocities remain below a

threshold value of approximately 0.6 m/s. When this threshold velocity is exceeded, the bed level suddenly changes, but no migration patterns of bedforms are visible. When flow velocities are high due to more energetic conditions, for example from October 16 to October 18, the bed level changes every outflow peak. But again when flow velocities remain low, for example from October 20 to October 31, the bed remains stable and no movement is visible for a long time. This corresponds with experiences during the fieldwork. It was observed that crests of bedforms remained at the same place relative to the frame for long time spans. The stability of the bed at low flow velocities does not imply that no bedload transport at all takes place: bedload transport may still take place, but not enough to change the location of the bedforms.

From September 20 up to September 24, flow velocities regularly exceed 0.6 m/s and the bedlevel slowly drops over the course of a few days. This slow decrease in bed level might indicate the slow passage of a single dune, but due to the highly three dimensional pattern of the bedforms, this is not certain. Also, if an ebb-dominated dune would slowly pass under the ADV's, the most seaward ADV (nr 3) would always give a slightly higher bedlevel than the most landward ADV (nr 1), but this is not the case. There is not one ADV which shows bed levels which are higher than those of the other ADV's for a longer time span. On October 1, a sudden rise of bedlevel of 30 centimetres takes place. This might be explained by the passage of a trough or scour hole between dunes or the filling up of a trough or scour hole.

At October 4, the bedlevel suddenly rises from -1.5 m +NAP to -1.1 m + NAP. This sudden and large rise of bedlevel is not due to bedform migration, but due to the migration of the channel as a whole. During the storm on October 4, the channel migrated several meters to the north and the measurement frame was located at the southern bank of the channel after the storm.

Since ebb currents are generally stronger than flood currents (see also paragraph 6.1), ebb currents more often exceed the 0.6 m/s threshold and the bed more often moves in the ebb direction than in the flood direction. This explains the ebb dominance of the bedforms.

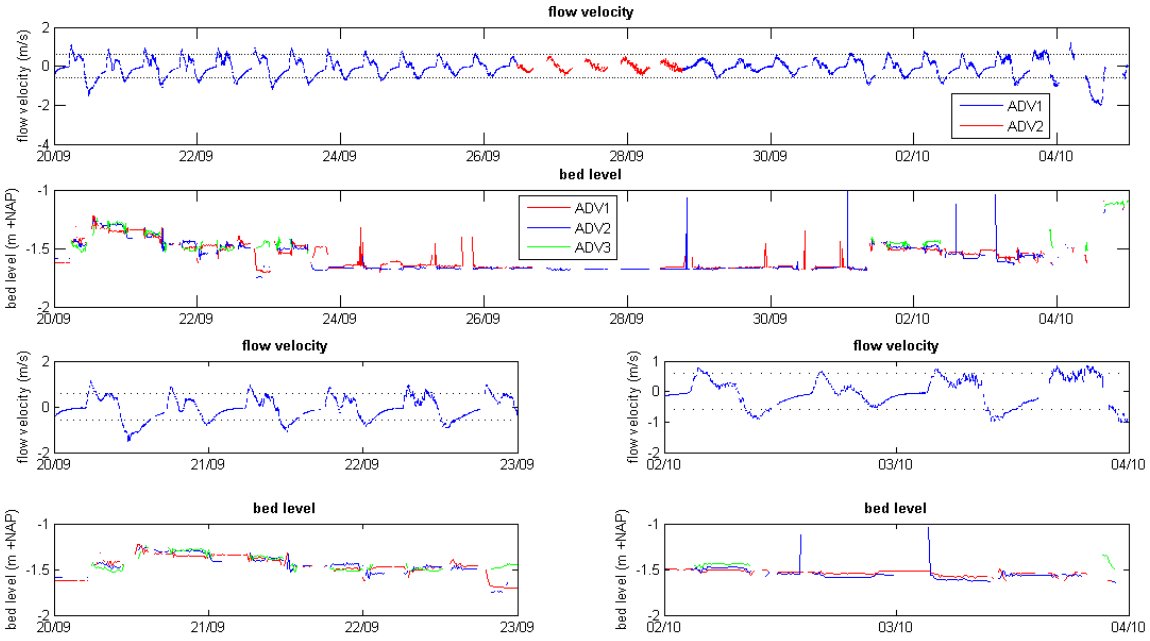

Figure 5.5 Flow velocity and bed level from September 20 to October 6, the period before and during the storm. Lower left panels: a close-up of the period September 20 to September 23. Lower right panels: a close-up of the period October 2 to October 4.

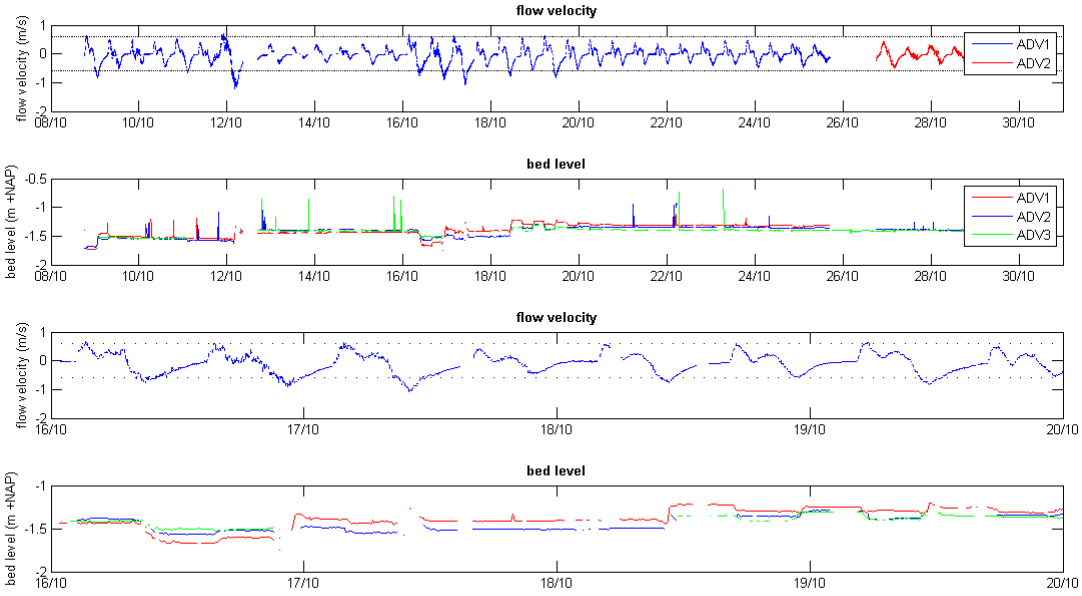

Figure 5.6 Flow velocity and bed level from October 8 to October 31, the period after the storm. Lower two panes: a close-up of the period October 16 to October 20.

As stated above, no migration patterns of bedforms can be detected from the bed level measurements. From the measurements no smooth increase or decrease in bedlevel is visible, instead bedlevel decreases or increases with sudden jumps.
Also when from the three measurement points the bed slope is analysed, no passing of bedforms can be seen under the three ADV's. Calculating bedload transports from bedform dimensions and migration rates therefore is impossible in this case. With more two-dimensional bedforms and a steady migration this may be possible in other cases.

5.3 Morphology and bedforms – overview

During low flow conditions in the Slufter inlet channel, no erosion of the outer channel bank takes place. During more energetic conditions, the outer channel bank starts eroding and sedimentation takes place at the inner bank. During storm, the high flood velocities cause great erosion, enhanced by the flooding of the beachflat, although it is impossible to see this process due to high water levels. The extremely high flow velocities during the ebb stage of a storm (up to 2 m/s) cause severe erosion of the banks. Ebb flow during the first tidal stage after the storm is still higher than normal, enhancing erosion of the outer bank even further. Channel migration mostly takes place where the channel crosses the beach flat.
A photo mosaic shows that the dunes in the channel are highly three dimensional with lengths in the order of meters and heights in the order of decimetres. In between dunes scour holes occur. The bed level does not change if flow velocities remain under 0.6 m/s. When flow velocities exceed this threshold, the bedlevel suddenly changes, but no passing of individual dunes can be determined. Therefore, calculating bedload transport from bedform dimensions and migration rates is impossible in this case.

6 Hydrodynamic processes in the channel

6.1 Flow velocity and water depth

The typical flow velocity pattern in the Slufter shows an inflow in two pulses, while outflow occurs in one single pulse (Figure 6.1). It takes about half an hour from low water slack before water levels at sea have increased so much that water can flow into the Slufter channel, which is located higher than the sea bed. Flow velocity increases quickly to decrease again after one hour. Velocities drop near zero or even negative values are measured, representing temporary outflow of the channel. A second inflow peak of longer duration but smaller magnitude follows the first. After high water slack, flow velocities drop very fast. In the first stage of the ebb, the flow velocities are determined by a water level gradient which in turn is determined by the water level at sea. However, water level at sea drops faster than the water level in the Slufter and at a certain moment, the water level at sea drops below the bed level of the Slufter inlet channel. Outflow velocity is now no longer directly determined by water level at sea, but by the tidal drainage and exfiltration of water in the Slufter itself, caused by low water levels in the channel mouth, where the Slufter still empties, and higher water levels in the backbasin area which is still partly filled. With the emptying of the Slufter basin, the water level gradient decreases and flow velocities decrease to near zero at the last stage of the tide. If, due to for example a set up of the astronomical tide, more water flows into the Slufter basin than during a tide with no setup, water volumes in the basin are higher than during a normal tide. Outflow velocities are therefore higher and outflow duration is longer. The final part of the tidal stage, where flow velocities in the Slufter channel near zero, is then shortened.

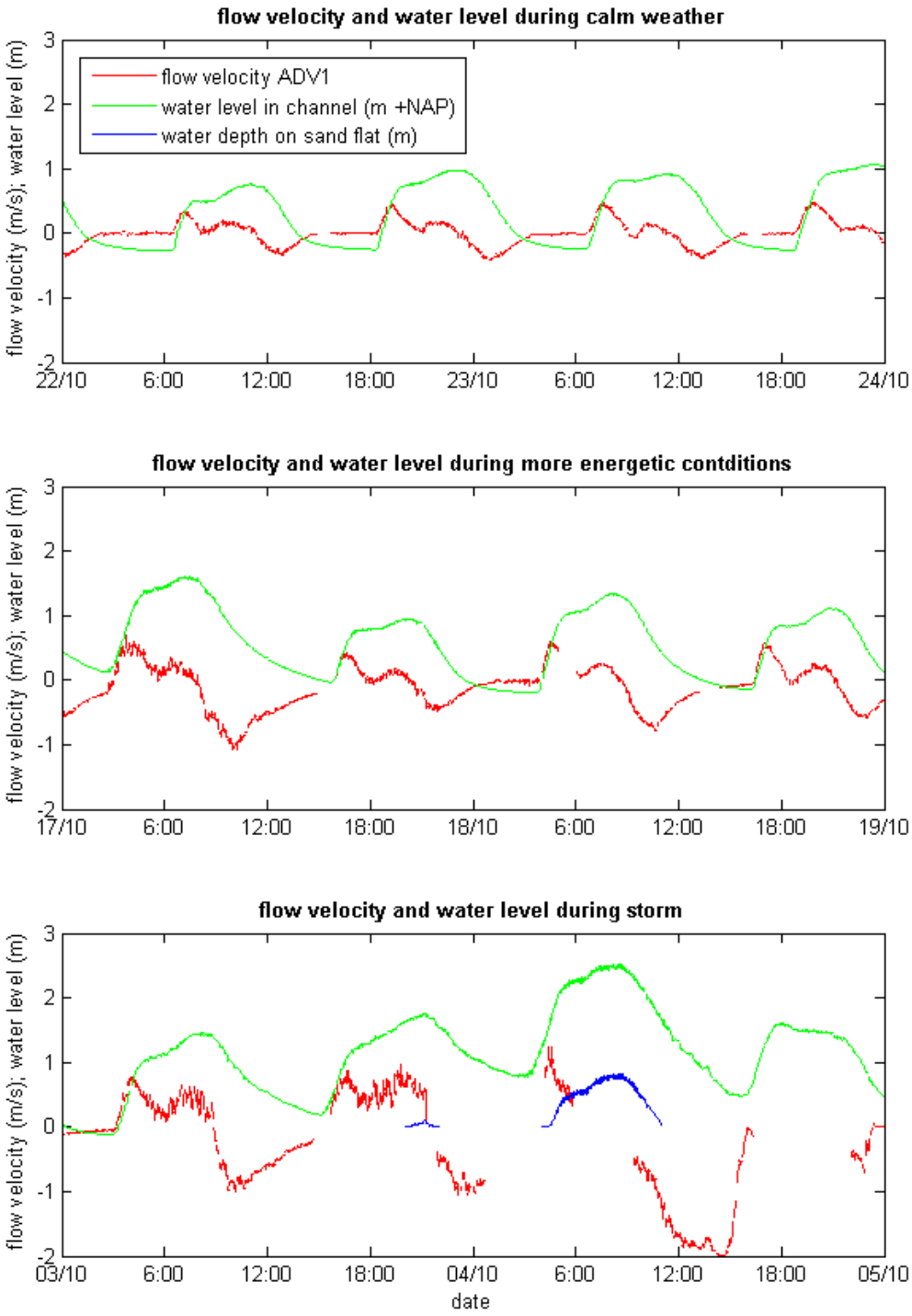

Figure 6.1 Flow velocity and water level in the channel during periods of calm weather (low waves, no setup), more energetic conditions (high waves, small setup) and storm (high waves, high setup). For storm, also the water height on the beach flat is given. Values are three-minute averages.

The main differences between the in- and outflow pattern at neap and spring tide are the maximum flow velocities, which are higher in the last case. The presence of a setup on

top of the astronomical tide or high waves causes the same changes in flow pattern: higher flow velocities for both inflow as well as outflow. This increase in flow velocity can be seen when the flow velocities during calm and more energetic conditions are compared. Under calm conditions, no setup was present and maximum flow velocities do not exceed 0.5 m/s. Under more energetic conditions, strong winds prevailed and a small setup and high waves were present. Under these conditions flow velocities increase to a maximum of 1 m/s (Figure 6.1). The storm is characterized by its high waves, high setup and extremely high flow velocities in the channel. The day before the storm, on October 3, flow velocities are higher than usual due to the already present wind setup at sea. Outflow velocities at October 3 and in the early morning of October 4 do not first drop to zero before the new inflow stage begins. This shows that the Slufter basin is not emptied fully before the next flood begins. The partial outflow in the ebb stage of the storm is caused by the large amounts of water that have to flow out of the channel in a limited amount of time and the wind- and wave-setup that push water into the basin, prohibiting outflow.

Water levels at October 4 were so high that water did not only flow in the Slufter basin via the channel, but also over the sand flat, as is shown by the water depth measurements which are performed on top of the sand flat (Figure 6.1). This inflow of water via the sand flat filled the Slufter basin to levels which were reached at sea, whilst flow velocities in the channel did not exceed 1.3 m/s. When after the high water slack water levels drop, water first flows from the sandflat to the channel. When water levels drop further, the sandflat falls dry and all water present in the Slufter has to flow out via the channel. This causes extremely high flow velocities of 2 m/s. Although the Froude number in the channel did not exceed 0.4, shooting water patterns were visible (Photograph 6.1).

Photograph 6.1 Supercritical flow patterns in the Slufter inlet during extreme outflow after the storm. The pole to which the datacables are mounted is visible, but the measurement frame is not, it is completely submerged.

6.2 tidal dominance

Due to the double inflow peak, tidal asymmetry is not easy to define. The period from highest flow velocity during inflow to the highest flow velocity during outflow is slightly smaller than the period from the lowest to the highest flow velocity. The ebb stage has a longer duration than the flood stage. Although ebb currents are low for a long time of the ebb stage, the maximum ebb currents are stronger than flood currents. The Slufter inlet is therefore classified as an ebb dominant tidal inlet.

As stated in paragraph 5.2, the bedforms in the channel had a seaward directed orientation, also pointing to ebb-dominance of the tide.

6.3 waves

To investigate whether waves travel into the inlet channel, a Fourier analysis (paragraph 3.5.1) was performed on the 4 Hz water level measurements. In addition, an analysis has been carried out on the water level measurements of the most seaward wave gauge on the

beach for comparison (see Witteveen 2010 and de Vries 2010 for more information on the locations of the wave gauges). The first ten minutes of measurements for several hours in a row have been analyzed. In this way, changing water levels due to tides had only limited influence on the analysis of each hour.

For calm weather conditions as well as more energetic conditions (see paragraph 6.1), practically no waves travel into the channel, while wind waves with a frequency around 10^{-1} Hz and infragravity waves with a frequency around 10^{-2} Hz are visible in the Fourier spectrum at the beach (Figure 6.2 and Figure 6.3). The spectral density of the waves present on the beach depends on the wave climate of the moment. During calm conditions, infragravity waves prevailed whilst during more energetic conditions, wind waves were dominant. The low-frequency waves partly migrate into the channel during the calm weather period, although their spectral density is much lower in the channel than on the beach.

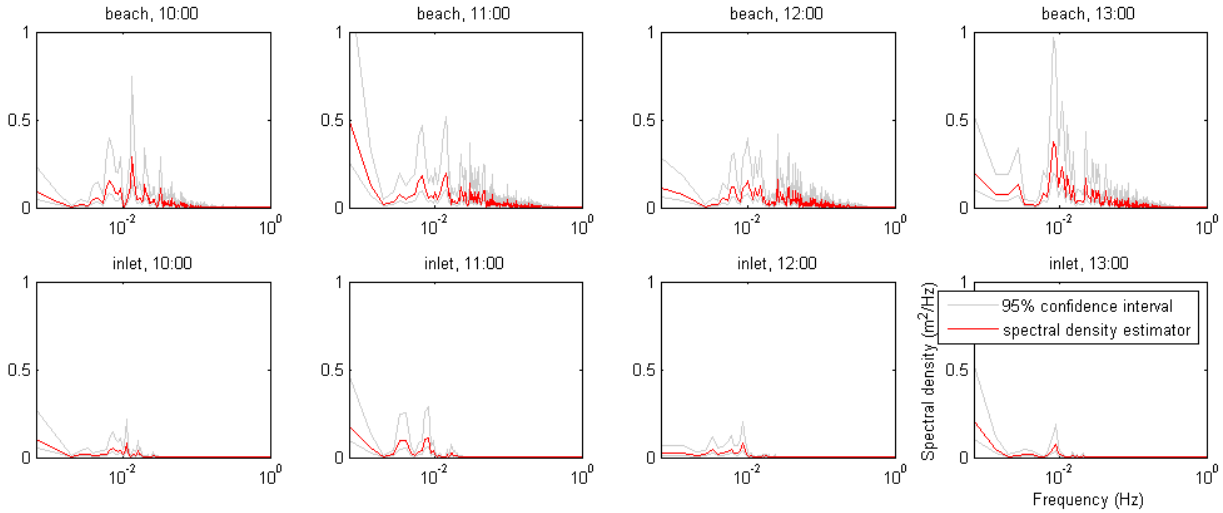

Figure 6.2 Fourier analysis results for four one-hour periods for the beach and the inlet during calm weather conditions. Analysis is of October 22. Highwater was at 14:25

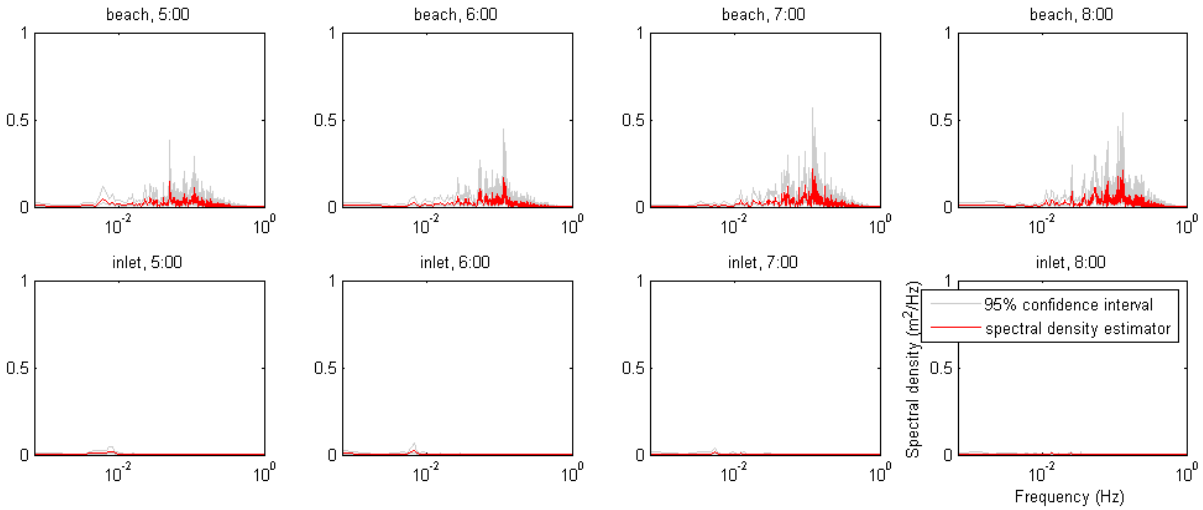

Figure 6.3 Fourier analysis results for four one-hour periods for the beach and the inlet during rough weather conditions. Analysis is of October 17. Highwater was at 8:05

During storm, the spectral density for wind waves is greatly increased on the beach (Figure 6.4). Also obvious peaks are visible for infragravity frequencies at and just below 10^{-2} Hz. In the inlet, peaks are visible at frequencies of 10^{-2} Hz (Figure 6.5). This shows that during the extreme high water levels of the storm, infragravity waves can penetrate into the inlet, but normal wind waves cannot.

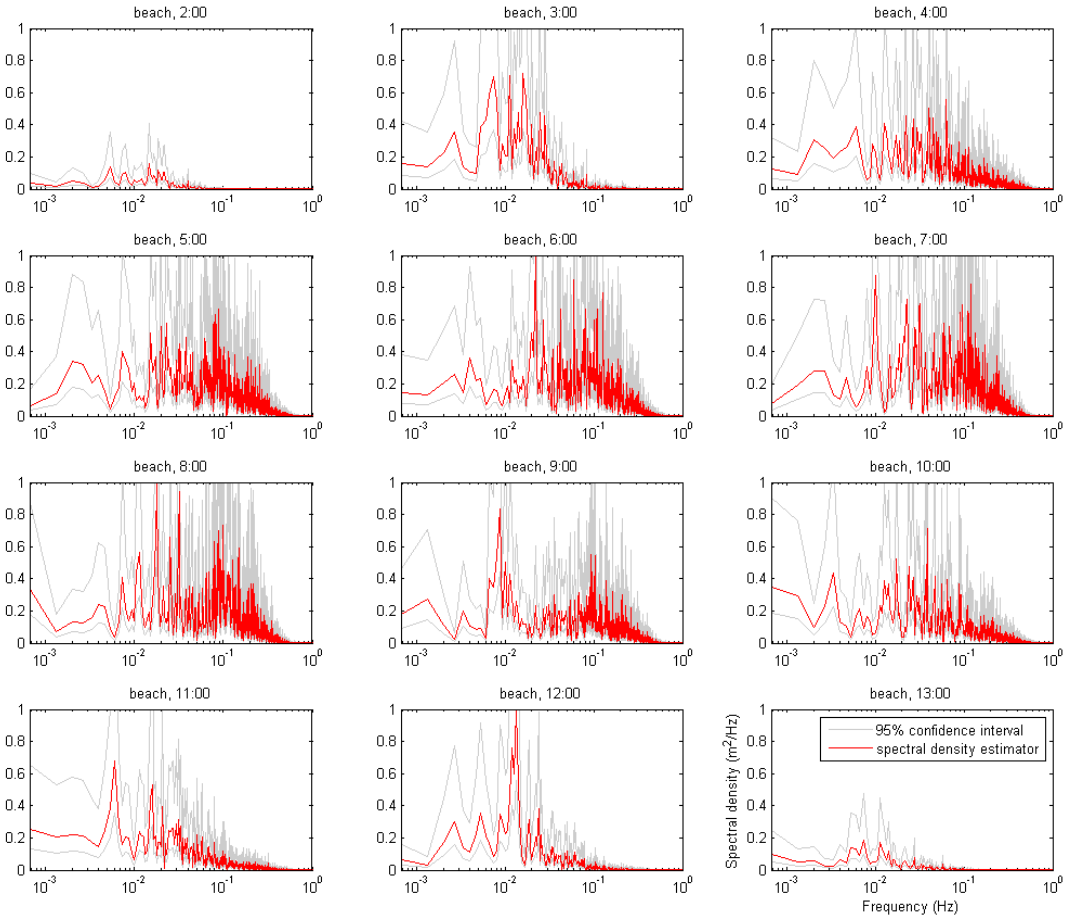

Figure 6.4 Fourier analysis for twelve one-hour periods for the beach during the storm. Analysis is of October 4, highwater was at 8:45

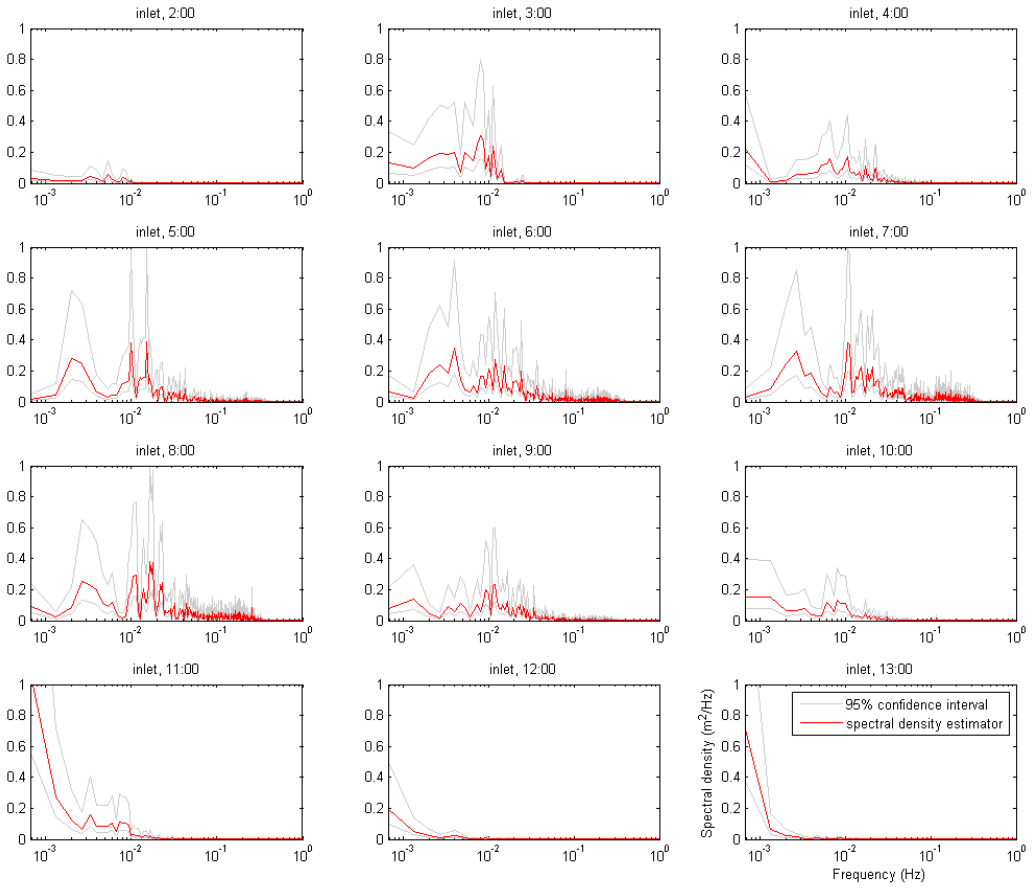

Figure 6.5 Fourier analysis for twelve one-hour periods for the Slufter inlet channel during the storm. Analysis is of October 4, high water was at 8:45

An explanation for the presence of infragravity waves in the inlet channel is the propagation of infragravity waves over the sand flat. When these waves, in the form of bores, have passed the sand flat and enter the channel behind it, they can cause the local water level to rise, causing a seaward directed gradient. The flow which is generated by this water level gradient has the same frequency as the long waves passing the sand flat. The peaks visible in the Fourier analysis of the channel during storm might therefore not be due to waves entering the channel from sea, but be the result of a flux forced outward by long waves which propagating over the sand flat.

To test this theory, a Fourier analysis of the water passing the sand flat has been made for comparison with the one from the channel (Figure 6.6). The waves passing the beach flat have a slightly higher frequency and thus a shorter period than the waves which were

found in the channel. Therefore it can be concluded that the long waves found in the channel are infragravity waves which travelled into the channel from sea, instead of forced waves from over the beach flat.

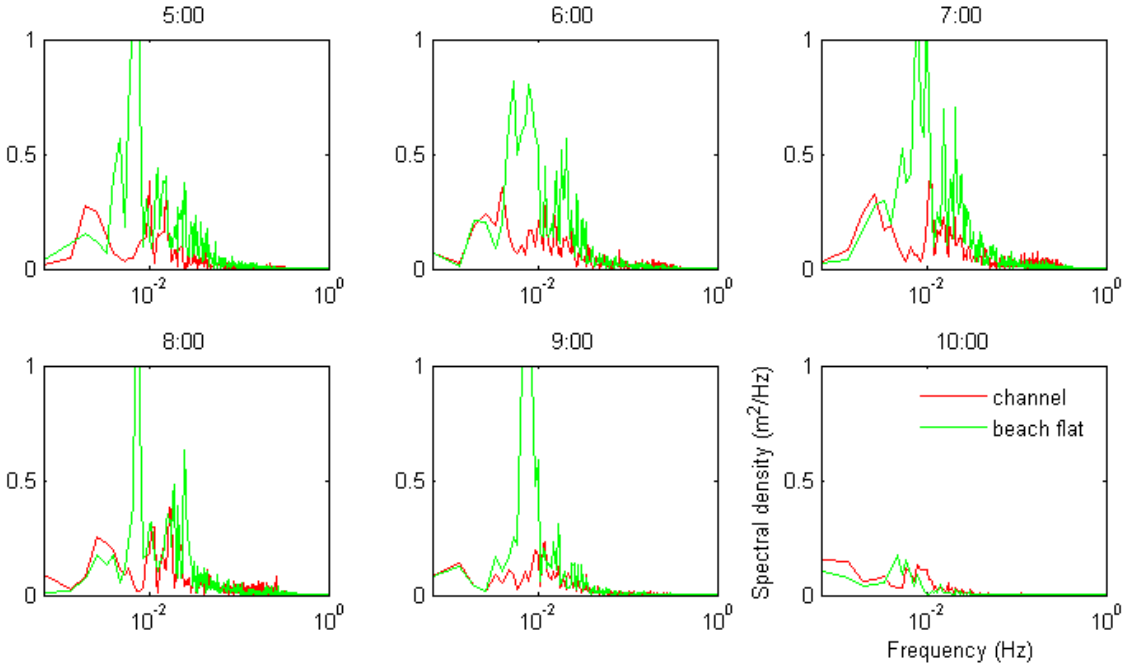

Figure 6.6 Fourier analysis for six one-hour periods of water levels in the inlet and on the beach flat during the storm. Analysis is of October 4. High water was at 8:45.

6.4 Hydrodynamic processes – overview

Flood flow in the Slufter inlet channel starts half an hour after low water slack. A typical velocity pattern in the inlet shows two inflow peaks: the first one with the highest flow velocity, but a short duration, the second one with lower flow velocities but a longer duration. After high water slack, ebb-directed flow velocities increase fast to a strong outflow peak, followed by lower flow velocities. In the last one to two hours before inflow starts again, flow velocities in the channel are almost zero. A wind- or wave-setup at open sea causes higher water levels in the Slufter basin, which in turn generate higher in- and outflow velocities. During storm, water enters the basin not only via the channel, but also via the beachflat. Water only leaves the basin via the channel, causing extreme

outflow velocities. The basin does not fully empty in one ebb tidal stage, causing the next ebb tidal stage also to have high outflow velocities.

Maximum ebb flow velocities are higher than maximum flood flow velocities. Therefore the Slufter is considered to be an ebb-dominated tidal basin. This is supported by the ebb-directed dunes on the bottom of the channel.

Under calm weather conditions, no waves enter the Slufter inlet channel. Only during storm, infragravity waves can enter the channel.

7 Sediment transport measurements and calculations

7.1 Bedload transport

7.1.1 Measured bedload transport

Bed level has been measured every ten minutes by the ADV's mounted on the frame. In paragraph 5.2 an overview of the bed level change during the course of the fieldwork is given. It appears that there is no bed level change when flow velocities stay below 0.6 m/s. From the sudden jumps in bed level, no migration patterns and velocities of bedforms can be deduced. Also when bed slope under the ADVs at different moments is analysed, no migration of bedforms can be seen under the three ADV's. Calculating bedload transports from bedform migration therefore is impossible in this case. With more two-dimensional bedforms and a steady migration rate it may be possible in other cases.

Critical flow velocities for bedload transport lie well below the 0.6 m/s needed for bedform change. The dunes are therefore considered relict bedforms which are not in equilibrium with the new, less energetic, hydrodynamic conditions. Bedload transport probably still takes place: sand particles are then rolling over the dunes, without changing the bed morphology.

Although quantification of bedload transport by means of dune-tracking is not possible, the net transport direction in the case of dune migration can be determined. Because maximum ebb flow velocities are higher than maximum flood flow velocities, they more often exceed the critical flow velocity for bed level change of 0.6 m/s. Also, all dunes in the channel show an ebb-dominated direction (see also Figure 5.4). These two factors point to a net export of bedload sediment via bedform migration.

7.1.2 Calculated bedload transport

To quantify bedload transport and to investigate patterns in bedload transport rates, transport has been calculated using the formulas of Bagnold (1966), Bailard (1981) and van Rijn (1984) during a calm weather period with low flow velocities, a period with higher than average flow velocities and a setup (i.e. more energetic weather conditions) and during storm.

For calculations, the depth-averaged flow velocity has been used, which is computed as the average of all ADV measurements. When a certain ADV did not give measurement results, for example because it was not submerged in the water, the average is calculated of the other measured velocities.

Calm weather conditions

The different methods give similar results under calm weather conditions, in magnitude as well as transport pattern (Figure 7.1). The van Rijn method gives much lower transports than the Bagnold and Bailard methods; often the transport as given by van Rijn equals zero. The reason for this lower transport is the T-factor in van Rijns computation method (paragraph 2.4.2). The T-factor in van Rijns computations states that only the bed shear stress exceeding the critical bed shear stress causes sediment transport. When flow velocities exceed critical values (i.e. bed shear stresses exceed critical stresses), van Rijn calculates bedload transport using only the flow velocity exceeding the critical value. When flow velocities do not exceed critical values, no transport takes place.

When the bedload transport rates for calm weather are added up over a period of 50 hours to include four complete tidal stages and multiplied by the approximate width of the channel (16 m), the bedload transport equals 0.014, -0.03 and 0.04 m^3 for the Bagold, Bailard and van Rijn computation methods, respectively. This means that the Bagnold and van Rijn computation methods calculate a small import of sediment via the channel, whilst the Bailard method calculates a small export. When the transports are recalculated to mm sedimentation or erosion that would occur if all this sediment was distributed evenly over the Slufter basin with its area of $4\ 10^6$ m^2, the sedimentation would be in an order of magnitude of 10^{-6} to 10^{-5} mm (table 7.1).

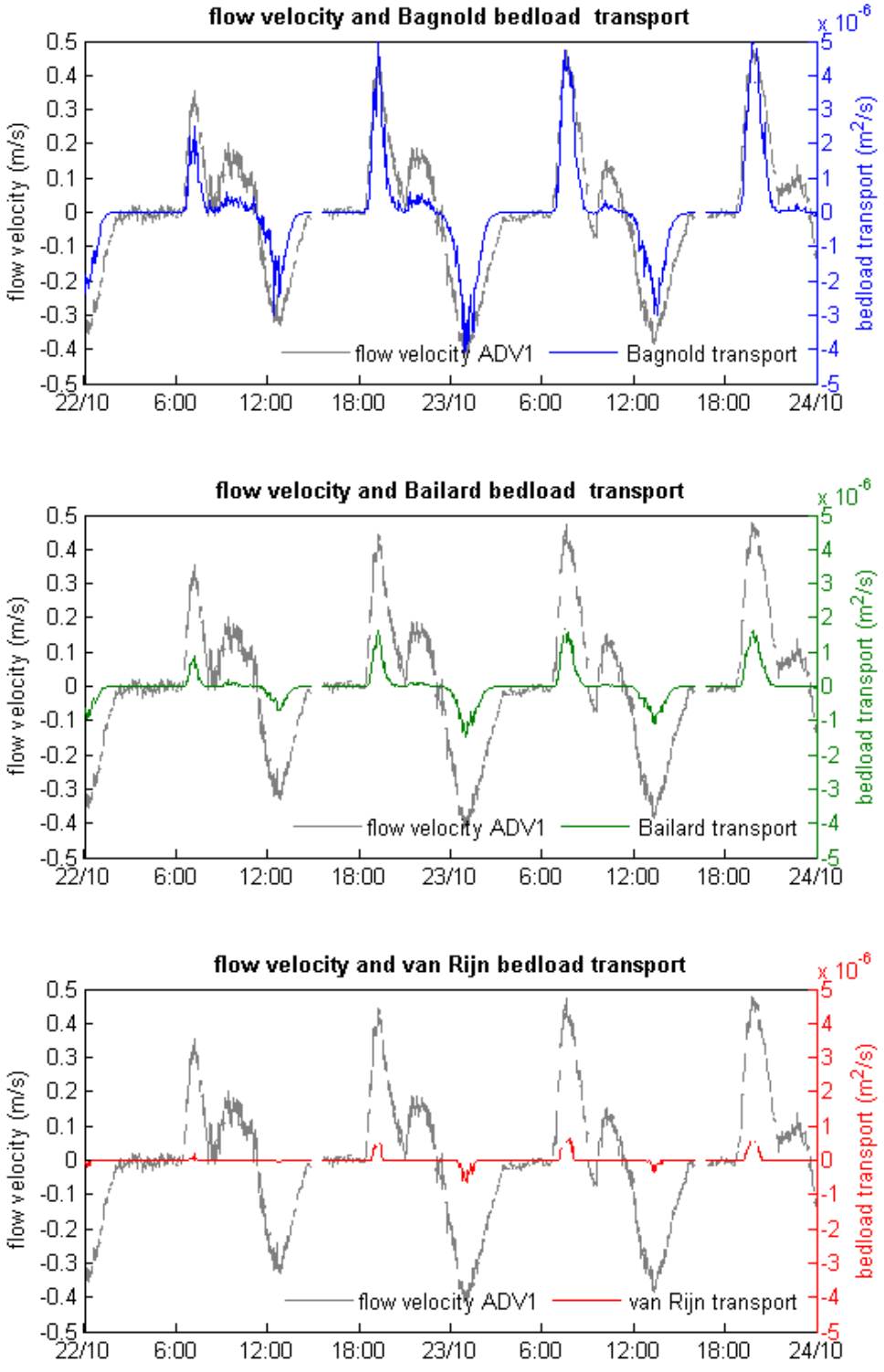

Figure 7.1 Flow velocity and bedload transport during calm weather conditions.

The import is only very small and so is its reliability. Near the beginning of motion, as is the case in this calm period, sediment transport is very difficult to predict and methods which have a term for the initiation of motion integrated in their formulas (such as the van Rijn method) give much lower transports than methods which do not include such terms.

More energetic conditions

Under more energetic weather conditions, the bedload transport as calculated by van Rijn does not give much lower transports than the Bagnold and Bailard methods, since flow velocities in this case regularly exceed critical values (Figure 7.2). As under calm weather conditions, all calculated bedload transports under more energetic conditions fall within the same order of magnitude.

When transports are summed over a fifty-hour period and multiplied by the width of the channel (16 m), total transports are -2.7, -1.9 and -2.8 m^3 for the Bagnold, Bailard and van Rijn computation methods, respectively. Again considering a basin area of 4 10^6 m^2, the erosion over two days lies in an order of magnitude of 10^{-4} mm, one or two orders of magnitude higher than under calm weather conditions (table 7.1)

These numbers show a net export of sediment via the channel. Import of sediment with the flood flow partly compensates the export of sediment during ebb flow, but ebb flow velocities are higher than flood flow velocities and transports are related to flow velocity with a third to fifth power, instead of linearly. These factors cause the export of sediment to exceed the import.

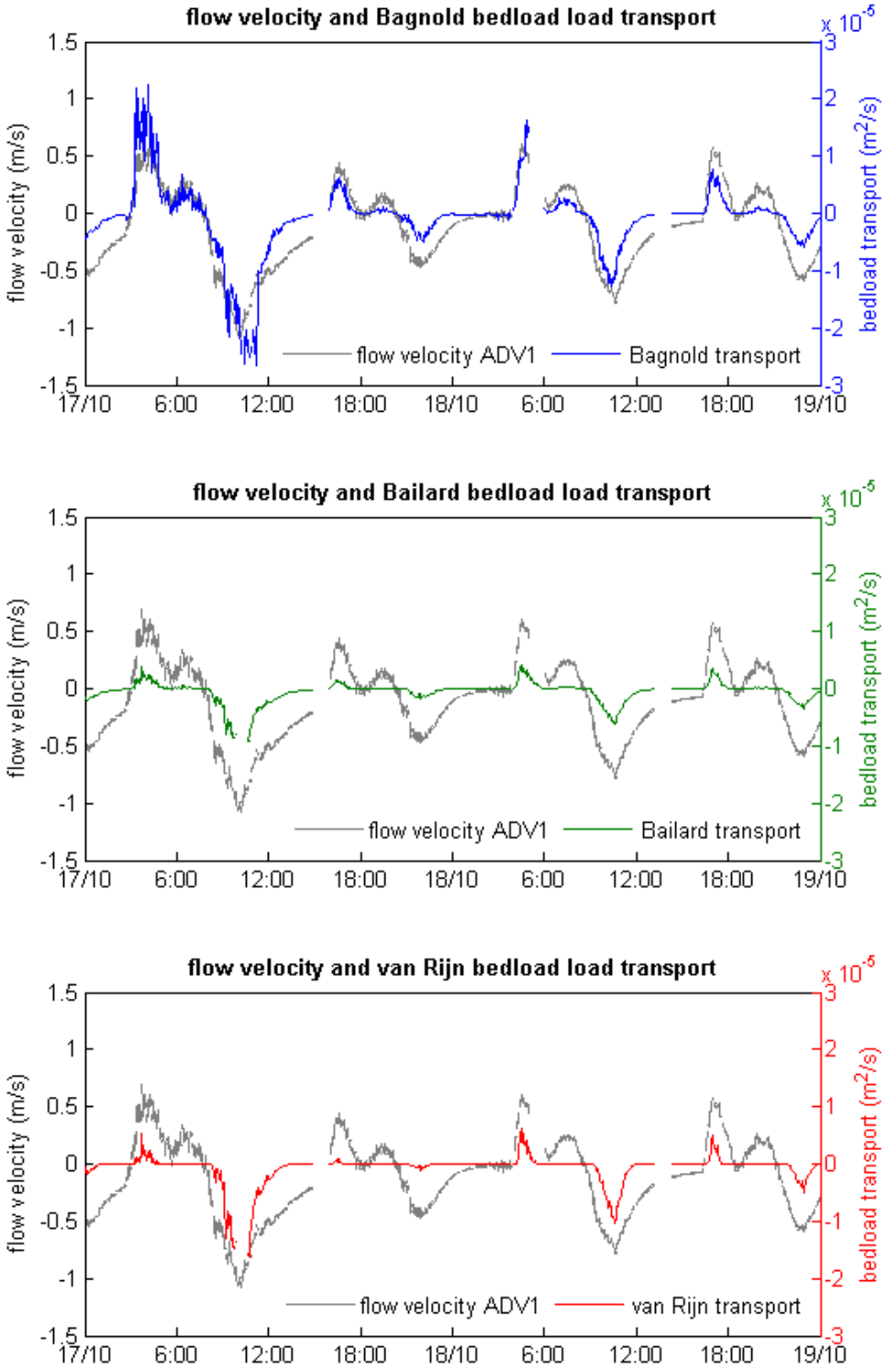

Figure 7.2 Flow velocity and bedload transport under more energetic weather conditions

Storm conditions

During storm conditions, bedload transport rates are an order of magnitude larger than transport rates under more energetic conditions and two orders of magnitude higher than under calm weather conditions. All calculated transport rates lie in the same order of magnitude and show large export rates during the peak outflow of 2 m/s (Figure 7.3).

It is difficult to predict transport rates after the storm, because directly after the storm, no measurements are available due to the migration of the channel. However, above average transports are expected because flow velocities probably remain high after the storm. In the first place because still a significant setup of a few decimetres was present which will generate both higher flow velocities at both inflow and outflow. Since the filled Slufter basin does not fully empty during one ebb tidal stage directly after the storm (see paragraph 6.1), the next ebb tidal stage will also facilitate outflow of water that entered the basin during storm and thus have higher flow velocities than is to be expected on tide and setup alone. This higher than normal flow velocities for the second ebb tidal stage after the storm cause higher than normal bedload transport rates.

Not surprisingly, all three different sediment transport models predict a strong export of bedload sediment for the period of October 3 and 4. Total transport amounts are -12.2, -17.0 and -34.0 m^3 for the Bagnold, Bailard and van Rijn computation methods, respectively. Recalculated this gives erosion rates in the order of magnitude of 10^{-3} mm. The large export can be explained with the extreme flow velocities during storm, especially during the ebb tidal stage. Also, the extended period of high flow velocities during storm events and the absence of periods with low flow velocities cause higher transports.

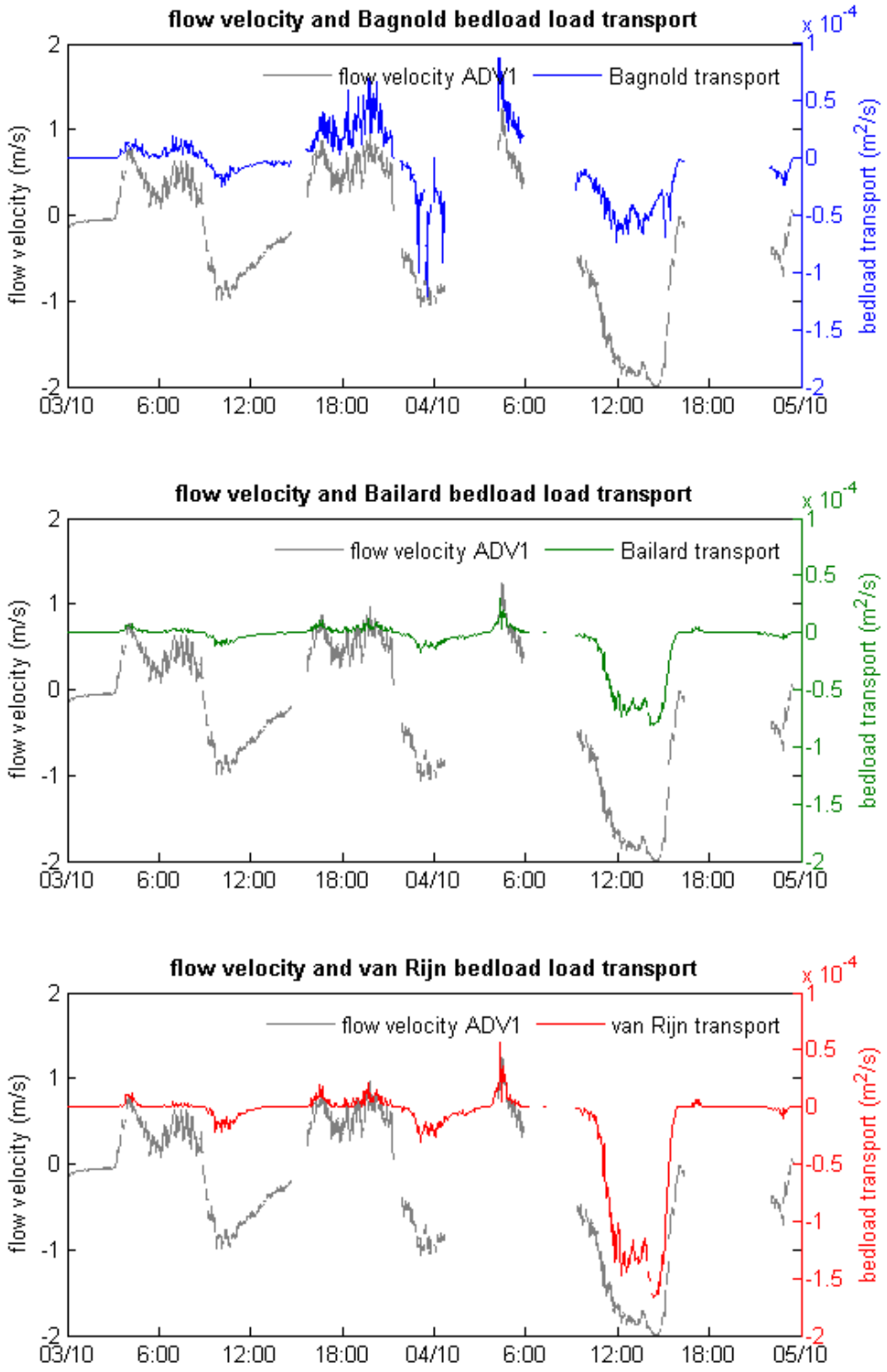

Figure 7.3 Flow velocity and bedload transport under storm conditions. Notice the different secondary y-axis of the top graph, it is an order of magnitude smaller than the middle and lower one.

Bedload transport on the long term

As can be seen from the above bedload transport computations, storms are of major importance to the total bedload transport over longer periods. During one tidal period under storm conditions, the amount of bedload transport is two orders of magnitudes larger than during one tidal period in calm weather. Despite the small net import of sediment under calm conditions as computed with the Bagnold and van Rijn methods, export of sediment during more energetic conditions and storm will probably dominate. Averaged over a year, net export of bedload sediment will take place through the channel, also because of the uncertainty of the net import of sediment under calm conditions.

Besides frequency and magnitude of storms, also the frequency of flooding of the beach flat has much influence, since a flooded beach flat is associated with a larger storage of water in the basin and, consequently, results in higher outflow velocities.

Due to the importance of individual storms and more energetic weather periods, it is impossible to quantify net bedload transport through the Slufter inlet over one or more years based on the present dataset. This would require flow velocity and water depth measurements over longer periods and long term information about weather conditions and setup.

7.2 Suspended load transport

7.2.1 Measurements of suspended sediment concentration

OBS measurement patterns

The suspended sediment concentration measurements that have been performed with the OBS are not of a constant quality. Where flow velocity measurements made with the ADV can be checked and deleted if quality is not sufficient, but no such method is available for OBS measurements. Since the OBS is an optical instrument, it is very sensitive for contamination. In addition, the sensor is very sensitive for grainsize effects.

Often, flotsam and seaweed attached to the OBS made its measurements useless for further investigation.

When the results of the OBS measurements were investigated, only the period from October 21 to October 24 appeared to give useful results for investigating the suspended sediment transport patterns in the Slufter inlet. From all other days, especially when higher flow velocities were recorded, no useful results could be obtained. One, but often more, of the three measurement series was characterized by spikes when others were not or showed very low values whereas others recorded large values. This lack of coherence makes it difficult to say which measurements represent the real suspended sediment signal.

The OBS measurement series of October 21 to October 24 show that suspended sediment concentrations rise and fall with flow velocities in the inlet (Figure 7.4). During the first stage of the flood, the suspended sediment concentration shows a peak which decreases when the flow velocities decrease. For the second stage of the flood, suspended sediment concentrations peak to a maximum value. During high water slack, suspended sediment concentrations do not decrease to zero because this slack period is only very short. The fine sediment has no time to settle and only a minor part will fall out of suspension. The outflow peak shows slightly smaller sediment concentrations than the second inflow peak. The reason for this might be that part of the suspended sediment has been deposited in the Slufter basin and is not available for the export anymore. In combination with the longer duration of the inflow of suspended sediment than the duration of outflow, this would suggest a net import of suspended sediment to the system.

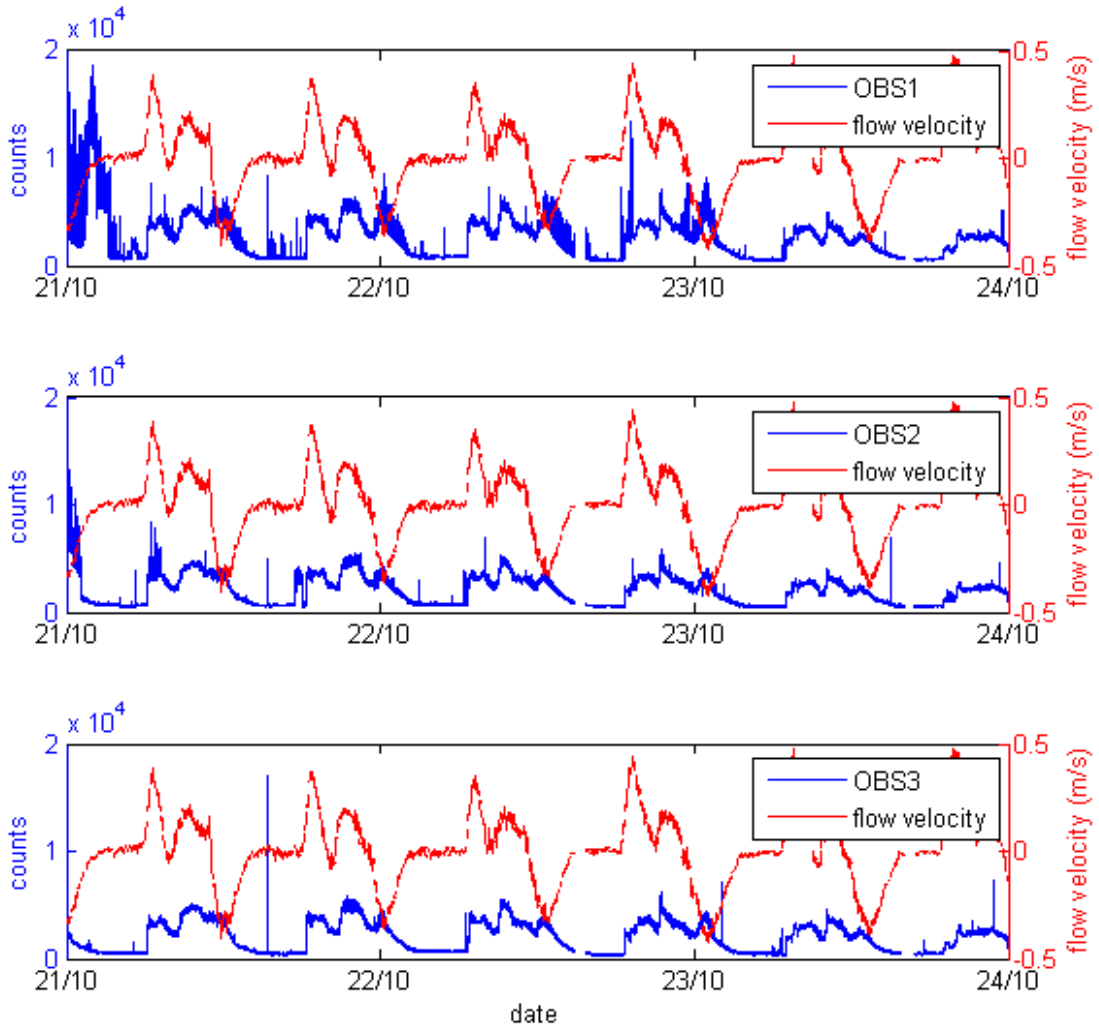

Figure 7.4 Measurements of the OBS compared to flow velocities in the channel for the period October 21 to October 24.

Quantifying suspended load transport from OBS measurements

In order to quantify the OBS measurements, calibration has been performed by taking water samples and comparing the sediment concentrations in these samples with the OBS measurements of the same moment.

Water samples were taken using a pump-sampling device, using flow velocities of about 0.8 m/s in the sampling tubes. Higher or lower velocities were not possible, which means that the water samples were not taken at the same speed as the flow velocity in the inlet channel of that moment. Also, samples were only taken when flow velocities in the channel were low, because of the location of the pump sampling device. When flow

velocities in the inlet were higher, the water levels also were too high to take samples. This means that samples were only taken at or just after low water, when suspended sediment concentrations were also low.

After analysis of the water samples, sediment concentrations have been plotted against the measured counts of the same moment (Figure 7.5). Water sample concentration and measurement counts do not show any correlation at all.

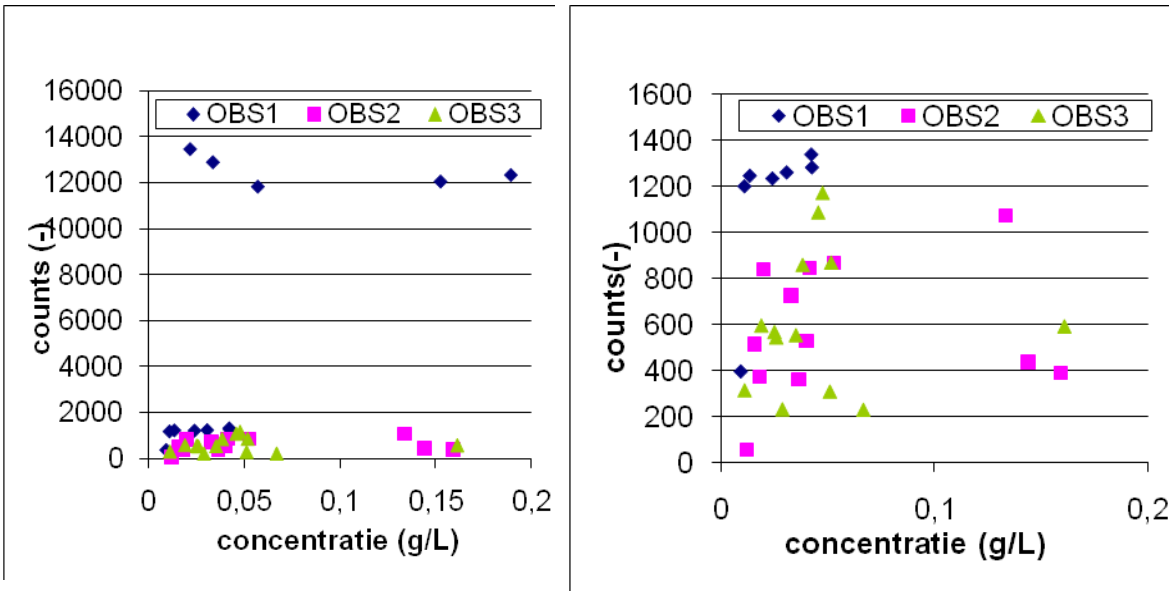

Figure 7.5 Measured counts plotted against measured suspended load concentration. Right figure is the same as left figure, but with an adjusted y-axis.

The above means that there is no way of accurately quantifying the OBS measurements. The calibration curves that are available are based on the local sand size and fall velocity. However, the OBS is very sensitive for grain size. When only sand of a known size is in suspension, measurements can be quantified to concentrations. In the Slufter inlet channel however, suspended sediment grain sizes may differ with the flow velocity and weather conditions. Specially the relative contributions of sand an mud to the total suspended sediment concentration is unknown, making quantification of the OBS measurements in the inlet channel impossible.

To quantify the concentrations based on the ADV measurements is not possible, since no calibration curves are available. The ADV performs different internal calculations on the

backscatter measurements before giving output. This is illustrated by the fact that ADV reflections of suspended sediment are equally high for storm and more energetic weather conditions, although concentrations during storm were almost certainly higher. Therefore, ADV measurements have to be investigated with care. Only general patterns can be deduced, but no detailed information will be available.

ADV measurements: acoustic reflection

Since an ADV needs sediment in suspension to measure the Doppler effect caused by the flow (see paragraph 3.2.1), it also provides information about suspended sediment concentrations. To see whether these measurements are useful for qualitatively analyzing suspended sediment concentration, the acoustic reflections measured by the ADV are compared with the optical backscatter signals measured by the OBS for the period October 21 to October 24. This comparison shows that the patterns measured by the ADV are very well comparable to those of the OBS (Figure 7.6).

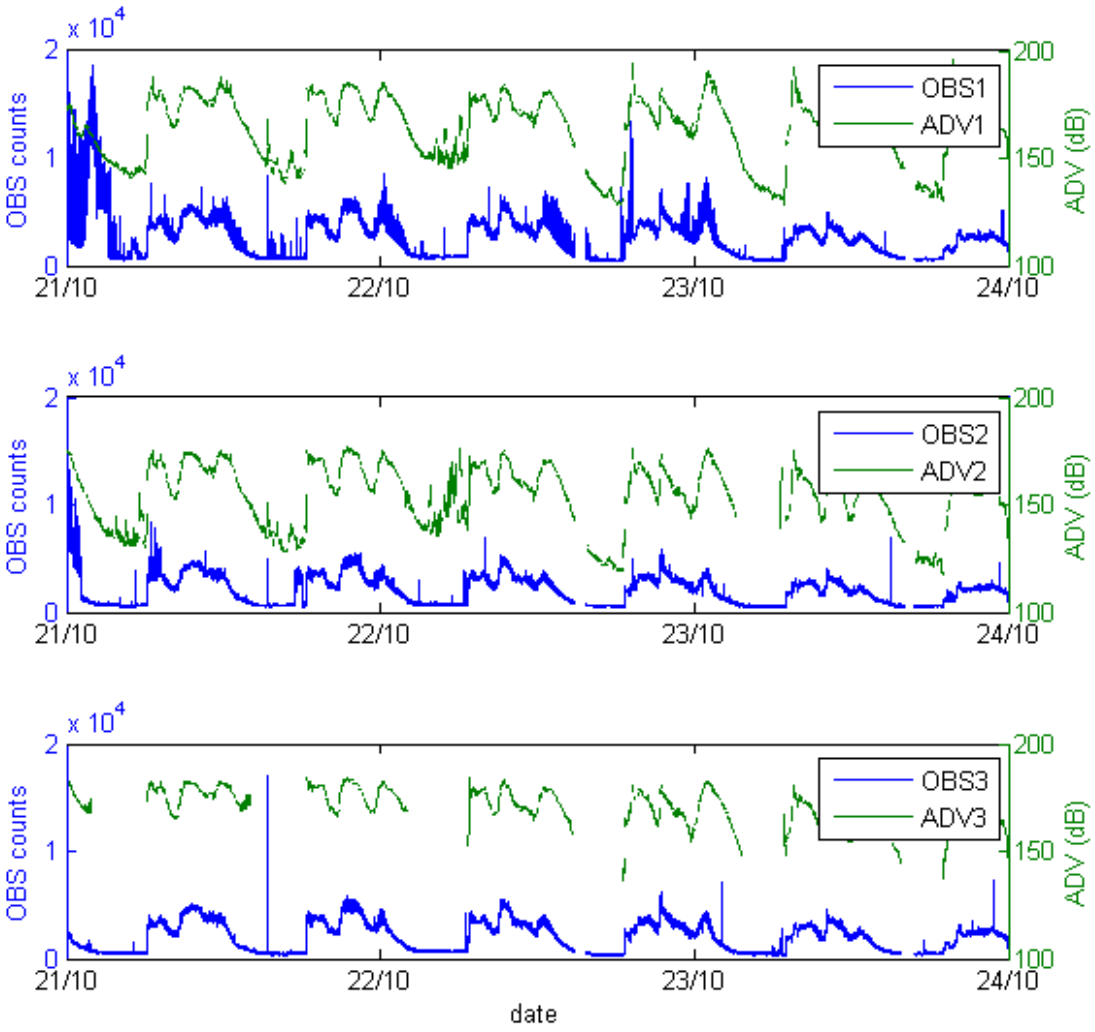

Figure 7.6 Comparison of OBS and ADV measurement results for the period October 21 to October 24. A gap in the ADV measurements series means that the ADV was dry at the time.

The main difference between the OBS and ADV measurements is that the ADV does not show the typical pattern of a lower peak followed by a higher peak during inflow and a lower peak during outflow as described above for the OBS. Instead, all peaks are approximately of the same height. With the ADV, the measurements do show a continuous decrease of sediment when flow velocities approach zero after the outflow stage, for example ADV1 at the last low water stage of October 22 and the first low water stage of October 23. This shows that although the flow velocity is zero, sediment needs time to fall out of suspension and suspended sediment concentrations gradually decrease through time. The backscatter values for the ADV's do not go below 120 to 130 dB,

suggesting an ever-present amount of suspended matter in the water, which does not have the time to fall out of suspension.
Although the concentration peak during outflow is not smaller than both concentration peaks during inflow, one could argue that also the ADV measurements suggest a net inflow of suspended sediment, since the inflow peaks have a much longer duration than the outflow peaks. However, statements about net transport based on the ADV measurements are very uncertain.

With the ADV measurements, it is possible to quantitavely investigate suspended sediment concentration patterns under more energetic conditions and during storm.
Under more energetic conditions, the measured ADV values are higher than those during calm weather (Figure 7.7), which is of course not surprising. However, the three distinct peaks in sediment concentration are not observed, during the second inflow event suspended sediment concentrations remain low. Also, the record is more irregular than that of calm weather, which might be caused by a larger contribution of resuspended sand in the water column due to the larger flow velocities. Opposing to calm weather conditions, the ADV backscatter values at more energetic weather conditions suggest a net export of sediment.

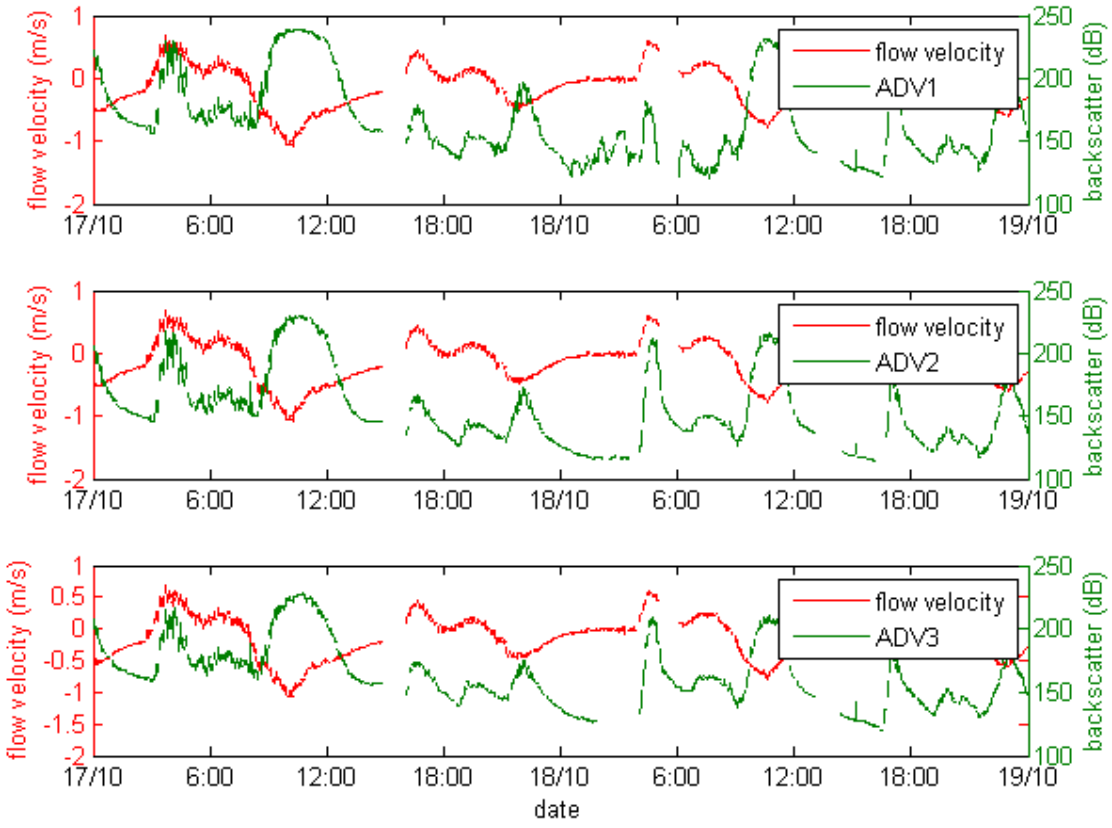

Figure 7.7 ADV suspended concentration measurements compared to flow velocity in a period with more energetic conditions, October 17 to October 19.

During storm, measurement values of acoustic backscatter are also higher than during fair weather, but not higher than during the more energetic weather record (Figure 7.8). The peak in backscatter values at noon at October 4 is not higher than the peaks which were measured earlier that day, for example at midnight and around five o'clock. It seems unlikely that suspended sediment concentrations were the same, considering the much higher flow velocities. Visual observations made during the high outflow during storm showed extremely large suspended sediment concentrations with clouds of sand moving through the water. Most probably the actual suspended sediment concentrations were higher than the concentrations during the increased inflow velocities in the more energetic weather period, but these differences were not detected by the ADV.

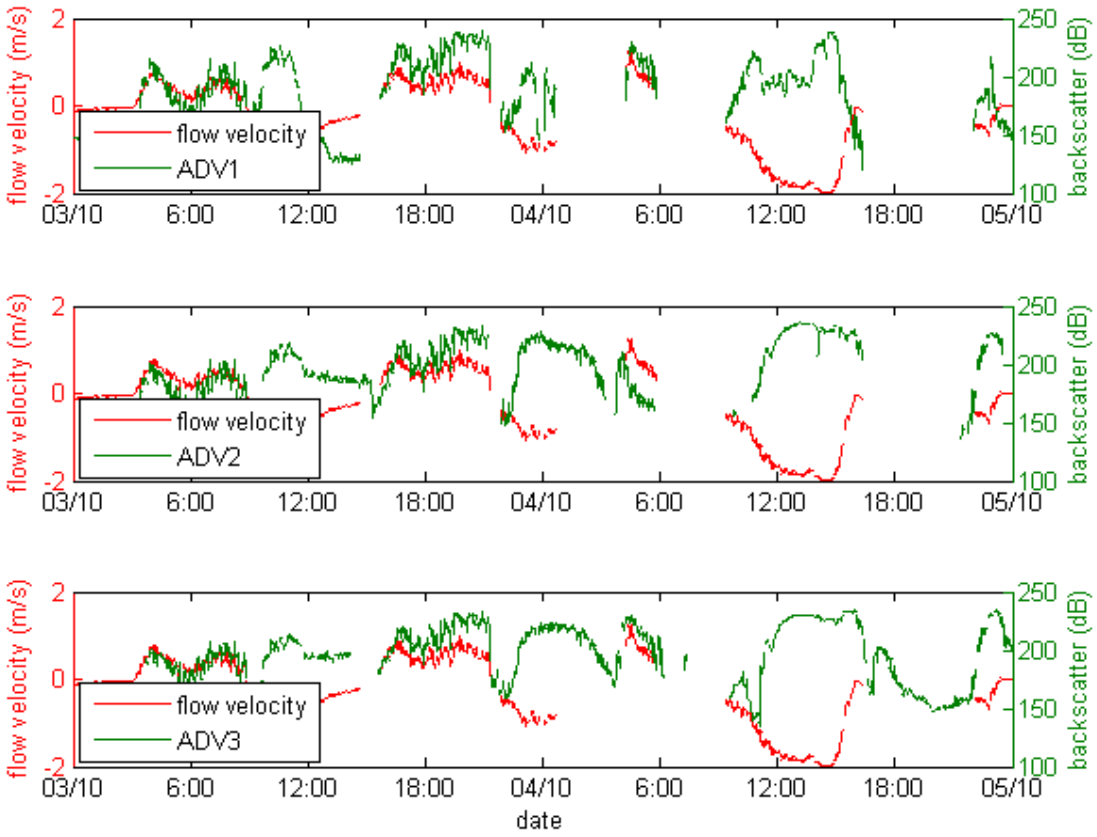

Figure 7.8 ADV suspended concentration measurements compared to flow velocity during the storm, from October 3 to October 5.

Quantifying suspended sediment concentrations with the help of ADV backscatter values has been successfully performed by several authors (Fugate and Friedrichs, 2002; Ha et al., 2009), but mostly in or with the extensive support of laboratory experiments. Also, for quantification of suspended sediment concentrations assumptions are made about the uniformity of the sediment composition which do not hold for the Slufter inlet channel. No calibration curves for the ADV backscatter and suspended sediment concentration are available. The ADV performs different internal calculations on the backscatter measurements before giving output. This is illustrated by the fact that ADV reflections of suspended sediment are equally high for storm and more energetic weather conditions, although concentrations during storm were almost certainly higher. Quantification of suspended sediment concentrations is not possible with the help of ADV backscatter values and the results can only be used to deduce general patterns.

Correlation

Suspended sediment concentrations seem to increase and decrease with local flow velocities. To investigate this further, cross correlations between sediment concentration measurements and flow velocities have been performed. For the period October 21 to October 24, a cross correlation has been performed for OBS backscatter measurements and flow velocity, and for ADV backscatter measurements and flow velocity. This way, the cross-correlations for the OBS and the ADV could be compared with each other (see Figure 7.9 for a typical example of an OBS and ADV measurement series). For the time period from October 21 to October 24, there is no time lag between suspended sediment concentrations and flow velocities, which suggests that the suspended sediment concentrations are indeed due to local flow velocities and have no time lag with flow due to large fall velocities.

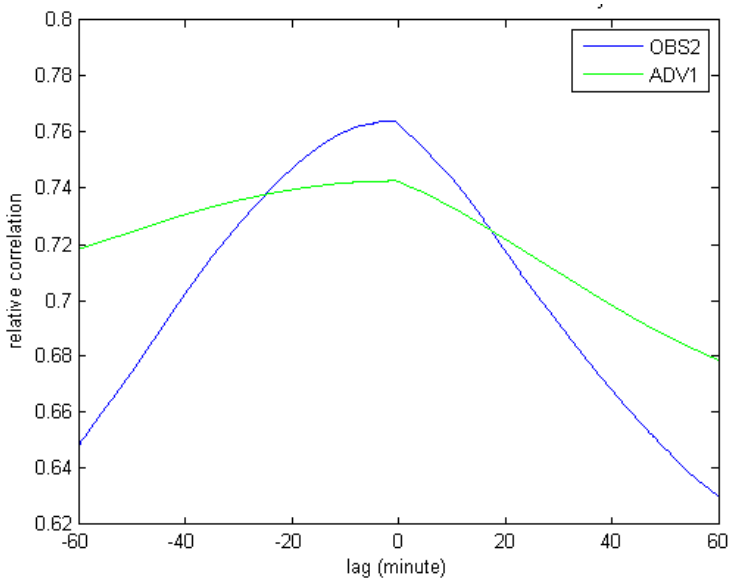

Figure 7.9 Cross correlation of OBS and ADV suspended sediment measurements with flow velocity, for the period October 21 to October 24.

For the ADV measurements, cross correlations have also been performed for more energetic weather conditions and during the storm. Under calm and energetic weather

conditions, there is no time lag between concentration measurements of the ADV and flow velocity (Figure 7.10). Under storm conditions, the maximum of the correlation curve lies around -30 minutes. An explanation could be that suspended sediment concentrations were already extremely high during the inflow of the storm, partly due to the high flow velocities in itself, partly due to wave action, stirring up the sediment. During outflow, concentrations did not increase very much and thus suspended sediment concentrations are not only a result of local flow velocities, but also of high sediment concentrations during inflow. However, the difference in correlation between zero lag and a lag of -30 minutes is not very large, which means that suspended sediment concentrations in the Slufter inlet channel are mostly dependent on local flow conditions.

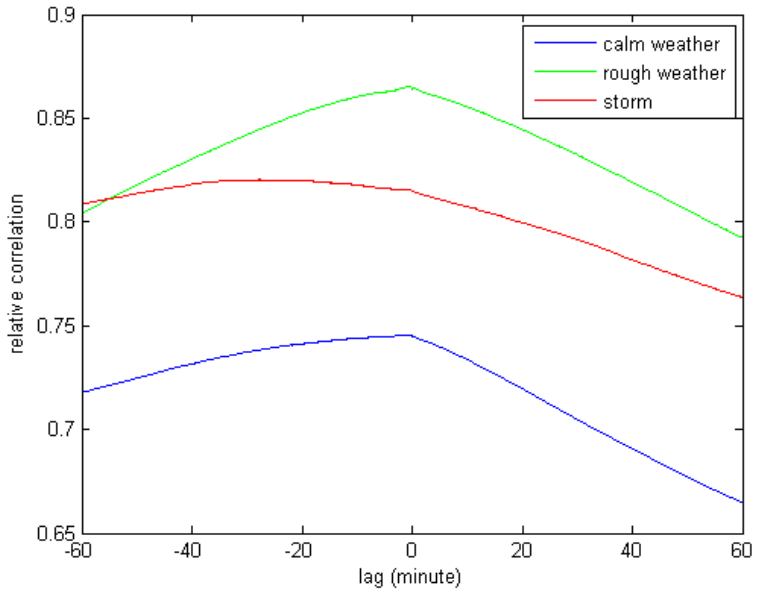

Figure 7.10 Cross correlation of ADV suspended sediment measurements with flow velocity, for a calm weather period, a rough weather period and storm. Every period has a duration of two days.

7.2.2 Concentration profiles and fall velocity

Suspended sediment concentration profiles in the Slufter inlet have been based on OBS and ADV measurements. These concentration profiles are then compared to profiles calculated with the van Rijn (1993) method (paragraph 2.5.3), using a grain size of 2.7 10^{-4} m. The only OBS measurements for which concentration profiles can be made are

those from October 21 to October 24, since only these measurements are reliable and don't show much spikes.

When comparing concentration profiles, the problem of different units arises. The OBS and ADV have different measuring methods and therefore output values are expressed in different units. The van Rijn calculations give a concentration in kg/m^3, which is not directly comparable to the output values of the OBS and ADV. To avoid this problem, all concentration profiles have been normalized from zero to one. The lowermost measurement location is assumed to have the highest concentration, which is set at one. All other measurements are given relative values. If for example the highest measurement point gives an output higher than the lowermost point, its relative concentration will also be higher than one.

The concentration profiles based on the OBS and ADV measurements do not always show a decreasing profile, instead, the uppermost measurement often shows a higher concentration than the middle measurement (Figure 7.11). In reality, such a concentration profile is highly unlikely, specially under calm conditions. These profiles are merely a result of the slightly different sensitivities of the different instruments. All instruments have their own sensitivity and thus their own calibration curves, but since these calibrations have not been implemented, a concentration profile is based on uncalibrated data. For the ADV, the internal processing of the measurements can also have its influence on the output.

When the highest measurements give higher, or equally high, concentrations of suspended sediment as the lower ones, this points to good mixing in the upper part of the water column. This good mixing will occur when mud is in suspension due to the low fall velocities of mud. When sand is in suspension, higher concentrations higher up in the water column are very unlikely.

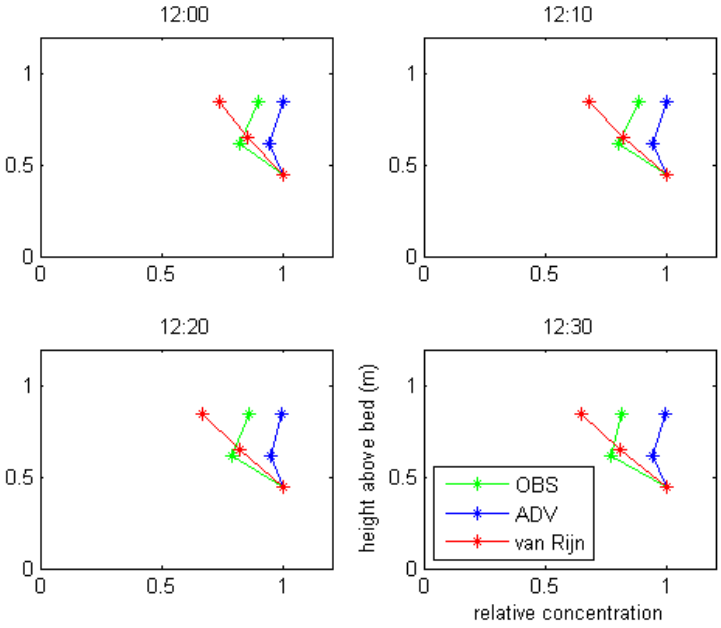

Figure 7.11 Measured and calculated concentration profiles at four moments during calm weather, on October 22

Concentration profiles during more energetic weather conditions do not differ much from those of calm weather (Figure 7.12). Under all conditions, the ADV measurements show relative concentrations near to one for all measurement heights, but during storm, the concentration profile as measured by the ADV shows an almost vertical line, which means that very good mixing occurs in the water column (Figure 7.13).

Measurements very near to the bed have not been made and most likely show higher concentrations than the current ADV measurements. Under storm conditions, the suspended sediment is very well mixed at the heights of the ADVs (45, 65 and 85 cm above the bed). This good mixing was also observed in reality: large clouds of sand flowed up in the water column and suspended sediment concentrations were very high near the surface.

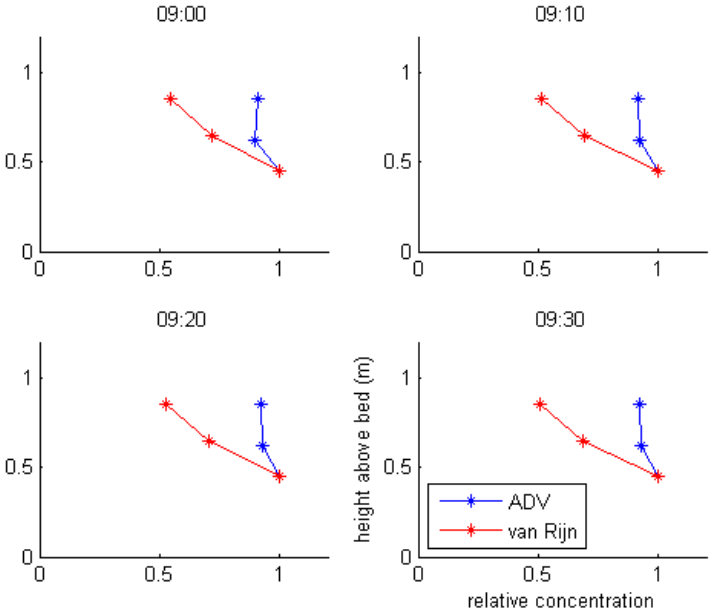

Figure 7.12 Measured and calculated concentration profiles at four moments during a more energetic weather period, on October 17

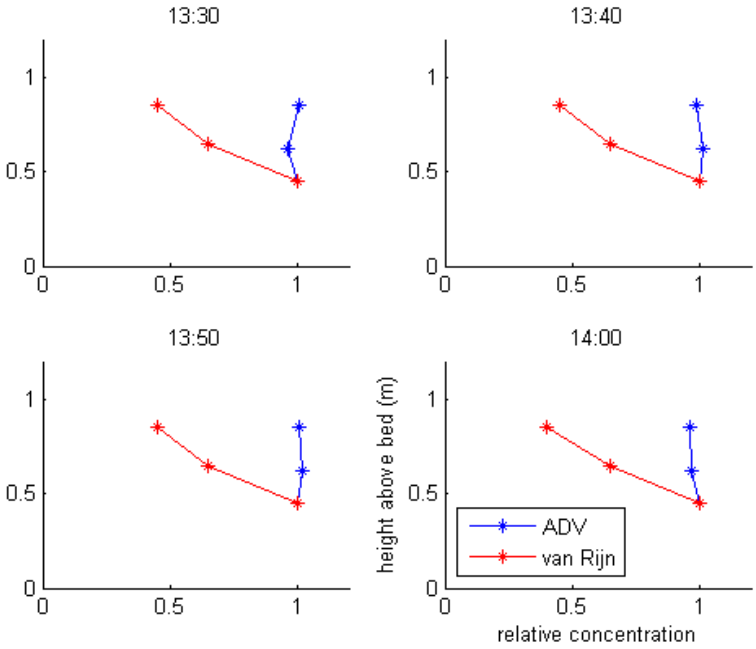

Figure 7.13 Measured and calculated concentration profiles for four moments during the storm, on October 4.

There is one obvious trend in all the concentration profiles (Figure 7.11, Figure 7.12 and Figure 7.13): the measured profiles of the ADV and OBS demonstrate a more vertical

homogeneous distribution than the calculated profile. This suggests that in the Slufter, the suspended sediment is better mixed than predicted by the van Rijn (1993) method.

The most likely reason for this better mixing is a smaller grain size in reality than is assumed in the calculations. The grain size used in calculations is determined from local bed material and has a median size of 0.27 mm. It is not surprising that the suspended sediment in the inlet does not only contain bed material, but also silt and mud. Silt and mud have a lower fall velocity and show a better mixing through the water column. More homogeneous concentration profiles are the result of this silt and mud content.

By adjusting the fall velocity used in the calculated concentration profiles, an estimated fall velocity can be used that provides a better fit with the measured concentration profiles. For calm weather conditions, a concentration profile is calculated with four different fall velocities: the original fall velocity based on local sand characteristics w_s, $0.5*w_s$, $0.1*w_s$ and $0.01*w_s$. The resulting profiles have been compared with the profiles as measured by the OBS and the ADV (Figure 7.14). It appears that the calculated profile using $0.01*w_s$ gives the best results for calm weather conditions. Recalculating this fall velocity to grain size gives a grain size of $2.1\ 10^{-5}$ m, an order of magnitude smaller than the original grain size of $2.7\ 10^{-4}$ m. This new grain size is probably not the only grain size present in the Slufter inlet.

In this particular case, the suspended sediment in the Slufter can be seen as a mixture of sand, silt and mud which can be represented by a grain size of $2.1\ 10^{-5}$ m. However, it should be kept in mind that the composition of the sediment in suspension changes with changing circumstances in the channel and that the found 'representative' grainsize of $2.1\ 10^{-5}$ m is not applicable in other cases. For example, during the strong outflow event of the storm, a lot of sand in suspension was observed, which would give a representative grainsize much more similar to the local sand size. However, the above calculated grainsize of $2.1\ 10^{-5}$ m suggests that under calm weather conditions, the sediment in suspension in the inlet channel is much smaller than the local sand.

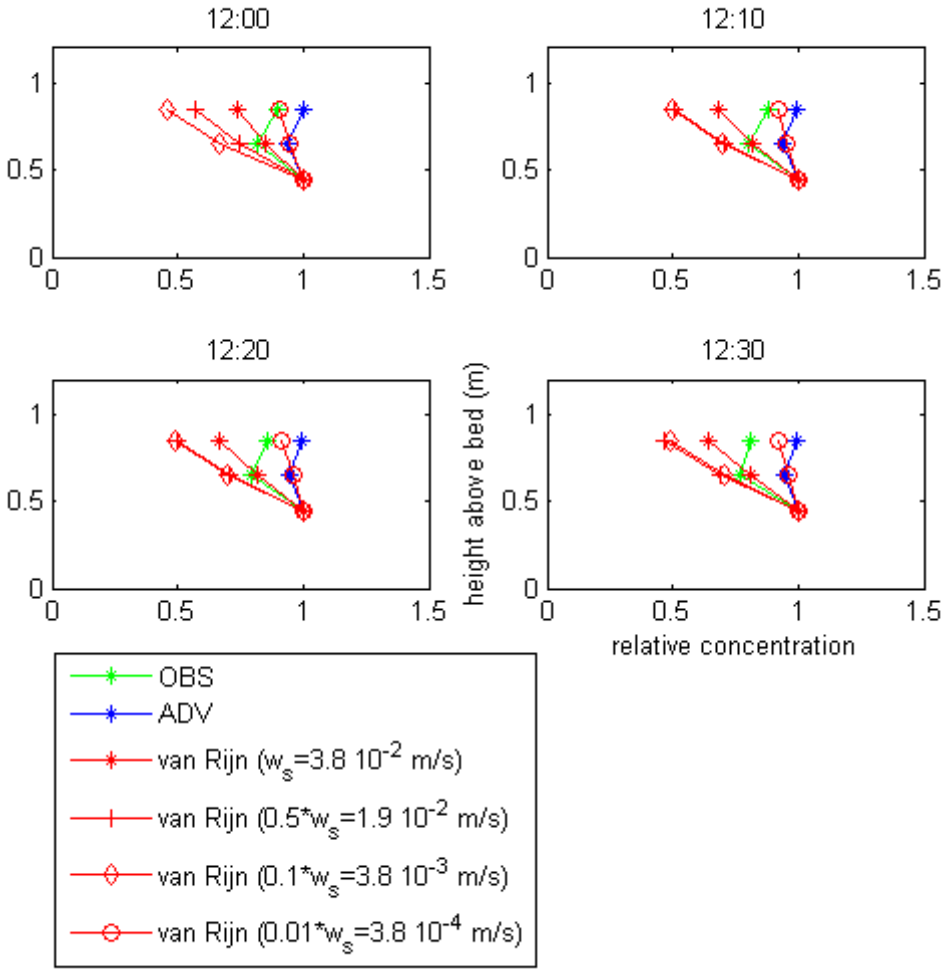

Figure 7.14 A comparison of concentration profiles as calculated by van Rijn (1993) and as measured by the OBS and ADV at four moments on October 22.

7.2.3 Calculation of suspended sediment transport

To quantify suspended load transport and to investigate its pattern, transport has been calculated using the models developed by Bagnold (1966), Bailard (1981) and van Rijn (1984) during a calm weather period with low flow velocities, a period with higher than average flow velocities and a setup (i.e. more energetic weather conditions) and during storm.

For calculations, the depth-averaged flow velocity has been used, which is computed as the average of all ADV measurements. When a certain ADV did not give measurement

results, for example because it was not submerged in the water, the average is calculated of the other measured velocities.

Calm weather

For calm weather conditions, the transport rates and patterns of suspended load sediment transport for the Bagnold and Bailard methods are quite similar. However, the van Rijn method gives no transport at all (Figure 7.15), which lies in the integration of a term for the initiation of motion (the T-factor) for the computation method. Flow velocities in the channel during calm weather do not exceed critical velocities as determined by van Rijn and therefore no transport is computed.

The Bagnold and Bailard computation methods give a large peak in transport rates during the first inflow peak of a tidal stage, but during the second peak of the inflow stage much less transport takes place due to the lower flow velocities. During outflow, there again is a distinct peak in the suspended transport rate.

Although quite small, the Bagnold method gives a small import of sediment over 50 hours ($4\ 10^{-2}$ m³), whilst the Bailard method gives a small export of sediment ($9\ 10^{-3}$ m³) When averaged over the whole Slufter area, the amounts of sedimentation and erosion lie in the order of 10^{-6} to 10^{-7} mm (table 7.1)

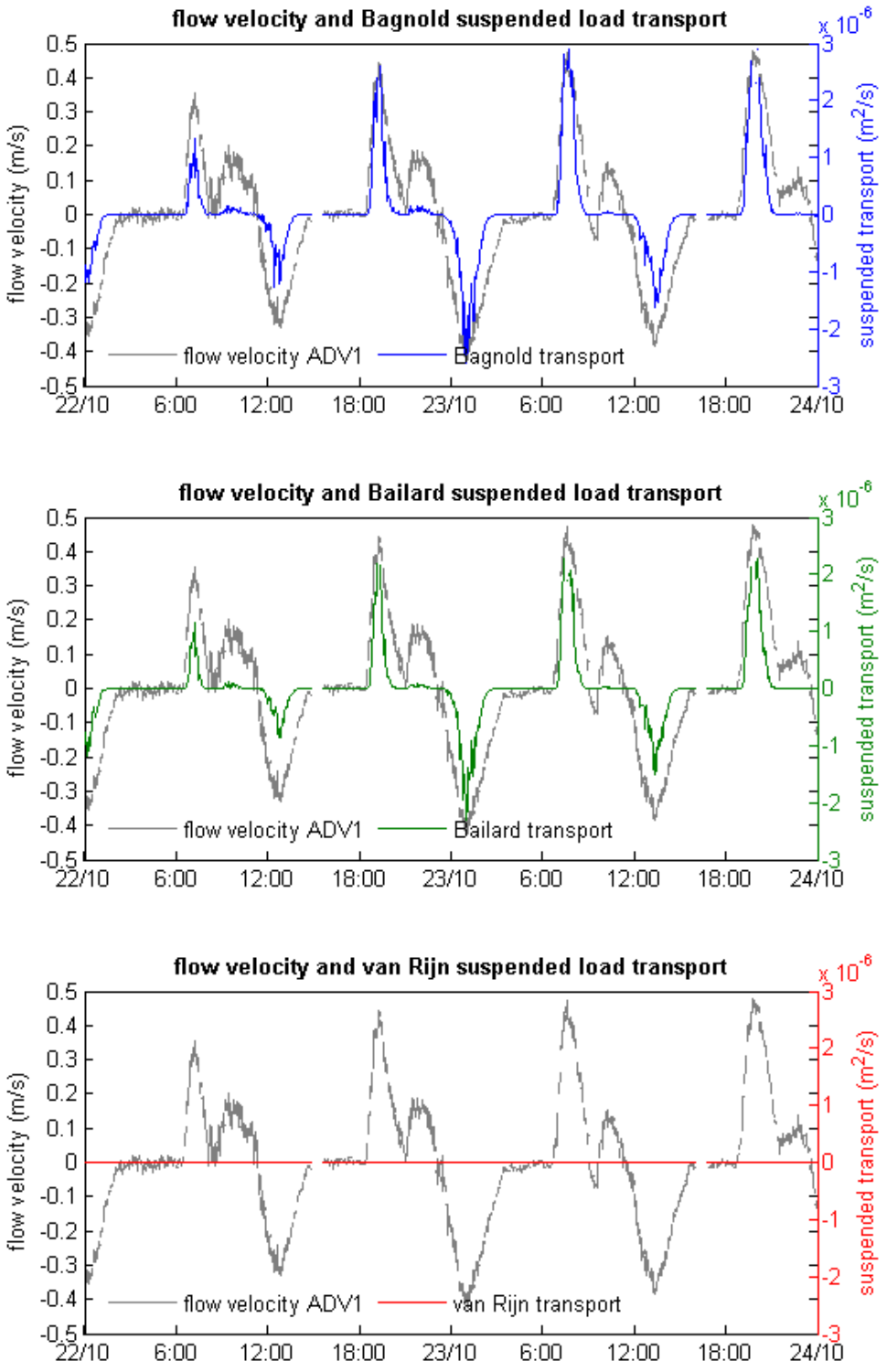

Figure 7.15 Suspended transport calculations for calm weather conditions.

Since the only good record of OBS measurements is made during calm weather, comparison with calculations is a useful way of testing the measurements. Making a comparison between OBS measurements and transport calculations, it should be noted that the calculated transports are negative during outflow of the channel and positive during inflow, while all OBS measurements are positive, regardless of out- and inflow (Figure 7.16). Both the OBS measurements and the transport calculations show peaks in backscatter counts and transport rate, respectively. However, for the OBS measurements the second inflow peak gives the highest backscatter values, while calculated transports at these moments are very low. Also, calculated transport rates decreases to zero when together with the flow velocity. The measured OBS values however stay relatively high and only decrease to the long-term minimum values when flow velocities are around zero for a longer time, after the outflow peak. The reason for this difference may be found in the kind of sediment in suspension. The models used assume sand is in suspension which reacts relatively direct to flow velocity due to its high fall velocity. However, in reality, sediment in suspension may be much smaller, with a low fall velocity and therefore a slower reaction to a decrease in flow velocity. Therefore, measured backscatter of the OBS remains relatively high when flow velocity is (almost) zero for only a short stretch of time.

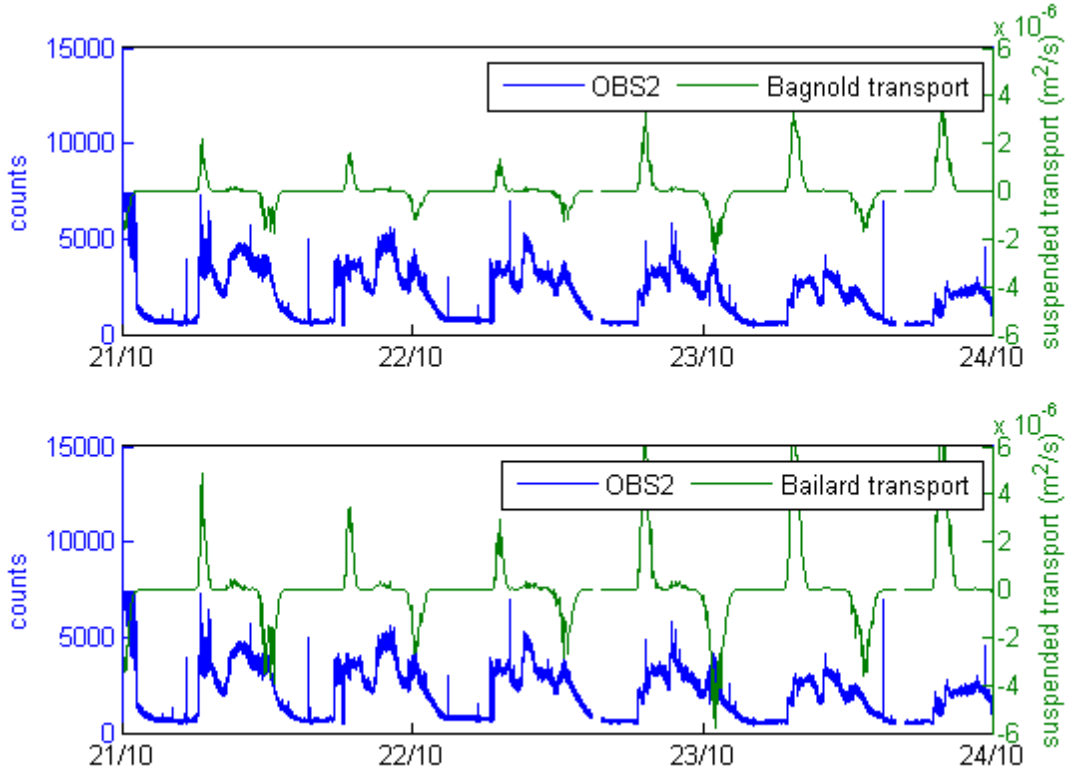

Figure 7.16 Comparison of OBS measurements and calculations of suspended sediment transport.

More energetic weather conditions

For more energetic weather conditions, the van Rijn method calculates small transport rates where flow velocities are largest and exceed the critical values. For the Bagnold and Bailard method the transports are larger (Figure 7.17). For the Bagnold and Bailard models, transport rates relate to flow velocity with a power of four, which is obvious in the outflow stage at October 17 between 6 and 12 o'clock. The outflow velocity is just a bit larger than one day later, but transport rates are much larger due to this nonlinearity. Since outflow velocities are usually larger than inflow velocities in the Slufter inlet channel, net transport is directed outward. Total transport amounts over 50 hours are -3.4, -4.8 and -0.8 m^3 for the Bagnold, Bailard and van Rijn methods respectively. This corresponds to an average erosion rate with an order of magnitude of 10^{-4} mm (table 7.1).

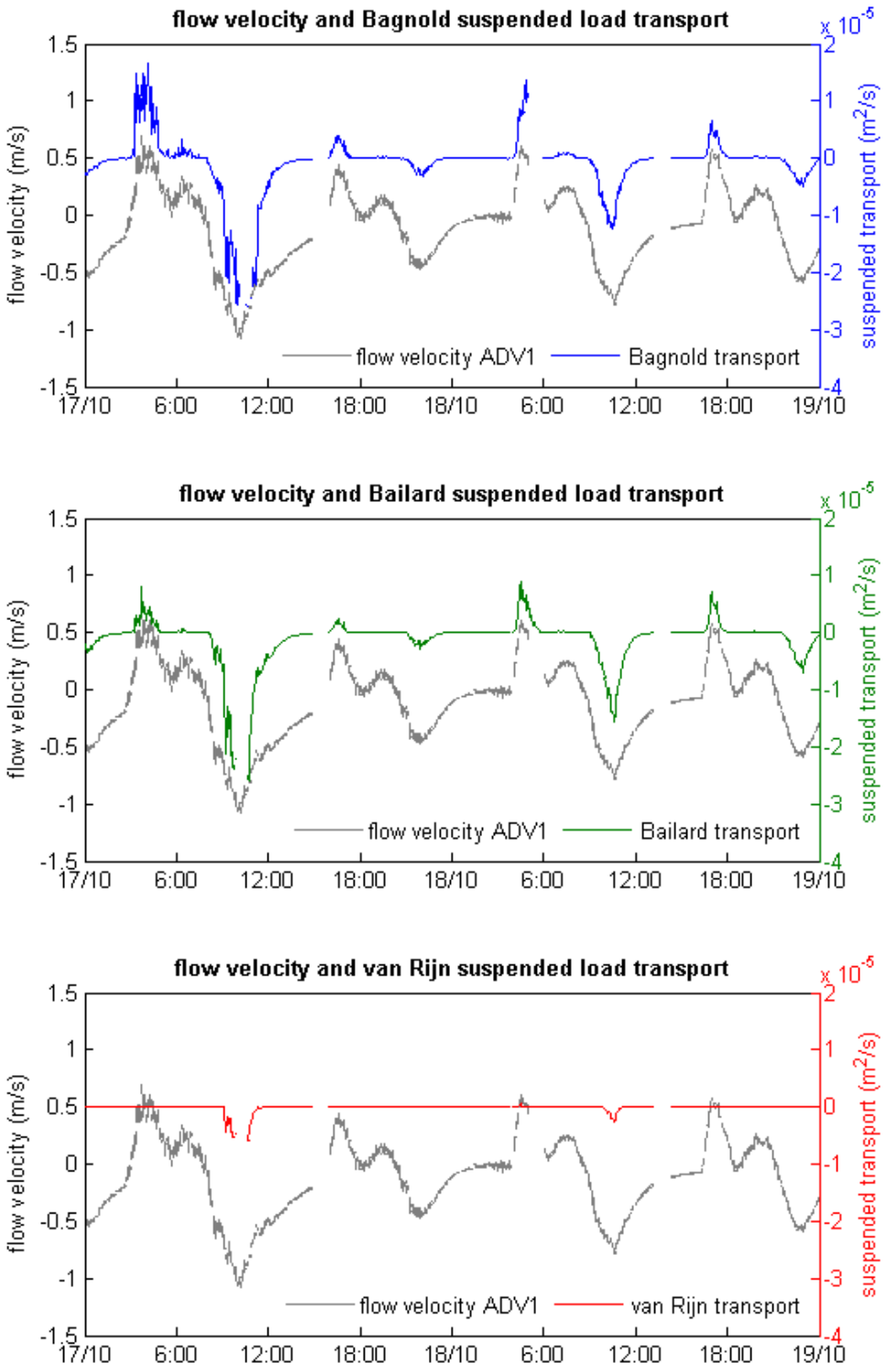

Figure 7.17 Suspended transport calculations for more energetic weather conditions.

Storm conditions

As could be expected, the suspended load transport rate reaches a maximum during the strongest outflow events of the storm and calculated values are much higher than under normal flow conditions (Figure 7.18). The biggest difference between the different computation methods is that transport rates calculated with the Bailard method are approximately twice as large as those calculated with the Bagnold and van Rijn methods. Due to the large suspended sediment transports calculated in the strong outflow event of the storm, the net transport pattern also shows a net export of sediment. Summed over fifty hours, the total transport is -30.0, -88.7 and -37.0 m^3 for the Bagnold, Bailard and van Rijn computation methods, respectively. Recalculated to average erosion over the whole area of the Slufter, this gives erosion in the order of magnitude of 10^{-3} to 10^{-2} mm, an order of magnitude larger than under energetic weather conditions. During one storm, ten times as much suspended sediment is exported through the channel than during the same time span under energetic weather conditions.

Suspended load transport on the long term

As with bedload transport, the frequency and magnitude of storms is very important for the net suspended load transport through the Slufter inlet on the long term. All models clearly indicate a net export of suspended sediment. Although it is unlikely that no suspended transport takes place at all under calm weather conditions, as the van Rijn computation method suggests, it appears to be of little influence on the total transport over long periods.

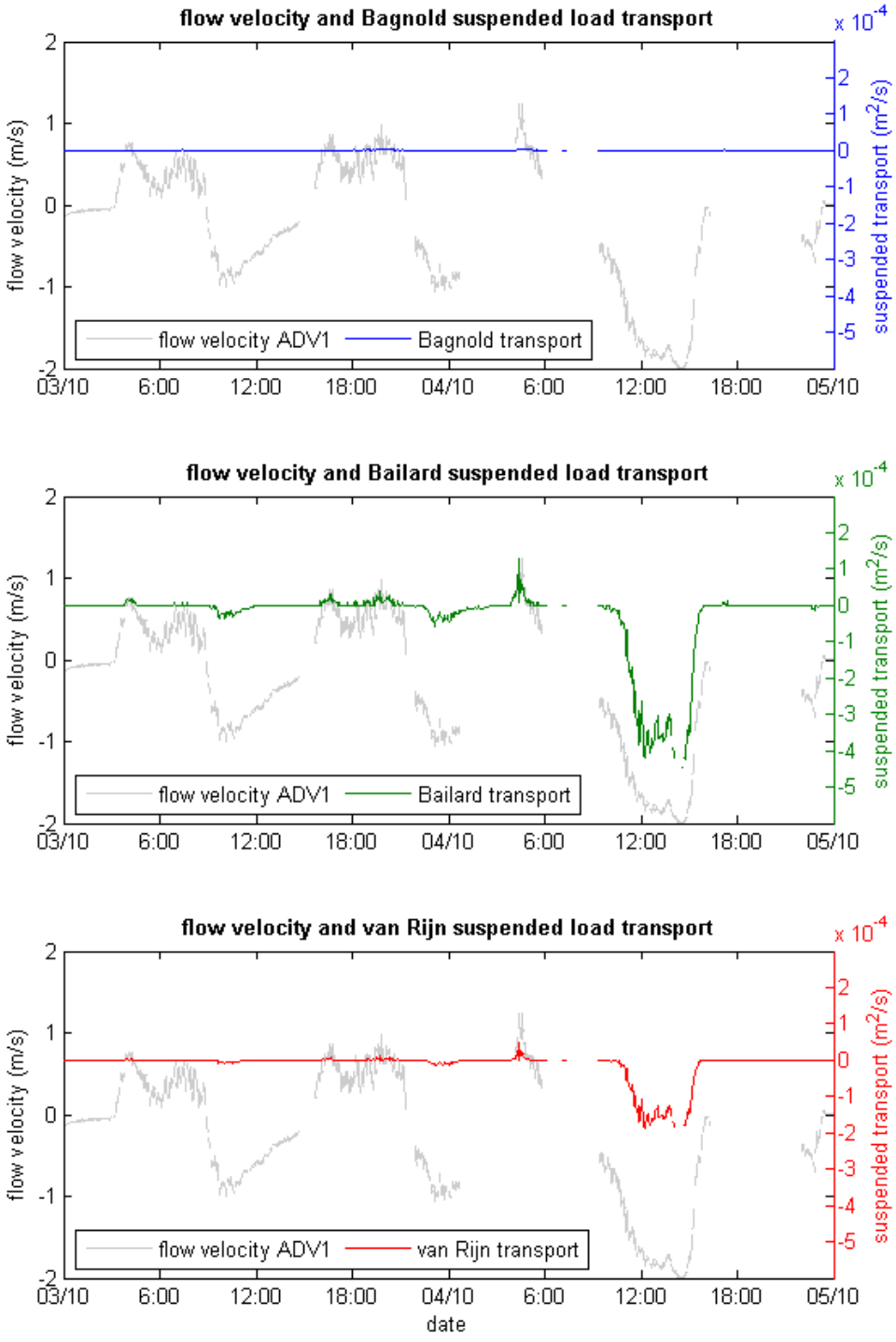

Figure 7.18 Suspended transport calculations for storm.

7.3 Total sediment transport

The total transport rate is assumed to be the sum of bedload and suspended load transport rates:

$$q_t = q_b + q_s \quad (7.1)$$

The total sediment transports over fifty hours for the periods of calm weather, more energetic weather conditions and storm are calculated and compared to the suspended load transports and bedload transports (table 7.1). a period of fifty hours instead of two days is chosen to include four complete tidal cycles. With a two-day period a peak ebb- or flood flow might have been left out, greatly influencing net transports.

7.3.1 Relative contributions of bedload and suspended load transport

When transports over fifty hours for calm weather conditions, more energetic weather conditions and storm are compared to each other, the transports under calm weather conditions appear to be insignificant with respect to the transports during more energetic weather conditions or during storm. During storm, transports are often three or more order of magnitude higher than under calm weather conditions.

Through the Slufter inlet channel, import of sediment is only calculated for calm weather conditions with the computation methods of Bagnold (1966) and van Rijn (1984a). Van Rijn (1984b) does not calculate any suspended load transport under calm weather conditions, but for all other cases export of sediment is found. Also for the seven week period export of sediment is found for bedload as well as suspended load sediment. The very small import under calm weather conditions as calculated by Bagnold and van Rijn is by far not large enough and does not occur often enough to compensate the export that occurs under more energetic conditions and storm.

When taking a look at the relative contributions of bedload and suspended load transport to the total transport, it is seen that bedload transport is highly dominant over suspended load transport under calm weather conditions for the Bailard and van Rijn computation

methods. Since no suspended load transport takes place under calm weather conditions according to van Rijn (1984b), bedload transport under these conditions equals the total transport. However, with increasing energetic conditions, the contribution of suspended load transport tot the total transport increases. For the Bagnold computation method, the contribution of suspended load transport to the total transport under calm weather conditions is relatively high. For more energetic conditions, the contribution of bedload transport increases with respect to the calm weather situation, but for storm, the contribution of suspended load transport to the total increases again.

It is hard to say what the relative contribution of bedload and suspended load in reality will be, since the calculations do not give uniform outcomes and measurement results are not available. For the time being, it can be concluded that on the long term, neither of both transport modes is highly dominant over the other.

	q_b (m^3)	q_b (mm)	q_s (m^3)	q_s (mm)	q_t (m^3)	q_t (mm)	% q_b	% q_s
Bagnold								
calm (2 d.)	0.0	$3.5\ 10^{-6}$	0.0	$9.9\ 10^{-6}$	0.1	$1.3\ 10^{-5}$	26	74
more energetic (2 d.)	-2.7	$-6.8\ 10^{-4}$	-3.4	$-8.5\ 10^{-4}$	-6.1	$-1.5\ 10^{-3}$	44	56
storm (2 d.)	-12.2	$-3.0\ 10^{-3}$	-30.3	$-7.6\ 10^{-3}$	-42.4	$-1.1\ 10^{-2}$	29	71
whole period (7 wks)	-35.2	$-8.8\ 10^{-3}$	-61.8	$-1.6\ 10^{-2}$	-97.0	$-2.4\ 10^{-2}$	36	64
Bailard								
calm (2 d.)	0.0	$-7.5\ 10^{-6}$	0.0	$-2.2\ 10^{-7}$	0.0	$-7.7\ 10^{-6}$	97	3
more energetic (2 d.)	-1.9	$-4.9\ 10^{-4}$	-4.8	$-1.2\ 10^{-3}$	-6.7	$-1.7\ 10^{-3}$	29	71
storm (2 d.)	-17.0	$-4.2\ 10^{-3}$	-88.7	$-2.2\ 10^{-2}$	-105.7	$-2.6\ 10^{-2}$	16	84
whole period (7 wks)	-29.2	$-7.3\ 10^{-3}$	-116.6	$-2.9\ 10^{-2}$	-145.9	$-3.7\ 10^{-2}$	20	80
van Rijn								
calm (2 d.)	0.0	$1.0\ 10^{-5}$	-	-	0.0	$1.0\ 10^{-5}$	100	0
more energetic (2 d.)	-2.8	$-7.0\ 10^{-4}$	-0.8	$-2.1\ 10^{-4}$	-3.6	$-9.1\ 10^{-4}$	77	23
storm (2 d.)	-34.0	$-8.5\ 10^{-3}$	-37.0	$-9.3\ 10^{-3}$	-71.0	$-1.8\ 10^{-2}$	48	52
whole period (7 wks)	-53.4	$-1.3\ 10^{-2}$	-42.9	$-1.0\ 10^{-2}$	-96.3	$-2.4\ 10^{-2}$	55	45

Table 7.1 Total sediment transport through the Slufter inlet channel over fifty hours. Only the transport over the whole period give the total transport over the whole fieldwork period, seven weeks. Also the percentage of the suspended load and bedload transport relative to the total transport is given.

7.3.2 Total transport during the fieldwork period and on the long term

Besides transport during a calm weather period, a more energetic weather period and a storm, the bedload, suspended load and total transport in the inlet channel have also been calculated over the whole fieldwork period of seven weeks (Table 7.1).
All different computation methods show a net export of sediment. When comparing the results for total transport, it is seen that the three different computation methods give similar exports. The Bailard (1981) method gives a suspended load export which is twice as high as the transports calculated by Bagnold (1966) and van Rijn (1984b), but all numbers still fall within the same order of magnitude.

The total transport as calculated during the fieldwork period is not representative for net total transport over longer periods. The frequency and magnitude of storms is a very important factor for the total net transport on the long term. A year with a lot of large storms may therefore show a different net transport than a year with few storms. Long periods of calm weather, for example during summer, may give a periodic import of sediment, although the amount of import will be relatively small.
Over a year, a net export of suspended as well as bedload sediment is most likely for the Slufter inlet channel. Most of the calculations performed indicate an export of sediment and the export during more energetic weather conditions and storm periods is so large that this export overrules the small import of sediment that occurs during calm weather. However, this export is calculated just for the inlet channel. For the Slufter basin as a whole, net transport not necessarily is export, due to the transport of sediment over the beach flat during storm. When the beach flat is inundated, water enters the Slufter basin via the beach flat, but leaves mostly via the channel. This implies import of sediment over the beach flat, although no measurements or calculations have been performed for this location. Taking this import of sediment over the beach flat into account, the long-term sediment transport direction and magnitude will be very different from the exports as calculated above.

8 Discussion

In this discussion section, first the stability of the Slufter and the net transport will be reflected, in the channel as well as for the system as a whole. Next some remarks about the measurements and computation methods for bedload and suspended load sediment will be made. To finish, some suggestions are made for future research in the Slufter inlet channel.

8.1 Stability of the Slufter and long term net transport

In comparison with most tidal inlets that have been covered by the literature, the Slufter inlet is a small system (van Puijvelde, 2009), which makes comparison difficult. When investigating sediment transport in tidal inlets, most literature covers tidal inlets in between barrier islands (e.g. (Bartholdy et al., 2002; Ernstsen et al., 2005; Fiechter et al., 2006) or estuaries (e.g. (Hoekstra et al., 2004; Kotaschuk & Best, 2005; Masselink et al., 2009). However, the Slufter is much smaller than most tidal inlets and estuaries and has a relatively small intertidal area and a large supratidal area. For most barrier systems and estuaries, the intertidal area is relatively larger. This means that in the Slufter, flow is almost always exclusively confined to the channel, while in for example estuaries flow during high tide takes place over the intertidal areas. This confinement of flow has a large influence on the deformation of the tidal wave in the system. Since no waves enter the channel and transport is thus tide-dominated, the deformation of the tidal wave in the Slufter is of large influence on transport rates. Assuming that a larger intertidal area would be present on both sides of the inlet channel, flood velocities would decrease with respect to the current situation, thereby decreasing the import of sediment. This would be of great importance to the stability of the Slufter as whole.

Although flow under normal conditions does not show much spatial variability due to its confinement to the channel, under storm conditions water also flows in over the beachflat, thereby causing large spatially variable for water as well as sediment. This second flow regime over the beach flat also makes the Slufter a exceptional tidal inlet; for

large tidal inlets in between barrier islands or estuaries, flow during storm is still mostly confined to the main channel and the intertidal areas.

When looking into the history of the Slufter, it can be assumed that the tidal inlet is stable, since its dimensions did not change drastically over the last 150 years. Silting up does not occur naturally, on the contrary. Several human attempts have been made to close the basin with dikes and artificial dunes, but severe storms repeatedly restored the link between the backbasin and the sea.
For the short term (up to ten years) it is difficult to make statements about the stability of the channel due to the regular relocation. It is unknown what will happen once the channel reached and starts to erode the dunes north of the gap in the dunes. A likely scenario that is in line with the opening of the channel after human closure, is an opening of a new channel more to the south, shortening the channel. Despite its large migration rate, the width and depth of the channel does not change significantly, thereby showing a short-term stability. It is expected that channel dimensions are stable, regardless its erosion to the north or possible relocation.

Sediment transport through the Slufter inlet channel is almost exclusively calculated as export. Only for calm weather conditions, the Bagnold (1966) and van Rijn (1984a) calculate a very small import of bedload sediment. However, under calm weather conditions all transports, bedload as well as suspended load, are very small with respect to transports under more energetic weather conditions and under storm and fall within the uncertainties of the calculation.
An important remark to make here is that these calculations are only valid for the channel itself. When under storm conditions the beach flats near the channel flood, an import of water and sediment takes place into the Slufter basin. Outflow takes place almost exclusively via the channel. Klein Breteler (2009) made a rough estimation of import of sediment via the beach flat during a storm of 100 m^3 per flooding event. Although, considering the assumptions made by Klein Breteler, this estimation will be an absolute maximum, it shows that significant import of sediment over the beach flat takes place during storm. When assuming 100 m^3 of bedload import for a single storm event, the net

import of transport for a single storm event would lie around 60 to 90 m^3. Apart from this import of sediment during storm, import is also assumed to take place under non-storm conditions due to aeolian transport since (south)western winds are dominant in the area. The above means that the long-term export for the Slufter basin as a whole is greatly reduced.

Suspended load sediment transport calculations calculate a net export of sediment under all circumstances, although transports under calm weather conditions are insignificant with respect to more energetic or storm conditions. However, some important remarks are to be made on the suspended load transport calculations. Most important to note is that the suspended transport calculations use the local bed sand characteristics, while sediment in suspension is a mixture of sand and much which cannot be described by these number. It is shown that for calm weather, the representative grainsize is an order of magnitude smaller than the grainsize used for calculations. A similar situation holds for more energetic weather conditions and storm: the grainsize used for calculation presumably is not the same as the representative grainsize of the suspended sediment.
In tidal inlets, there are a lot of factors which play a role in the erosion and sedimentation of suspended sediment, but which are not taken into account in the computation methods used. Biological factors, enhanced sedimentation in vegetated areas and the settling- and scour lag mechanism are examples of processes that have a big influence on the total sediment budget of the Slufter but which have not been taken into account. Despite the calculated exports, it is very well possible that sedimentation of fine sediment takes place, specially under storm conditions when the supratidal area floods. Low water levels, prolonged low flow velocities and the presence of vegetation all favour sedimentation on the marshes. Under calm weather conditions, sedimentation on the marshes does not take place as they are not flooded, but the OBS as well as the ADV measurements show suspended sediment concentration patterns which suggest a net import of sediment under calm weather conditions. Although estimations of sedimentation in the Slufter backbasin are almost impossible to make without further assumptions, it is likely that the calculated net export of suspended sediment overestimates the real net transports.

When looking at the long term sediment budget for the Slufter as a whole, the export of sediment probably will be smaller than what is expected on the basis of the calculations made in this study. Smaller exports are in correspondence with the apparent stability of the system.

When assuming small import for suspended sediment under calm weather conditions as indicated by the OBS and ADV measurements and a large export under storm conditions, the net transport pattern would show a similar pattern as found by Lumborg and Pejrup (2005) in the Danish Wadden sea (figure 8.1), although the relative contributions of storm and calm weather transports might be different, with a different net transport direction on the long term as a result. For bedload transport, the situation in the Slufter might be mirrored from that of the Danish Wadden sea: large import of bedload sediment during storm and a smaller export of sediment under more energetic conditions. During calm weather, almost no transport takes place. Again, the net transport direction on the long term depends on the differences in transport rate between the different situations.

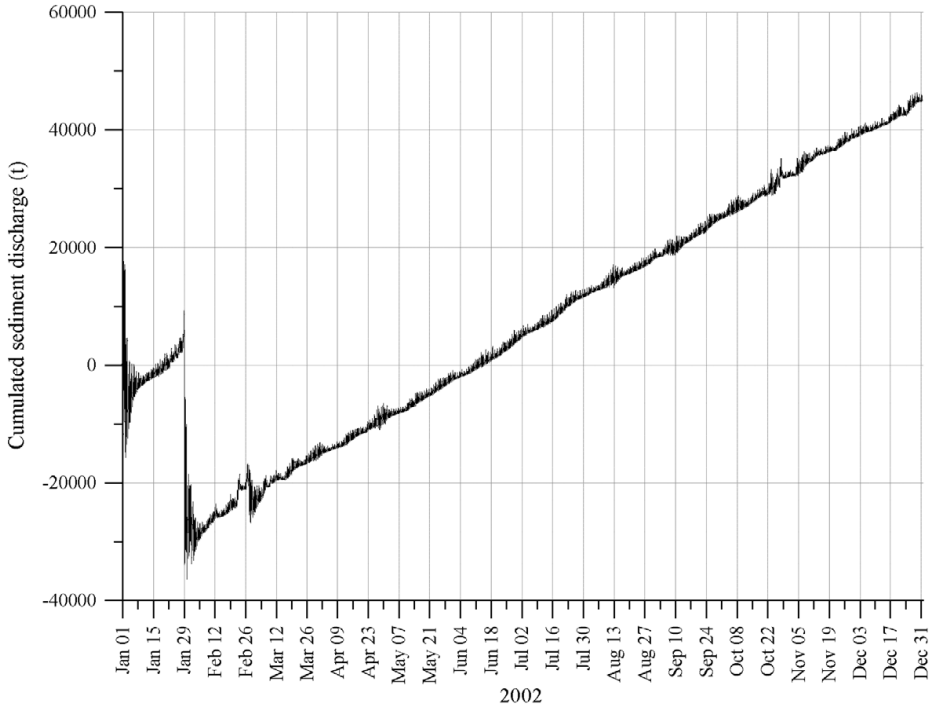

Figure 8.1 Sediment transport in the Danish Wadden sea. During calm weather, there is a slow, continuous import of sediment, during storm a sudden large export, for example on January 39 (Lumborg and Pejrup, 2005)

8.2 Remarks on measurements and calculations

8.2.1 Bedload sediment transport

When calculating bedload transport from bedform migration, it is assumed that the bedform migration is equal to bedload transport. For example, Hoekstra (2004), assumes that all bedload transport translates to bedform migration and that by calculating the net amount of sediment that passes a certain point via bedform migration, the net bedload transport is calculated. In the case of the Slufter, however, the situation is more complicated since the critical flow velocity for the migration of bedforms (0.6 m/s), is much larger than critical flow velocities for bedload sediment transport.
This raises the question how bedload transport takes place when bedforms do not migrate, if it takes place at all. If it does not, this would suggest that calculated bedload transport rates are systematically overestimated by the different computation methods used. Better investigation of bedload transport on a very small scale (lengths of single dunes) could give more insight in the processes at hand here.

One major shortcoming of the bedload transport calculations is that bedforms were not taken into account in these calculations; calculations were performed for a flat bed. However, bedforms are of significant influence to bedload transport because bedforms increase the local roughness of the bed, thereby increasing sediment transports. Bedload transport calculations could be improved by taking bedform roughness into account in roughness predictors.
The bedload transport calculations during calm weather conditions have a limited reliability. Apart from the question how much transport really takes place over bedforms at low flow velocities (see also above), calculating transport close to the initiation of motion is always difficult. Calculated net im- or export is so small that it lies within the uncertainties of the calculation methods. A sensitivity analysis of bedload transport could shed more light on this problem.

Finally, bedload transport calculations have been performed with an assumed channel width of 16 meters. However, with high water levels, the width of the channel is much larger, influencing the total transports of the channel.

8.2.2 Remarks on suspended load sediment transport

Despite the OBS measurements, the suspended sediment pattern in the Slufter inlet is not clear, especially during storm. OBS and ADV measurements show that suspended sediment concentrations in general follow flow velocity, but the exact pattern and magnitude of the peaks cannot be determined from these measurements. One problem in measuring suspended sediment concentrations with an OBS and to a lesser extent with and ADV is biofouling. In situations with high flow velocities, a lot of seaweed, plants from the backbasin and plastic ropes from boats at sea ties itself around the measurement instrument, making measurements useless. Unfortunately, these high-flow velocity events are the most interesting ones to measure. Spiked measurements are not always easy to distinct from good measurements.
The estimated grain size of 2.1 10^{-5} m as obtained in paragraph 7.2.2 is only a rough estimation of the grain size for sand in suspension. For more energetic weather conditions or even storm conditions, another, probably coarser, representative grain size is needed.

8.3 Recommendation for further research

Sediment transport in the Slufter inlet channel becomes much more insightful when more is known about the behaviour of bedforms on the channel bed and about suspended sediment concentrations and composition. More insight in these subjects might lead to answers about sediment transport under different circumstances and transport patterns and directions.

To gain more insight in the behaviour of bedforms, they should be monitored with a much higher spatial and temporal resolution than has been done in this research. Measuring equipment similar to ripple profilers for regular measuring of bed morphology can provide much information when visual observations are impossible due to high water

levels and flow velocities. Observing bedforms at low tide and low flow velocities, as has been done here, is not enough, observations should be made at high temporal resolutions when bedforms are actually expected to move, i.e. at high flow velocities.
Also, since bedform patterns did show a two-dimensional pattern in the period prior to this fieldwork study (van der Vegt, personal communication; Kramer, 2009), longer monitoring on the dimensions and patterns of the bedforms in the channel might be useful.

This study has shown that using OBS measurements in the Slufter inlet channel is of little use due to varying grainsize composition and partly due to biofouling. To still be able to gain basic insight in the suspended sediment composition and patterns in concentration and composition, water samples should be taken often. Taking samples with a pump has a lot of practical drawbacks. Simply filling a bottle by submerging it into the channel water might not be a very precise way of determining suspended sediment concentrations, but it is a very easy one. At least with this method basic questions about the change of suspended sediment concentration through time and its composition might be answered, on which basis plans for further research can be based.

9 Conclusion

Morphology

- With increasing flow velocities in the Slufter inlet channel, the northward migration rate of the channel also increases.
- Bedforms in the channel have lengths in the order of meters and heights in the order of decimetres and are highly three-dimensional. All bedforms show an ebb-dominated morphology
- Bedform migration or bedlevel change does not take place when flow velocities do not exceed 0.6 m/s.

Hydrodynamics

- Flow in the channel is ebb dominated; maximum ebb flow velocities are higher than maximum flood flow velocities, the ebb duration is longer than the flood duration, as is the period from maximum ebb flow to maximum flood flow.
- During storm, infragravity waves enter the channel due to increased water levels. Otherwise, waves do not enter the Slufter inlet channel.

Bedload sediment transport

- Due to sudden changes in bedlevel when flow velocities are higher than 0.6 m/s, the dune tracking technique could not be applied on the bedforms in the channel. No bedload transport can therefore be calculated from dune tracking measurements.
- Practically no bedload sediment transport is calculated under calm weather conditions. Under more energetic weather conditions and storm conditions, an export is calculated. During storm, transport rates are an order of magnitude higher than under more energetic conditions.

Suspended load transport

- Suspended sediment concentrations are the result of local flow velocities.
- Comparison of transport patterns from measurements and calculations show good agreement under calm weather conditions.
- Quantifying OBS and ADV suspended sediment measurements is not possible in the Slufter inlet.
- Suspended sediment transport calculations show hardly any transport under calm weather conditions. In other cases, an export of suspended sediment is calculated. Transport rates during storm are an order of magnitude larger than transport rates during energetic weather conditions.
- Calculated and measured concentration profiles under calm weather conditions show that fall velocities for sediment in suspension are two orders of magnitude lower than the initial fall velocity used in calculations. Under calm weather conditions, the sediment in suspension has a representative grain size of $2.1\ 10^{-5}$ m instead of $2.7\ 10^{-4}$ m, the local sediment grainsize that was used in transport calculations. Silt and mud play an important role in the suspended sediment transports.

Total load transport

- On the long term, the Slufter inlet channel shows a net export of bedload as well as suspended load sediment
- The frequency and strength of storms over a year is of major importance to the total and net sediment transports. The strong export during storm events mostly determines the net export of sediment through the inlet channel over a year.
- With increasing flow velocities, the contribution of suspended sediment transport to the total transport increases. Over long periods, both bedload and suspended load are important contributors to the total transport budget.
- Since there are processes that cause an import of sediment, but which do not take place in the inlet channel, the net export of sediment for the whole system is probably smaller than what has been calculated in this study.

Objectives of research

Over long periods, the Slufter inlet channel shows an export of sediment for suspended as well as bedload sediment. Since waves do not enter the inlet, except for infragravity waves during storm, the tide is the main factor governing sediment transport.

Under neap tide conditions, flow velocities are smaller, which will enhance import of bedload sediment. Under spring tide conditions, flow velocities are generally larger which will enhance export of bedload and suspended load sediment. However, external factors, such as wind setup which causes higher flow velocities in the channel, are of major importance to sediment transport. Since sediment transport rates under calm weather conditions are negligible to those under storm conditions, and because sediment transport rates under storm conditions are an order of magnitude higher than under more energetic conditions, storm are of major importance for determining the net transport budgets through the inlet channel for long periods.

10 References

Allen, J.R.L., P.F. Friend, A. Lloyd et al. (1994), Morphodynamics of intertidal dunes: A year-long study at lifeboat station bank, wells-next-the-sea, eastern england. Philosophical Transactions: Physical Sciences and Engineering 347(1682), pp.291-344.

Anthony, D. & J.O. Leth. (2002), Large-scale bedforms, sediment distribution and sand mobility in the eastern north sea off the danish west coast. Marine Geology 182(3-4), pp.247-263.

Bagnold, R.A. (1966), An approach to the sediment transport problem from general physics. Geological Survey Prof. Paper 422-I

Bailard, J. (1981), An energetics total load sediment transport model for a plane sloping beach. Journal of Geophysical Research 86(C11), pp.10938-10954.

Bartholdy, J., A. Bartholomae & B.W. Flemming. (2002), Grain-size control of large compound flow-transverse bedforms in a tidal inlet of the danish wadden sea. Marine Geology 188(3-4), pp.391-413.

Brockhus, H. (2010). Title unknown. Unpublished MSc, Utrecht University.

Buijsman, M.C. & H. Ridderinkhof. (2008a), Long-term evolution of sand waves in the marsdiep inlet. I: High-resolution observations. Continental Shelf Research 28(9), pp.1190-1201.

Buijsman, M.C. & H. Ridderinkhof. (2008b), Long-term evolution of sand waves in the marsdiep inlet. II: Relation to hydrodynamics. Continental Shelf Research 28(9), pp.1202-1215.

Camenen, B. & P. Larroudé. (2003), Comparison of sediment transport formulae for the coastal environment. Coastal Engineering 48(2), pp.111-132. DOI: DOI: 10.1016/S0378-3839(03)00002-4

de Swart, H.E. & J.T.F. Zimmerman. (2009), Morphodynamics of tidal inlet systems. Annual Review of Fluid Mechanics(41), pp.203-229.

de Vries, J. (2010). Infragravity wave behaviour in a secondary tidal inlet, at the slufter, the Netherlands. Unpublished MSc, Utrecht University.

Dyer, K., M. Christie & A. Manning. (2004), The effects of suspended sediment on turbulence within an estuarine turbidity maximum. Estuarine, Coastal and Shelf Science 59(2), pp.237-248.

Elgar, S., B. Raubenheimer & R. Guza. (2005), Quality control of acoustic doppler velocimeter data in the surfzone. Measurement science and technology 16(10), pp.1889-1893.

Elias, E.P.L., J. Cleveringa, M.C. Buijsman et al. (2006), Field and model data analysis of sand transport patterns in texel tidal inlet (the netherlands). Coastal Engineering 53(5-6), pp.505-529. DOI: 10.1016/j.coastaleng.2005.11.006 ER

Elias, E.P.L. & A.J.F. van der Spek. (2006), Long-term morphodynamic evolution of texel inlet and its ebb-tidal delta (the netherlands). Marine Geology 225(1-4), pp.5-21.

Engel, P. & Y.L. Lau. (1980), Computation of bedload using bathymetric data. Journal of the hydraulics division 106, pp.369-380.

Ernstsen, V.B., R. Noormets, C. Winter et al. (2005), Development of subaqueous barchanoid-shaped dunes due to lateral grain size variability in a tidal inlet channel of the danish wadden sea. Journal of Geophysical Research 110

Fiechter, J., K.L. Steffen, C.N.K. Mooers et al. (2006), Hydrodynamics and sediment transport in a southeast florida tidal inlet. Estuarine, Coastal and Shelf Science 70(1-2), pp.297-306.

Finelli, C.M., D.D. Hart & D.M. Fonseca. (1999), Evaluating the spatial resolution of an acoustic doppler velocimeter and the consequences for measuring near-bed flows. Limnology and Oceanography 44(7), pp.1793-1801.

Fugate, D. & Friedrichs, C. (2002), Determining concentration and fall velocity of estuarine particle populations using ADV, OBS and LISST. Oxford: Pergamon.

Gao, S. & M. Collins. (1994), Tidal inlet stability in response to hydrodynamic and sediment dynamic conditions. Coastal Engineering 23(1-2), pp.61-80.

Green, M.O. & I.T. MacDonald. (2001), Processes driving estuary infilling by marine sands on an embayed coast. Marine Geology 178(1-4), pp.11-37.

Ha, H., W. Hsu, J. Maa et al. (2009), Using ADV backscatter strength for measuring suspended cohesive sediment concentration. Continental Shelf Research 29(10), pp.1310-1316.

Hawkins, A.B. & M.J. Sebbage. (1972), The reversal of sand waves in the bristol channel. Marine Geology 12, pp.M7-M9.

Hisgen, R. G. W. & Laane, R. W. P. M. (2008). Geheimen van de kust, van zwin tot marsdiep. (1st ed.). Diemen: Uitgeverij Veen Magazines B.V.

Hoekstra, P., P. Bell, P. van Santen et al. (2004), Bedform migration and bedload transport on an intertidal shoal. Continental Shelf Research 24(11), pp.1249-1269.

Hoque, M.A., B.G. Ahad & E. Saleh. (2009), Sediment transport and morphodynamics of the tidal inlet and adjacent coastlines of salut-mengkabong lagoon, sabah, malaysia. Journal of Coastal Research 2, pp.1360-1364.

Huettel, M., E. Precht & F. Janssen. (2006), Near-bottom performance of the acoustic doppler velocimeter (ADV) – a comparative study. Aquatic Ecology 40(4), pp.481-492.

Jinchi, H. (1992), Application of sandwave measurements in calculating bed load discharge. Erosion and Sediment transport monitoring programmes in river basins, proceedings of the Oslo symposium 210, pp.63-70.

Kim, S., C. Friedrichs, J. Maa et al. (2000), Estimating bottom stress in tidal boundary layer from acoustic doppler velocimeter data. Journal of Hydraulic Engineering 126(6), pp.399-406.

Klein Breteler, R. (2009). Wave-induced sediment transport at the small tidal inlet 'Slufter' of Texel, the Netherlands. (MSc graduation, Utrecht University, The Netherlands), (www.uu.nl/igitur)

Kotaschuk, R. & J. Best. (2005), Response of sand dunes to variations in tidal flow: Fraser estuary,
canada. Journal of Geophysical Research 110(F04S04)

Kramer, W.M. (2009). Tidal hydrodynamics and sediment transport processes in 'de slufter', the netherlands. Unpublished MSc, Utrecht University, The Netherlands.

Liu, J.T. & L.-. Hou. (1997), Sediment trapping and bypassing characteristics of a stable tidal inlet at kaohsiung harbor, taiwan. Marine Geology 140(3-4), pp.367-390.

Lumborg, U. & M. Pejrup. (2005), Modelling of cohesive sediment transport in a tidal lagoon-an annual budget. Marine Geology 218(1-4), pp.1-16.

Masselink, G., L. Cointre, J. Williams et al. (2009), Tide-driven dune migration and sediment transport on an intertidal shoal in a shallow estuary in devon, UK. Marine Geology 262(1-4), pp.82-95.

Meyer-Peter, E. & R. Mueller. (1948), Formulas for bed-load transpor, stockholm, sweden. Sec. Int. IAHR congress

Mori, N., T. Suzuki & S. Kakuno. (2007), Noise of acoustic doppler velocimeter data in bubbly flows. Journal of Engineering Mechanics 133(1), pp.p122-4p.

Nield, J.M., D.J. Walker & M.F. Lambert. (2005), Two-dimensional equilibrium morphological modelling of a tidal inlet: An entropy based approach. Ocean Dynamics 55(5-6), pp.549-558. DOI: 10.1007/s10236-005-0023-4 ER

Pacheco, A., A. Vila-Concejo, O. Ferreira et al. (2008), Assessment of tidal inlet evolution and stability using sediment budget computations and hydraulic parameter analysis. Marine Geology 247(1-2), pp.104-127. DOI: 10.1016/j.margeo.2007.07.003 ER

Pope, N., J. Widdows & M. Brinsley. (2006), Estimation of bed shear stress using the turbulent kinetic energy approach - A comparison of annular flume and field data. Continental Shelf Research 26(8), pp.959-970.

Ranasinghe, R. & C.B. Pattiaratchi. (2000), Tidal inlet velocity asymmetry in diurnal regimes. Continental Shelf Research 20(17), pp.2347-2366.

Siegle, E., D.A. Huntley & M.A. Davidson. (2004), Physical controls on the dynamics of inlet sandbar systems. Ocean Dynamics 54(3-4), pp.360-373. DOI: 10.1007/s10236-003-0062-7 ER

Soulsby, R. (1997). Dynamics of marine sands, a manual for practical applications. Wallingford, England: Thomas Telford.

Stanev, E.V., G. Brink-Spalingk & J.O. Wolff. (2007), Sediment dynamics in tidally dominated environments controlled by transport and turbulence: A case study for the east frisian wadden sea. Journal of Geophysical Research 112

Ten Brinke, W.B.M., A.W.E. Wilbers & C. Wesseling. (1999), Dune growth, decay and migration rates during a large-magnitude flood at a sand and mixed sand-gravel bed in the dutch rhine river system. Special publication International Association of Sedimentology 28, pp.15-32.

Thompson, C., C. Amos, T. Jones et al. (2003), The manifestation of fluid-transmitted bed shear stress in a smooth annular flume - a comparison of methods. Journal of Coastal Research 19(4), pp.1094-1103.

Traynum, S. & R. Styles. (2007), Flow, stress and sediment resuspension in a shallow tidal channel. Estuaries and Coasts 30(1), pp.94-101.

van de Kreeke, J. & A. Hibma. (2005), Observations on silt and sand transport in the throat section of the frisian inlet. Coastal Engineering 52(2), pp.159-175.

van den Berg, J.H. (1987), Bedform migration and bedload transport in some rivers and tidal environments. Sedimentology 34, pp.681-198.

van der Molen, J. (2002), The influence of tides, wind and waves on the net sand transport in the north sea. Continental Shelf Research 22(18-19), pp.2739-2762. DOI: DOI: 10.1016/S0278-4343(02)00124-3

Van Goor, M.A., T.J. Zitman, Z.B. Wang et al. (2003), Impact of sea-level rise on the morphological equilibrium state of tidal inlets. Marine Geology 202(3-4), pp.211-227. DOI: 10.1016/S0025-3227(03)00262-7 ER

van Puijvelde, S.P. (2009). Morphodynamics of the slufter, morphodynamical processes in a small tidal inlet in the Netherlands. (MSc thesis, Utrecht University, faculty of geosciences),

van Rijn, L.C. (1984), Sediment transport, part II: Suspended load transport. Journal of Hydraulic Engineering, ASCE 110(11)

van Rijn, L. C. (1990). Principles of fluid flow and surface waves in river, estuaries, seas and oceans (2nd ed.). The Netherlands: Aqua publication.

van Rijn, L.C. (1984), Sediment transport, part I: Bed load transport. Journal of Hydraulic Engineering, ASCE 110(10)

van Rijn, L. C. (1993). Principles of sediment transport in rivers, estuaries and coastal seas (1st ed.). Amsterdam: Aqua publications.

Vila-Concejo, A., O. Ferreira, A. Matias et al. (2003), The first two years of an inlet: Sedimentary dynamics. Continental Shelf Research 23(14-15), pp.1425-1445. DOI: 10.1016/S0278-4343(03)00142-0 ER

Vinther, N., J. Nielsen & T. Aagaard. (2004), Cyclic sand bar migration on a spit-platform in the danish wadden sea - spit-platform morphology related to variations in water level. Journal of coastal research 20(3), pp.672-679.

Witteveen, M. (2010). Cross-shore suspended sediment transport and morphological response on a beach plain during fair weather conditions and during a storm event at the Slufter, Texel. Unpublished MSc, Utrecht University.